PNL-3160-1
UC-70

NOTICE
This is a draft report. The information presented is of preliminary nature and is not intended to be referenced in open literature.

Assessment of Effectiveness of Geologic Isolation Systems

VARIABLE THICKNESS TRANSIENT GROUND-WATER FLOW MODEL

VOLUME 1. FORMULATION

A. E. Reisenauer

December 1979

Prepared for the
Office of Nuclear Waste Isolation
under its Contract with the
U.S. Department of Energy

Pacific Northwest Laboratory
Richland, Washington 99352

FOREWORD

The Assessment of Effectiveness of Geologic Isolation Systems (AEGIS) Program is developing and applying the methodology for assessing the far-field, long-term post-closure safety of deep geologic nuclear waste repositories. AEGIS is being performed by Pacific Northwest Laboratory (PNL) under contract with the Office of Nuclear Waste Isolation (ONWI) for the Department of Energy (DOE). One task within AEGIS is the development of methodology for analysis of the consequences (water pathway) from loss of repository containment as defined by various release scenarios.

Analysis of the long-term, far-field consequences of release scenarios requires the application of numerical codes which simulate the hydrologic systems, model the transport of released radionuclides through the hydrologic systems to the biosphere, and, where applicable, assess the radiological dose to humans.

Essentially three modeling technologies are involved in assessing the water pathway release consequence. These models are: 1) hydrologic models that define the groundwater flow field and provide water flow paths and travel times, 2) transport models that describe the movement and concentrations of the radionuclides in the flow field, and 3) dose models that determine the resultant radiation doses to individuals and/or populations. Figure i is a schematic flow diagram for the release consequence analysis.

The various input parameters required in the analysis are compiled in data systems. The data are organized and prepared by various input subroutines for use by the hydrologic and transport codes. The hydrologic models simulate the groundwater flow systems and provide water flow directions, rates, and velocities as inputs to the transport models. Outputs from the transport models are basically graphs of radionuclide concentration in the groundwater plotted against time. After dilution in the receiving surface-water body (e.g., lake, river, bay), these data are the input source terms for the dose models, if dose assessments are required. The dose models calculate radiation dose to individuals and populations.

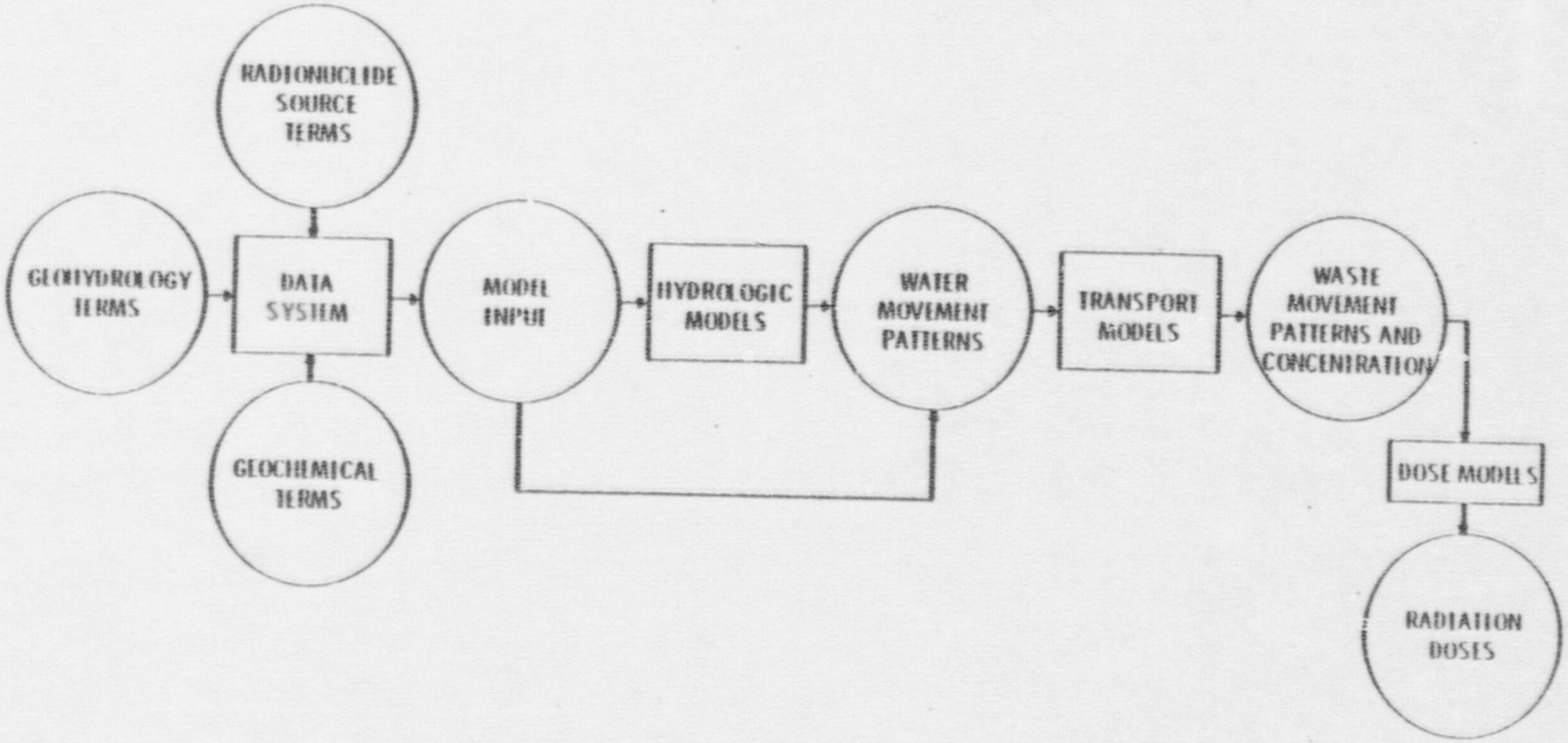

FIGURE i. Schematic Diagram of Consequence Analysis

Hydrologic and transport models are available at several levels of complexity or sophistication. Model selection and use are determined by the quantity and quality of input data. Model development under AEGIS and related programs provides three levels of hydrologic models, two levels of transport models, and one level of dose models (with several separate models). The models and data systems are documented as follows:

- HYDROLOGIC MODELS:

PNL-3162 PATHS Groundwater Hydrologic Model - first level (simplest) idealized hybrid analytical/numerical model for two-dimensional, saturated groundwater flow and single component transport; homogeneous geology.

PNL-3160 VTT (Variable Thickness Transient) Groundwater Hydrologic Model - second level (intermediate complexity) two-dimensional saturated groundwater flow, Boussinesq approximation, finite difference approach; two-dimensional (quasi three-dimensional) multiaquifer capability; heterogeneous geology.

PNL-2939 FE3DGW (Finite Element, Three-Dimensional Groundwater Hydrologic Model - third level (high complexity) three-dimensional, finite element approach (Galerkin formulation) for saturated groundwater flow; heterogeneous geology.

- TRANSPORT MODELS:

PNL-2970 GETOUT Transport Model - first level one-dimensional analytical solution considering radioactive chain decay with capability for only simple release and hydrologic functions; single speciation, constant flow rate, dispersion and sorption three-member straight delay chains.

PNL-3179 MMT (Multicomponent Mass Transport) Model - second level, one-dimensional numerical, discrete parcel random walk (DPRW) algorithm; chain decay, single speciation, equilibrium sorption, time-variant leach rate and dispersion, n-membered straight or branched decay chains.

- DOSE MODELS:

PNL-3180 ARRRG - drinking water, external exposure to aquatic food, water and shorelines, and FOOD - terrestrial food.

PNL-3209 PABLM - Combination of ARRRG and FOOD with additional features related to chronic releases.

BNWL-B-264 KRONIC - chronic external dose from air pathways.

BNWL-B-351 SUBDOSA - acute external dose from air pathways.

BNWL-B-389 DACRIN - chronic or acute inhalation dose from air pathways.

- DATA SYSTEMS:

PNL-3139 SIRS (Sorption Information Retrieval System) - storage and retrieval system for experimental data on sorption/desorption analyses for a wide variety of radionuclides, groundwater compositions, and rocks and minerals.

PNL-3161 CIRMIS (Comprehensive Information Retrieval and Model Input Sequence) Data System - storage and retrieval system for model input and output data, including graphical interpretation and display.

This is the first of 3 volumes of the description of the VTT hydrologic model.

Return of the form on the last page of this report is required in order to remain on the Distribution List for future revisions of the model.

ACKNOWLEDGMENT

This research was supported by the Waste Isolation Safety Assessment Program being conducted by Pacific Northwest Laboratory. This program was sponsored by the Office of Nuclear Waste Isolation, managed by Battelle Memorial Institute for the Department of Energy under Contract EY-76-C-06-1830. On 1 October 1979, WISAP became the Assessment of Effectiveness of Geologic Isolation Systems (AEGIS) Program and the Waste/Rock Interactions Technology (WRIT) Program. This report was issued by AEGIS.

CONTENTS

FIGURES

INTRODUCTION

Any modeling effort requires some simplifying assumptions to bridge the gap between reality and our current knowledge or understanding of the system being modeled and practicability. In most modeling fields certain basic simplifying assumptions are routinely accepted, whereas others require justification based on data gathered and observations made on the real-world system being modeled. In the set of equations we will write in this section, a large amount of the modeling effort and associated assumptions have already been made (cf., Bear et al. 1972). The set of assumptions and modeling effort discussed in Chapter 4 of Bear's report takes us from the complex world of porous media particles and the associated tortuous flow paths for ground water to the regime of representative elementary volumes and the fluid flow continuum. These assumptions are generally accepted in the field of ground-water hydrology and are complex enough that they will not be presented here. The equations we write to describe an aquifer system will be for a fluid flow continuum in porous media. However, it is not sufficient for a mathematical model to be based on a sound set of equations which describe the physical system. The model must also be based on technically sound hydrologic information and reasonable simplifying assumptions regarding these hydrologic interpretations. The advent of high-speed digital computers has paved the way for making computer simulation of complex ground-water systems a practical reality.

The digital computer model is designed to simulate the hydraulic-head response to natural and man-made aquifer stresses in a multi-layered two-dimensional aquifer system. The real ground-water system is, of course, a three-dimensional system, including precipitation percolating from the surface through unsaturated soil into the uppermost aquifer. In some cases along rivers or streams or at the base of lakes and ponds, the aquifers are discharging into or being recharged from these surface-water bodies. These conditions formulate one type of boundary condition for our mathematical model. The units we call separate aquifers are really water saturated layers in the soil and rock matrix which make up the earth's crust. These units are generally more permeable than the geologic units directly below them and sometimes above. As a result, the water in an aquifer tends to flow in a horizontal direction along the bedding plane of the more permeable geologic formation since the resistance to flow is less. The less permeable (aquitard) or sometimes impermeable (aquiclude) layers below and sometimes above the aquifer materials retard or completely block the vertical flow. These less permeable layers are designated as the base and top of the aquifer unit. When a more permeable layer exists below the upper aquifer unit's base, another aquifer may exist. When the aquitard material between aquifers is somewhat permeable, there can be water transfer between the aquifer units, depending on the water potential or pressure in the units. For most regional ground-water models which are currently being used, a simplifying assumption is made which transforms this three-dimensional system to a layered two-dimensional system with interaquifer transfer via a potential-driven leakage term. The mathematical model which utilizes this set of simplifying assumptions is the multi-aquifer formulation of the Boussinesq equations.

MATHEMATICAL FORMULATION FOR THE VARIABLE THICKNESS TRANSIENT (VTT) MODEL

Often an exact solution of the general, three-dimensional, saturated flow equation and free-surface boundary condition is not required to obtain useful results. VTT utilizes the Dupuit-Forchheimer or Boussinesq approximate method, which assumes a simplified, two-dimensional horizontal view of the ground-water system. This allows the free-surface boundary condition and the flow equation to be combined into a single equation amenable to practical numerical solution techniques. For simplicity we will refer to this method as the Boussinesq Flow Model.

Let x, y, z be the coordinates of a fluid particle, then dx/dt, dy/dt and dz/dt are the components of "pore velocity," and the Darcian seepage velocities are:

$$V_x = n_e \frac{dx}{dt} \tag{1}$$

$$V_y = n_e \frac{dy}{dt} \tag{2}$$

$$V_z = n_e \frac{dz}{dt} \tag{3}$$

where:

n_e = effective porosity.

Now, if we let $z = h(x, y, t)$ represent the coordinate of the free surface and formally differentiate with respect to time, we have:

$$\frac{\partial z}{\partial t} = \frac{\partial h}{\partial x}\frac{dx}{dt} + \frac{\partial h}{\partial y}\frac{dy}{dt} + \frac{\partial h}{\partial t} \tag{4}$$

Substituting the Darcian velocities and rearranging we have:

$$n_e \frac{\partial h}{\partial t} + V_x \frac{\partial h}{\partial x} + V_y \frac{\partial h}{\partial y} - V_z(h) = 0 \qquad (5)$$

The Dupuit assumptions used in this model may be simply stated as: $\phi(x, y, z, t) = \phi(x, y, \overline{z}, t)$ where $\overline{z}$ = average height of the water particles above reference datum. This is equivalent to stating that flow is essentially horizontal, so that vertical flow components can be neglected and that the slope of the water table surface is slight (< 5°). If we assume an incompressible fluid and full saturation, then our equation of continuity written in terms of Darcian velocities becomes:

$$\frac{\partial V_x}{\partial x} + \frac{\partial V_y}{\partial y} + \frac{\partial V_z}{\partial z} = 0 \qquad (6)$$

Since we wish to average in the z direction, we must integrate this equation from the base of the aquifer to the free surface or:

$$V_z \Big|_{z\,=\,0\,=\,\text{base of aquifer}}^{z\,=\,h} = V_z(h) = \frac{\partial V_x}{\partial x} + \frac{\partial V_y}{\partial y} \qquad (7)$$

Defining ϕ as the head in units of length, $\phi = P/\rho g + z$, the value of ϕ is equal to z at the free surface, since P = 0 at that point. Using this result along with the first Dupuit assumption and our earlier equation ($z = h(x, y, t)$), we have:

$$h(x, y, t) = \phi(x, t, \overline{z}, t) \qquad (8)$$

From this result Darcy's law can be rewritten as:

$$V_x = -\overline{K} \frac{\partial h}{\partial x} \qquad (9)$$

$$V_y = -\overline{K}\frac{\partial h}{\partial y} \tag{10}$$

where:

$K(x, y)$ = vertically averaged value of hydraulic conductivity at location (x, y)

Substituting Equations 9 and 10 into 5 we have:

$$n_e\frac{\partial h}{\partial t} - \overline{K}\left[\left(\frac{\partial h}{\partial x}\right)^2 + \left(\frac{\partial h}{\partial y}\right)^2\right] - V_z(h) = 0 \tag{11}$$

Now replacing $V_z(h)$ with the expression obtained from substituting the results of Equations 9 and 10 into Equation 11.

$$n_e\frac{\partial h}{\partial t} - \overline{K}\left[\left(\frac{\partial h}{\partial x}\right)^2 + \left(\frac{\partial h}{\partial y}\right)^2\right] - h\frac{\partial}{\partial x}\left[\left(\frac{\overline{K}\partial h}{\partial x}\right) + \frac{\partial}{\partial y}\left(\frac{\overline{K}\partial h}{\partial y}\right)\right] = 0 \tag{12}$$

Rearranging Equation 12 yields:

$$n_e\frac{\partial h}{\partial t} - \frac{\partial}{\partial x}\left(\frac{\overline{K}h\partial h}{\partial x}\right) - \frac{\partial}{\partial y}\left(\frac{\overline{K}h\partial h}{\partial y}\right) = 0 \tag{13}$$

or in gradient vector notation

$$n_e\frac{\partial h}{\partial t} - \nabla\cdot(\overline{K}h\nabla h) = 0 \tag{14}$$

Equation 13 is termed the Boussinesq equation. To this point for simplicity of development we did not include source terms and have assumed that the aquifer base elevation is the zero reference elevation. To expand Equations 13 or 14 to handle an aquifer with varying bottom elevation $h_b(x, y)$, and to include source/sink or accretion terms, we must do the following:

* assume that the bottom slope is slight, as we did for the free-surface slope;
* replace h in Equations 13 or 14, which was a result of integrating from z = 0 to z = h by $h-h_b$, since our integration is now done from $z = h_b$ to z = h;
* add the accretion term, N.

The resulting equation is the Boussinesq equation for unsteady flow:

$$\bar{n}_e \frac{h}{t} = \nabla \cdot \bar{K} (h-h_b) \nabla h + N \tag{15}$$

where:

$\bar{n}_e$ (x, y) = vertical average of the effective porosity of the aquifer (dimensionless)

h (x, y) = elevation of the free surface from some reference elevation (L)

h_b (x, y) = elevation of the aquifer bottom from the reference elevation (L)

N (x, y) = accretion rate (LT^{-1})

$\bar{K}$ (x, y) = vertically averaged value for hydraulic conductivity at point (x, y) (LT^{-1})

ASSUMPTIONS

The basic assumptions of the Boussinesq flow model for describing saturated unconfined flow are:

- Flow is by an incompressible fluid that saturates a rigid, porous soil matrix.
- Compressibility effects of the fluid and soil matrix can be neglected under conditions of unconfined or free-surface flow; however, they are incorporated into the storage term for confined flow.
- Hydraulic conductivity and effective porosity can be represented by the vertical average values and are isotropic but inhomogeneous throughout the region.
- The free-surface slope and the aquifer bottom slope are both assumed to be slight ($<5°$).
- Vertical velocities are assumed to be small and therefore can be neglected.
- Coefficient distributions and dependent variables are assumed continuous over the simulation region.
- Flow in the capillary fringe is neglected.
- Seepage surfaces cannot be handled and are therefore neglected.

The Boussinesq formulation as presented above allows one to approximate the elevation of the free surface in a single unconfined aquifer at every (x, y) location. Many times in a real system, one wishes to simulate a multi-aquifer system, in which one or more of the aquifers are confined, although these confined aquifers may be unconfined in some places. Also there may be transfer of water between the aquifers. This kind of a multi-aquifer system can be handled by a multi-aquifer set of Boussinesq equations with potential driven interaquifer tranfer or leakage terms. For a multilayered system the equations would be:

$$S^{i} \frac{\partial h^{i}}{\partial t} = \frac{\partial}{\partial x}\left(T^{i} \frac{\partial h^{i}}{\partial x}\right) + \frac{\partial}{\partial y}\left(T^{i} \frac{\partial h^{i}}{\partial y}\right) + N^{i} + \sum_{j=1}^{i-1} C_{j \to i} \left(h^{j} - h^{i}\right)$$

$$+ \sum_{j=i+1}^{n} C_{j \to i} \left(h^{j} - h^{i}\right) \tag{16}$$

where:

$i = 1, 2, \ldots n$

n = number of layers

$C_{i \to j} = C_{j \to i}$ = interaquifer transfer coefficient between layer i and j

$S^{i} = n_e^{i}$ for unconfined system or storage coefficient for the confined system

T^{i} = transmissivity for a confined system is K^{i} times the thickness of aquifer or $K^{i}(h^{i} - h_{i})$ for an unconfined or water table aquifer

N^{i} = the flux or stress term applied to layer i

As with any mathematical model there are specific data requirements, boundary conditions, and initial conditions which must be specified. Equation 16 as presented is the transient equation. When the left-hand side of Equation 16 is replaced by zero, the steady-state equation results. As mentioned previously, the transient equation allows one to investigate the effects of seasonal fluctuations and rates of change, whereas the steady-state equation allows one to investigate the ultimate effect of any water use policy. Use of the transient model requires that the storage coefficient distribution be known, whereas the steady-state model does not require this distribution.

SPECIFIC DATA REQUIREMENTS FOR THE PHYSICAL PARAMETERS

The following are the specific data requirements:

- Hydraulic conductivity ($K=k/\mu$, where k = intrinsic permeability and μ = fluid viscosity); transmissivity ($T=Kb$, where b = saturated thickness of the aquifer material).

  The Boussinesq flow model requires as an input the saturated hydraulic conductivity or transmissivity distribution throughout the region being modeled and for each aquifer being modeled. The values required by the Boussinesq model must represent the vertical average of the K or T of the saturated thickness of the aquifer.

  Hydraulic conductivity or transmissivity reflects the ability of the rock and soil matrix to allow water transmission. The K or T distribution is usually determined via appropriately conducted pumping tests, where the well is fully penetrating and perforated throughout saturated aquifer material. Data from these type of field measurements are expensive to obtain, and therefore the K or T distribution is extrapolated from a small number of these measurements. This initial distribution is further modified during the model calibration phase to obtain better agreement between model-predicted potentials and observed potentials. Hydraulic conductivity can also be estimated from laboratory studies of aquifer material samples, lithologic data and inverse mathematical modeling methods.

- Storage coefficient (or effective porosity n_e and vertical compressibility of the soil matrix [α]).

  The transient form of the Boussinesq equation requires the distribution of the vertical averaged value of the storage coefficient for each aquifer throughout the region being modeled. This parameter controls the rate at which the water and disturbances in the potential surface propogate throughout the groundwater system. In the case of an unconfined system, the storage coefficient is dominated by the effective porosity of the aquifers soil matrix.

Contributions to the storage coefficient based on soil matrix compressibility and water compressibility are ignored. In the case of confined systems, the storage is a function of the aquifer soil matrix compressibility (α), effective porosity (n_e), with storage = $\rho g(\alpha + n_e\beta)$.

Storage or effective porosity can be determined via pumping tests with observations wells, lithologic data from core samples, and laboratory or in situ measurement techniques. In addition, storage coefficients can be determined during model calibration when adequate transient data on potentials exist.

- Interaquifer transfer coefficients ($C_{j \to i}$)

  The multiaquifer Boussinesq Flow Model requires an interaquifer transfer coefficient, which is a measure of the hydraulic interconnection between aquifer systems. This value is a function of the thickness and hydraulic conductivity of the aquitard separating the aquifer systems. This value must be determined at each (x, y) location where an aquitard exists between the aquifers. This value arises naturally in the other three dimensional formulations in the form of (X,Y,Z) hydraulic conductivity distributions. It is generally obtained via model calibration of inverse modeling techniques.

INITIAL CONDITIONS

The Boussinesq flow model requires initial conditions. The Boussinesq flow model requires one average potential value for each aquifer for each (x, y) grid location throughtout the region being modeled.

BOUNDARY CONDITIONS

Like all mathematical models, the Boussinesq model requires that boundary conditions be specified. Boundary conditions are difficult to formulate and result from interpretations of potential data, well logs, and lithologic data. The physical extent of the aquifer and or aquifers are defined. This includes a geometrical description of the positions in space of the aquifer materials such as:

* the lateral boundaries of the aquifer or aquifer systems
* contour maps of the base and top of the aquifer or aquifer systems.

Along each of the lateral boundaries, the conditions which describe the physical situation which exists must be determined. These include:

* Lateral Flow Boundary

  This results from not extending the model to the geologic boundaries of the aquifer or aquifer systems. At these boundaries the rate that water is flowing into or out of the aquifer of aquifer system must be specified.

* No Flow Boundaries

  These occur when the model has been extended to the geologic boundaries of the aquifer where the aquifer materials and impermeable barriers meet.

* Held or Time Varying Potential Boundaries

  These occur at large lakes and rivers, where the saturated aquifer materials are in contact with large bodies of water whose water surface elevations are essentially unaffected by aquifer potentials.

RECHARGE - DISCHARGE LOCATIONS AND RATES

Typically when modeling an aquifer system which extends to the major recharge areas of the aquifer, the following types of data are used to estimate aquifer recharge:

- precipitation records
- surface slope
- temperature record
- surface soil types
- vegetation cover and land use
- evapotranspiration data.

Man-made recharge or discharge must also be accounted for by determining:

- location of pumping and recharge wells
- use of water and infiltration mechanisms (e.g., septic tanks, irrigation infiltrations, settling ponds).

Along flow boundaries where the area being modeled does not extend to geologic boundaries, the flow across this boundary must be determined via pump test and geologic studies conducted along this boundary.

Figure 1 illustrates graphically the phenomena which must be considered in calculating the distribution of aquifer stress values throughout the region being modeled.

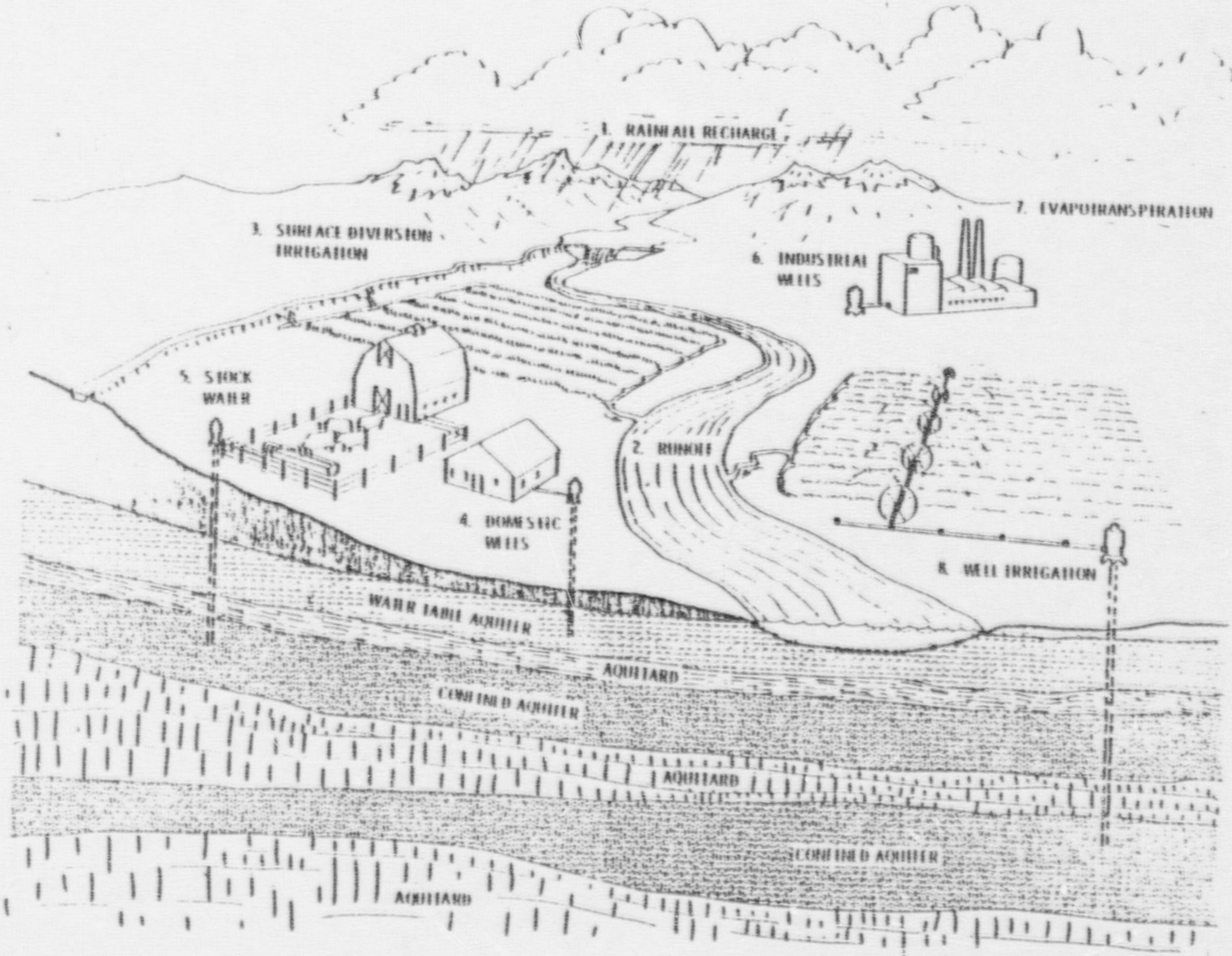

FIGURE 1. Nodal Recharge/Withdrawal Phenomena

NUMERICAL FORMULATION OF THE SYSTEM EQUATIONS

For numerical formulation, a horizontal x-y coordinate grid system was adopted with uniform nodal spacing. R represents the region of flow and r_{ij} the sub-area associated with node ij (Figure 2).

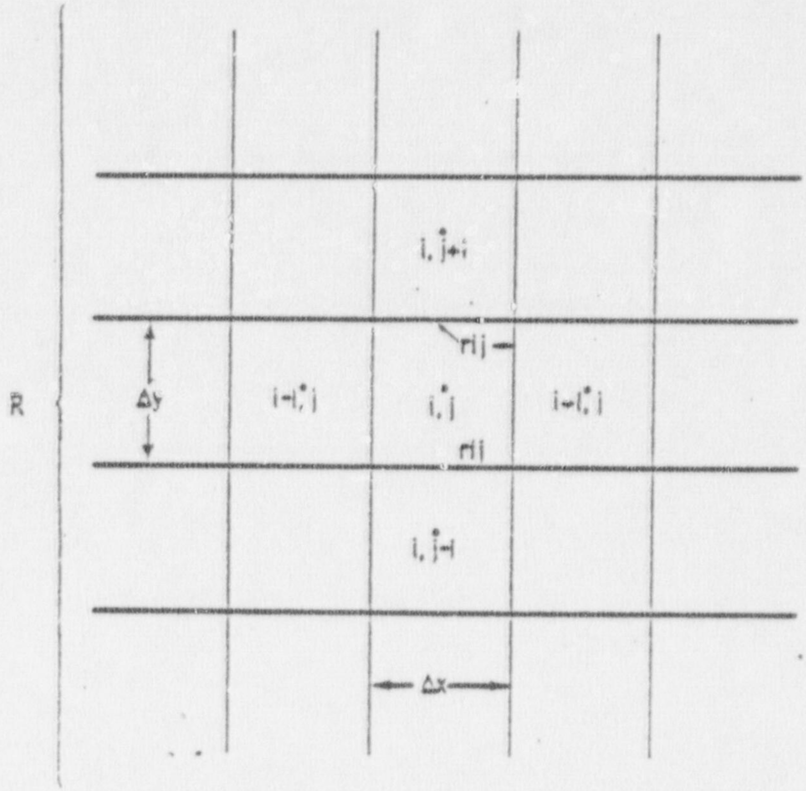

FIGURE 2. The Finite Difference Grid with the Nodal Numbering System

The differential equation, Equation 11, is then converted to finite difference form by integrating around the node area r_{ij}. Now:

$$\int_r \int_{ij} \left[\underline{\nabla} \cdot K(h - h^b)\underline{\nabla}h - \phi\frac{\partial h}{\partial t} + N \right] dxdy = 0 \qquad (17)$$

By Green's theorem in the first form (Kellogg 1954):

$$\int_r \int_{ij} \nabla \cdot K(h - h^b)\nabla h\,dx\,dy = \oint_{\Gamma_{ij}} K(h - h^b)\,\frac{\partial h}{\partial n}ds \tag{18}$$

where n denotes the outward pointing normal to the curve Γ which bounds the area r_{ij}. The line integral is taken in the anticlockwise direction. Using Equation 18, Equation 17 reduces to:

$$\oint_{\Gamma_{ij}} K(h - h^b)\,\frac{\partial h}{\partial n}ds - \int_r \int_{ij} (n_e\frac{\partial h}{\partial t} - N)\,dx\,dy = 0 \tag{19}$$

In Figure 2 the corner points of the node area are at (i-1/2, j-1/2), (i+1/2, j-1/2), (i+1/2, j+1/2), and (i-1/2, j+1/2). The area of r_{ij} is $\Delta x\Delta y$. The integrals of Equation 19 are approximated as follows, with the integral along Γ_{ij} divided into the integrals along the four sides of r_{ij}:

$$\int_{i-1/2,\ j-1/2}^{i+1/2,\ j-1/2} K(h - h^b)\frac{\partial h}{\partial n}dx = (K\Delta h)_{i,j-1/2}\ \frac{h_{ij} - h_{i,j-1}}{-\Delta y}\ \Delta x \tag{20a}$$

$$\int_{i+1/2,\ j-1/2}^{i+1/2,\ j+1/2} K(h - h^b)\frac{\partial h}{\partial n}dy = (K\Delta h)_{i+1/2,\ j}\ \frac{h_{i+1,\ j} - h_{ij}}{\Delta x}\ \Delta y \tag{20b}$$

$$\int_{i+1/2,\ j+1/2}^{i-1/2,\ j+1/2} K(h - h^b)\ \frac{\partial h}{\partial n}dx = (K\Delta h)_{i,\ j+1/2}\ \frac{h_{i,\ j+1} - h_{ij}}{\Delta y}\ \Delta x \tag{20c}$$

$$\int_{i-1/2,\ j+1/2}^{i-1/2,\ j-1/2} K(h - h^b)\frac{\partial h}{\partial n}dy = (K\Delta h)_{i-1/2,\ j}\ \frac{h_{ij} - h_{i-1,j}}{-\Delta x}\ \Delta y \tag{20d}$$

$$\int_r \int_{ij} (+n_e\frac{\partial h}{\partial t} - N)\,dx\,dy = n_{eij}\ \frac{h_{ij}^k - h_{ij}^{k-1}}{\Delta t}\ \Delta x\Delta y - N_{ij}\Delta x\Delta y \tag{20e}$$

where the superscript k denotes the iteration number and where the $K\Delta h$ half way between node center in the j-1 direction is

$$(K\Delta h)_{i,j-1/2} = 1/2[K_{ij}(h_{ij}^{k} - h_{ij}^{b}) + K_{i,j-1}\ (h_{i,j-1}^{k} - h_{ij}^{b})],$$

A fully implicit representation of the time derivative has been used in Equation (20e). Combining the above approximations results in the finite difference approximation to the Boussinesq equation for a square grid system, $\Delta x = \Delta y$:

$$-(K\Delta h)_{i-1/2,j}\ h_{i-1,j}^{k} + \Big[(K\Delta h)_{i-1/2,j}+(K\Delta h)_{i+1/2,j}+(K\Delta h)_{i,j-1/2}$$

$$+(K\Delta h)_{i,j+1/2}+n_{e_{ij}}\frac{(\Delta x)^2}{\Delta t}\Big]\,h_{ij}^{k}-(K\Delta h)_{i+1/2,j}\ h_{i+1,j}^{k}$$

$$= (K\Delta h)_{i,j-1/2}\ h_{i,j-1}^{k}+(K\Delta h)_{i,j+1/2}\ h_{i,j+1}^{k}+n_{e_{ij}}\ \frac{(\Delta x)^2}{\Delta t}\ h_{ij}^{k-1}+N_{ij}^{k-1}\ (\Delta x)^2 \quad . \qquad (21)$$

For node on boundaries along which the hydraulic potential is specified in time and space (and therefore no calculation is needed):

$$h_{ij}^{k} = H_{ij}^{k}$$

The impermeable boundaries of the region must be approximated in the grid system by shapes selected from Figure 3. This avoids right angles which cause stagnation points and singularities in the mathematical solution of the ground-water flow equation.

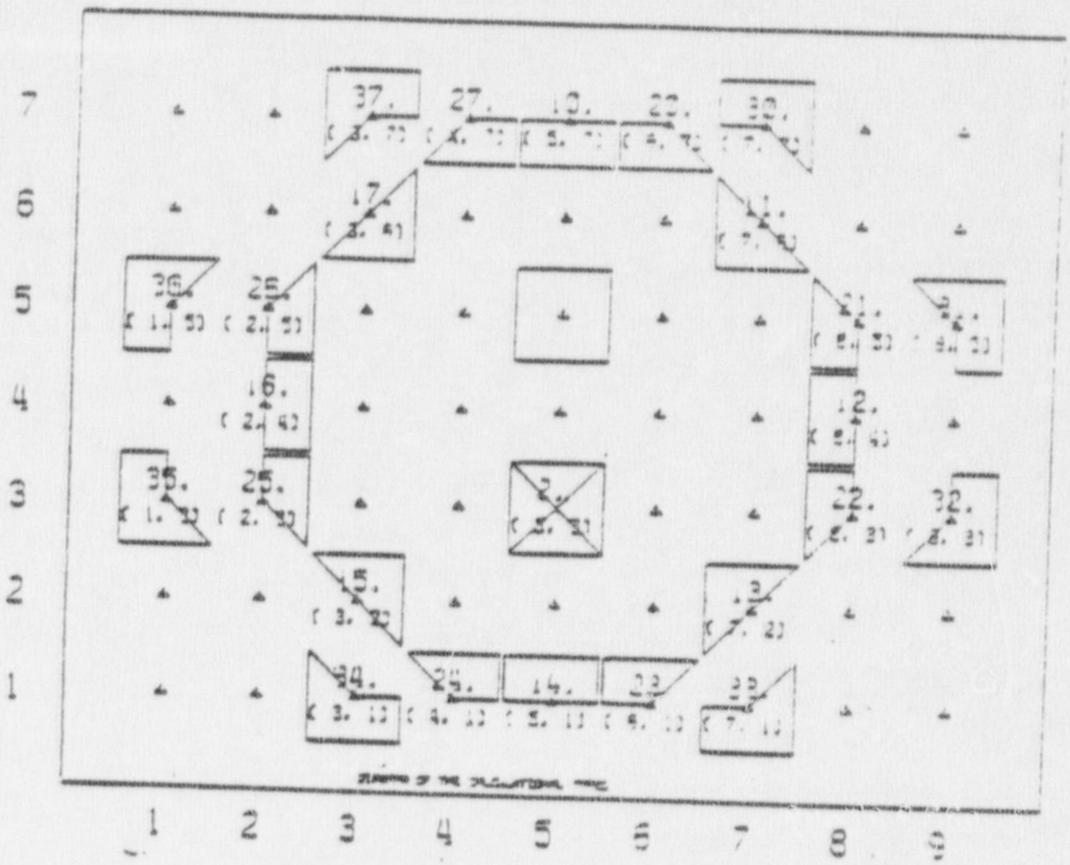

FIGURE 3. Schematic Showing Shapes and Rotation of Available Boundary Condition Types

The boundary conditions are put into finite difference form by applying the technique described above to a node area at the boundary of the region R. The boundary types are illustrated in Figure 3. The associated nodal area r_{ij} can be either inside or outside the octagon. The finite difference equations are derived by setting the appropriate portions of the integral on Γ_{ij} in Equation (18) to zero when the segment is impermeable, and by inputting $N_{ij} = N_{ij}n$ when the flux across the segment is specified. In finite difference form, 24 different equations correspond to each of the different boundary point subregions illustrated in Figure 3. Either a specified flux or no flow can be imposed by each of the 24 equations. The accretion term, whether infiltration or withdrawal, in finite difference form becomes $N_{ij} = q_{ij}(\Delta x)^2$ (units L^3/T) to be specified at each node. Accretion at the fractional boundary nodes must have the nodal area properly reduced from $(\Delta x)^2$.

The partial differential equation and boundary conditions subsequently become a set of $\hat{N}$ finite difference equations, one for each node of the region R being modeled. The boundary conditions have been effectively absorbed into the equations for their respective boundary nodes.

It should be noted that the finite difference equations can be derived in the same form by other techniques, such as Taylor series expansion. The equations for nodes on impermeable boundaries are equivalent to those obtained by introduction of a point external to the region for purposes of forming the normal derivative.

Boundary Definitions

To simulate the system, a model depends on segmenting the physical continuum into a discrete grid. Each grid segment is then represented by a single node within the model. The VTT Model uses a finite difference algorithm with a uniform grid and requires that each node within the Cartesian coordinate system be marked with a calculation type as:

- within the aquifer
- external to the aquifer
- a water or held potential boundary node [$h = H(x,y,t)$]
- an impermeable boundary for the aquifer with $q = 0$ (aquifer boundary nodes, where the flux is known, are treated as the mathematical equivalent to an impermeable boundary node with the appropriate accretion term; i.e., $q \neq 0$).

To facilitate the marking of calculational boundary types to avoid right angles along no-flow boundaries, and to simplify representation of complex boundaries, a systematic method of representing interior, exterior, and boundary nodes was adopted. Figure 3 illustrates the different kinds of nodal types used in the VTT code. There are basically four nodal types; others simply arise to handle the various shapes and orientations of the impermeable boundaries.

is a water boundary, i.e., held potential boundary node $h = H(x,y,t)$.

is an external node outside of the aquifer.

is an internal or nonboundary node which lies within the aquifer.

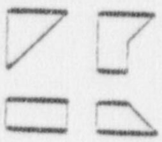

these basic shapes with all their possible rotations are used to represent the 24 kinds and shapes of impermeable boundary nodes.

Solution Techniques

Three different solution techniques were selected to solve essentially the same set of equations, thus, resulting in three separate versions of the same model. Each of these is designed for use in specific problems. These will be described in general to avoid lengthy mathematical discussions.

The VTT version of the model solves the transient form of the system of finite different equations by using the successive line overrelaxation technique. For transient problems the solution is stable and convergent with sufficient speed to make solution of large matrices practical.

The VTTSS3 version of the model solves the steady-state system of finite difference equations resulting from the integration of Equation (17) when the transient term $n_e \frac{\partial h}{\partial t}$ is set to zero. This set of equations is solved by using a Newton iteration technique (Kellogg 1954). This version is primarily used for a system of aquifers in which one is unconfined and, therefore, the equations are nonlinear. Convergence of this method is quadratic in nature and for most ground water problems the solution is reached in four to five iterations.

The VTTSSZ version of the model solves the same system of steady-state equations discussed in the preceding paragraph, except that it uses a Colesky decomposition method (Kellogg 1954). This version if used when all the aquifers being simulated are confined. This method is many times faster than the Newton version, and since the system of equations will be linear, no iteration is required.

REFERENCES

1. Bear, Jacob. 1972. Dynamics of Fluids in Porous Media. American Elsevier: New York Publishing Co. Inc.

2. Kellogg, O. D. 1954. Foundations of Potential Theory. Dover: New York.

3. Acton, Forman, S. 1970. Numerical Methods that Work. Harper and Row: New York.

DRAFT

To: BWIP & DOE Hydrology Task Group and related investigators.

From: University of Arizona Subcontractor to Rockwell,
Hanford Operations.

Date: 6/25/87

Re: PROPOSAL FOR THE STUDY OF PRESSURE DISTURBANCE PROPAGATION THROUGH SUBSURFACE HYDROSTRATIGRAPHIC UNITS

PROPOSAL SUMMARY

The investigation here proposed explores the effects of surface pressure disturbances on the baseline potentiometric surface as expressed by existing monitoring wells at the Hanford BWIP site, Richland, Washington. The goal is to predict the possible magnitude of a disturbance caused by exploratory shaft drilling, and subsequently determine if LHS test interpretations are impacted. As is discussed, the aformentioned goal can be realized through the study of the attenuation of barometric pressure disturbances as they propagate through subsurface hydrostratigraphic units.

A relatively simple experiment is outlined which if conducted, will provide the essential information towards solving this problem. The experimental methodology, data analysis, and specific data requirements are all brought forth.

In the consideration of time constraints in conducting the investigation, computational tools for the data analysis already exist and are not the limiting factor. However, data requirements include time intervals which run against current deadlines, and thus expediency in initiating data acquisition is highly recommended.

Introduction

The investigation here proposed is motivated by the desire to understand and predict the effects of surface pressure disturbances, in particular the drilling of an exploratory shaft, on the baseline potentiometric surface as expressed by existing monitoring wells, at the Hanford BWIP site, Richland, Washington. The concern is that the disturbance of the baseline would interfere with the interpretation of LHS testing. Should it prove possible to begin drilling the shaft without significantly affecting the water levels in the monitoring wells, then the drilling phase should not need to be delayed any further. Thus, the goal of this study is to compute the possible magnitude of the expected drilling disturbance.

The scope of this proposal is to outline the recommended procedure for the investigation. It is proposed that the aformentioned goal can be realized through the study of the attenuation of barometric pressure disturbances as they propagate through subsurface hydrostratigraphic units. The proposed investigative methodology, analysis and data requirements are presented.

Methodology

If the drilling disturbance were uniformly distributed over the entire area of interest we might simply use the known tidal efficiency of the formation to compute the corresponding well disturbance. However this is not the case, since the disturbance is not so widely distributed. Thus in order to estimate such magnitudes, certain alternative information must be known.

This information includes 1) the magnitude of the surficial disturbance and the area over which its force is applied, 2) the increase in the total stress at any given point of interest within a given formation of interest, and 3) the percentage of the stress increase which will be realized by the formation pore pressure. Thus, with the knowledge of the response in pore fluid pressure due to the surface disturbance, the gradient between a point within the well and formation are known and the corresponding change in water level can be predicted, and the information necessary in the attempt to predict the impact of exploratory shaft drilling on LHS ~~test~~ interpretation is gained.

The information under (1) above can be estimated. The information under (2) above can be computed from equations existing in the soil mechanics literature (Scott and Shoustra, 1968). However, the information under (3) above is dependent upon the compressible properties of the fluid and formation matrix of interest. Fortunately, we only need know the ratio of the compressabilities, and an easily conducted experiment to measure them is discussed below.

The increase in pore fluid pressure due to an increase in total stress within the formation is given (Narisimhan et al., 1984, Scott and Shoustra, 1968) by:

$$\delta P_f = \delta \sigma_T \frac{1}{1 + (\phi C_w / C_m)}$$

where: δP_f = change in formation fluid pressure
$\delta \sigma_T$ = " " total stress
C_w = compressibility of water
C_e = " " matrix
ϕ = porosity
$\phi C_w/C_e$ = ratio of compressibilities

Thus, for an observed ratio of δP_f to $\delta \sigma_T$ the compressibility ratio can be computed, and thus the pore pressure response to any given change in total stress is computable.

Fortunately, to conduct the experiment needed to obtain this information, nature provides a continually changing surface pressure disturbance expressed in the barometric record. It should be possible to take advantage of this natural phenomena within the scope of the proposed investigation, and obtain all of the aformentioned informational needs with relative ease.

The barometric time series is easily monitored at the surface within the study area. Since it is a distributed pressure source, the increase in total formational stress given some arbitrary change in barometric pressure is known. Then, by simply monitoring a well shut in to monitor formation pressure, the percentage of the total stress borne by pore water pressure is observable.

Analysis

Subsequently, translating the two time series of 1) surface barometric pressure and 2) formation pressure from the shut-in well into a ratio of the amplitudes of the respective signals is similar to the concept of computing a barometric efficiency, although now formation pressure is being considered instead of water level fluctuations. Recent work at the University of

Arizona has examined barometric efficiency computations, and suggests that where amplitude ratios are to be examined critically, a frequency based approach will allow for the consideration of phase lag phenomena which might affect the results. Thus, such an approach is here recommended.

Note that through this analysis, information is gained only regarding the formation in which the experiment is conducted, and the results are not general across the verticum of formations. Thus, the experiment must be conducted in the Priest Rapids if this is indeed the formation upon which the DOE wishes to conduct its drilling test predictions.

Proposed Data Needs

To begin the investigation as proposed, the following data needs are outlined:

1) The data should include I) atmospheric pressure, II) formation pressure from a shut in well, and III) water level (or pressure) fluctuations from a well open to the atmosphere that is relatively close to the shut in well (the wells should be located together within the region in which the formation can be considered relatively uniform).

2) Initially, the data should include a minimum of 30 days of observations with an hourly-spaced frequency from each of the above three. Since this need may run into future deadlines, it is suggested that the first 15 days of data be collected at minute spaced intervals if possible for immediate analysis. Subsequent data can be collected hourly. To reach conclusions

that can be considered statistically significant, data should be continually collected into the future until such time as it is demonstrated that data acquisition is no longer of value in the investigation.

References

Narasimhan, T.N., B.Y. Kanehiro, and P.A. Witherspoon, 1984, "Interpretation of earth tic. esponse of three deep, confined aquifers," Journl Geophs Res, 83(B3), 1913-1924

Scott, R.F., and J.J. Schoustra, 1986, SOIL: Mechanics and Engineering, McG-w-Hill, p.59-69

Effects of River Stage Variations on
Water Levels in Well DC-15

Alan S. Cuddy
June 19, 1987

Introduction.

Drilling of the exploratory shafts in the Hanford and Ringoid sediments may cause water level disturbances in wells monitoring the Grande Ronde basalts, thus complicating the analysis of the LHS test data. Stage variations of the Columbia river are suggested as a possible analog to shaft drilling operations. The disturbance of water levels in the wells may result either from downward leakage or surface loading from drilling fluids. This report examines the effects of river stage variations on water levels in well DC-15.

Method.

Well DC-15 was chosen for this analysis for several reasons.

1. It is the only well in the Hanford reservation which lies close to the Columbia river and monitors the Grande Ronde (Figure 1). It is unlikely to be isolated from the river by hydrologic barriers.

2. It lies far away from recent drilling activities and is less likely than other wells to be affected by drilling disturbances.

3. It was drilled earlier than other wells which monitor the Grande Ronde and is less likely than other wells to show recovery effects from its construction.

4. The top of the Grande Ronde in DC-15 lies 2118 feet below the surface (Cross, 1983). This is similar to the depth of the Grande Ronde ~~in~~ at the shaft site where it lies roughly 2687 feet below the surface (as seen in RRL-2).

Figure 2 shows a hydrograph for DC-15. The hydrograph is based on weekly readings with a steel tape. The water levels in the well show a linear increase with time as well as smaller fluctuations which may be due to any combination of variations in barometric pressure, river stage, nearby well drilling or testing, irrigation, and other unknown causes.

In order to evaluate the relationship between river stage and water levels in DC-15, the effects of the linear trend and barometric fluctuations were subtracted from the water levels leaving a residual water level which is a function of all remaining unaccounted factors including the effects of river stage variation. The residual was calculated with a program (THEIS) developed by Ross Wolford and Rick Nevulis at the

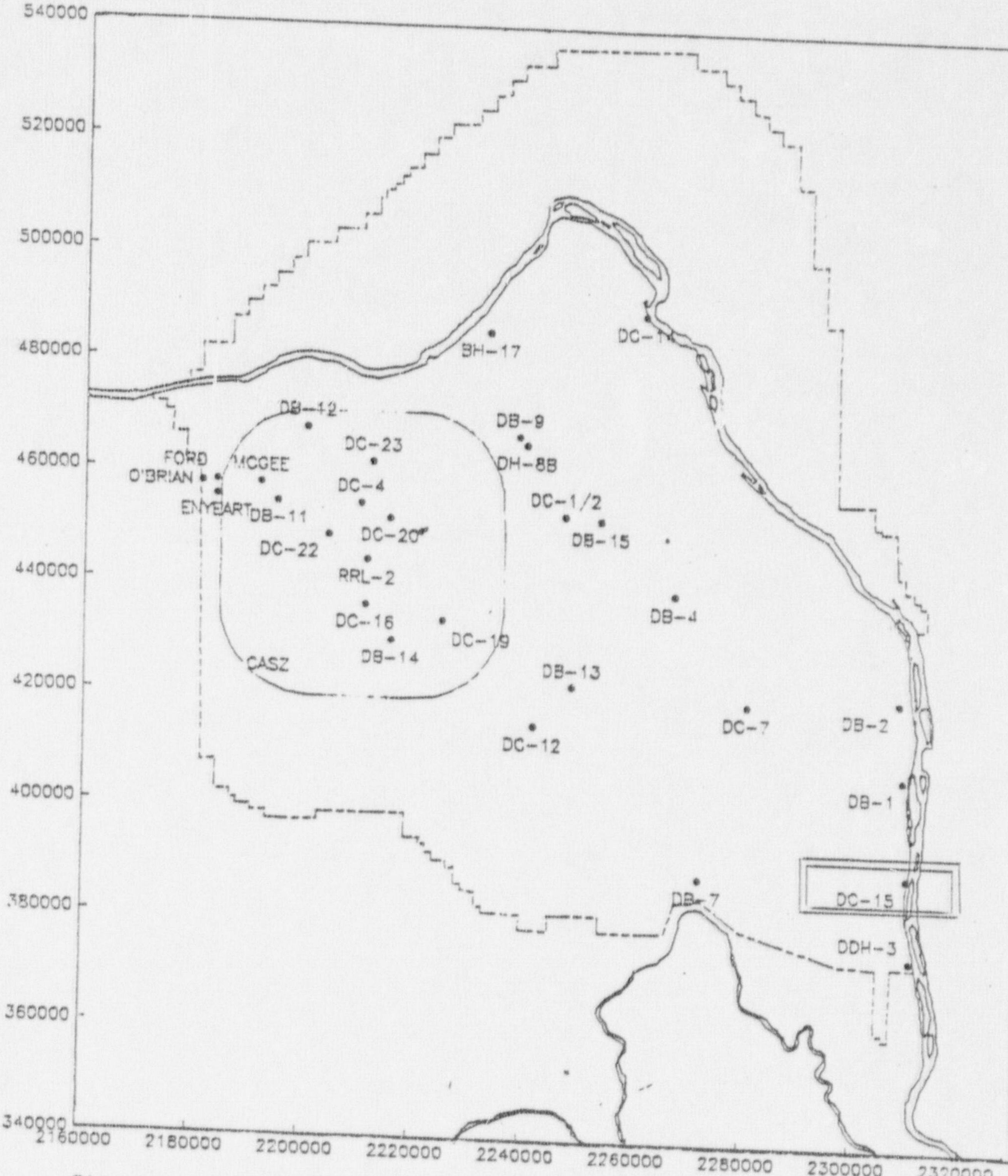

Figure 1. Map of well locations showing DC-15.

BOREHOLE NUMBER: DC−15
HYDROGEOLOGIC UNIT: COMPOSITE GRANDE RONDE

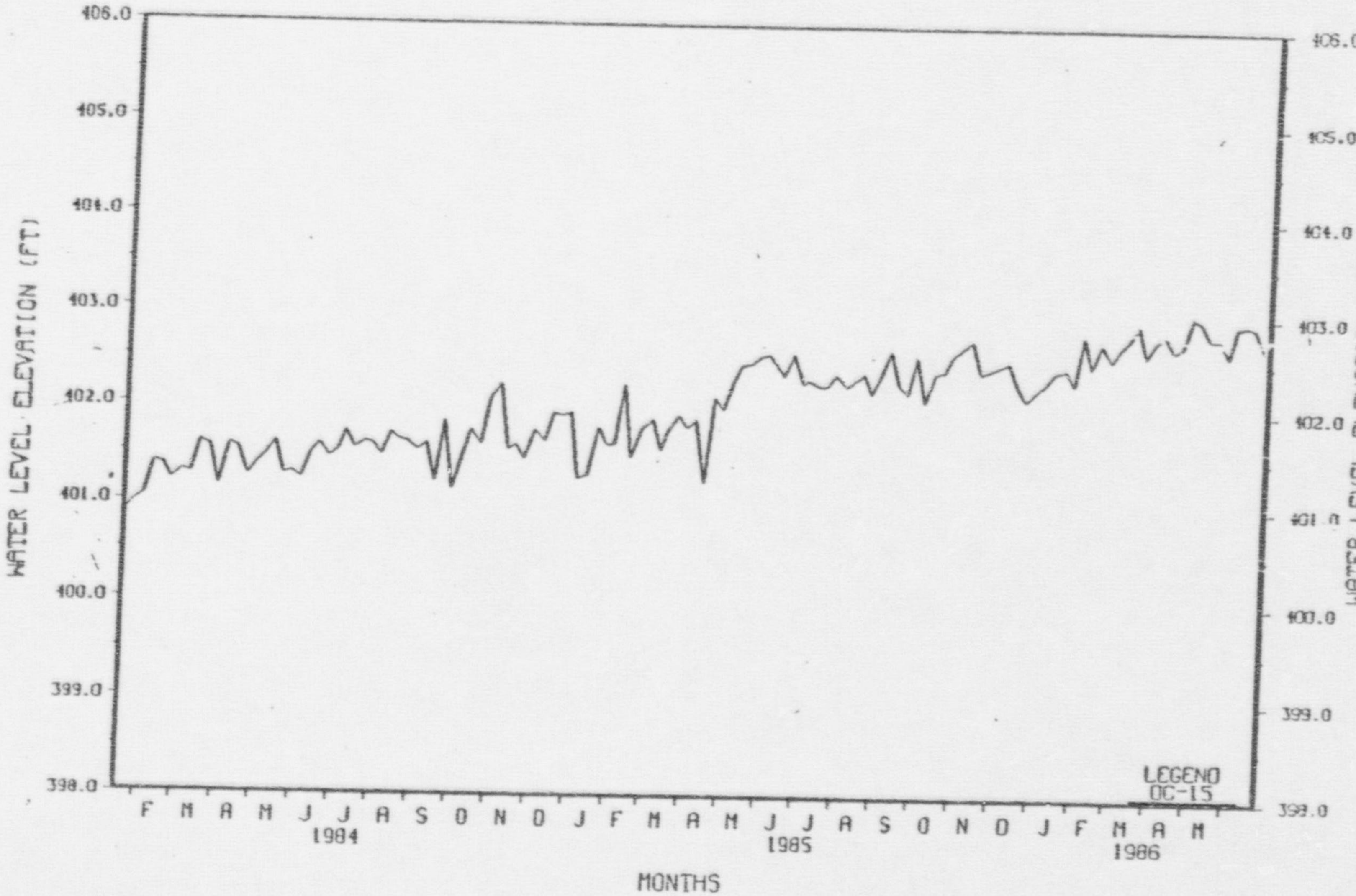

Water levels are unadjusted for atmospheric pressure.

Department of Hydrology at the University of Arizona. The program estimates barometric efficiency and a regression line for the data and subtracts a predicted water level from the observed water level to give a residual water level. These residuals are plotted in Figure 3.

The river stage data were collected every two hours. This stage data showed high variability and were smoothed before correlating by averaging the data over a seven day period. Figure 4 shows a plot of the river stage with time. The plot shows a yearly cycle in the river stage with high stages corresponding to the spring runoff. These yearly cycles have large amplitude and a low frequency and for these reasons would be more strongly propagated through the basalt than the other fluctuations in the river.

Correlations were calculated between the river and the water level residuals with lags ranging from 0 to 26 weeks in 1-week increments. The lagging of the data during the correlation calculations determines if the river effects are delayed while traveling to the well. The correlations were calculated with a program written by Rick Nevulis at the Department of Hydrology at the University of Arizona. A correlogram is shown in Figure 5. The plot shows that the highest correlation of roughly 0.4 occurs at a lag of 0. The correlation of 0.4 is not high but is significantly different from zero at the 5% level indicating that the river does have an effect on the water levels in DC-15. The highest correlation occurrs at zero lag and indicates that the effect is propagated instantaneously and therefore is a result of loading rather than downward leakage.

Conclusions.

Two conclusions can be drawn from this study.

1. The river stage flucuations have a small but significant effect on the water levels in the Grande Ronde basalt in DC-15.

2. The effect of the river is a result of surface loading rather than leakage.

Additional work related to this study is recommended and includes:

1. Conduct similar analyses for wells DDH-3, DC-7, DB-1, DB-2, and BH-17 which lie near the river and monitor the Wanapum and Grande Ronde basalts.

2. Conduct a regression analysis on the well residuals as a function of river stage to determine the magnitude of the effect of a unit change in river stage on the water levels.

3. Check the analysis by calculating barometric efficiencies

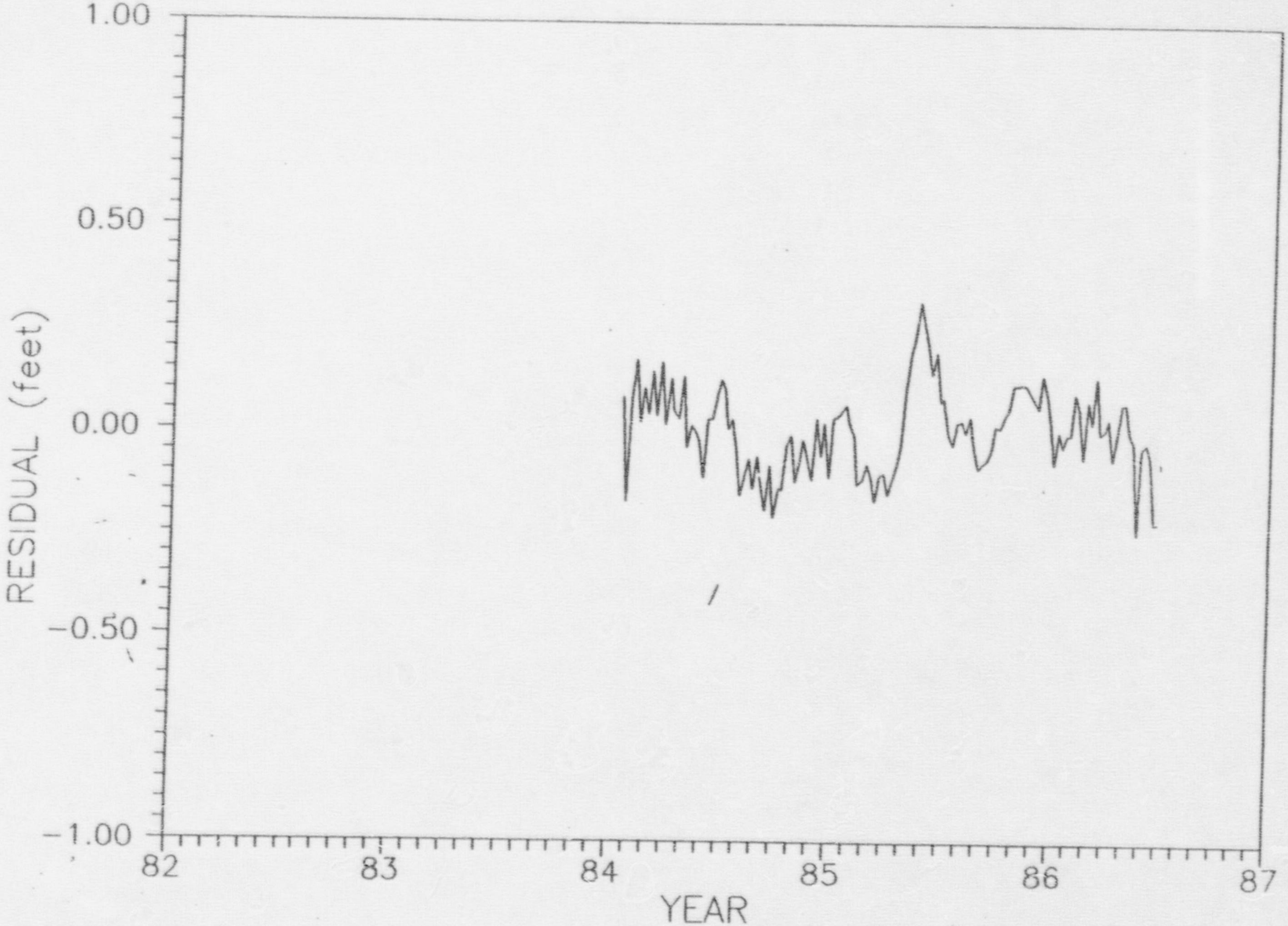

Figure 3. DC-15 residuals after removing linear trend and barometric effects.

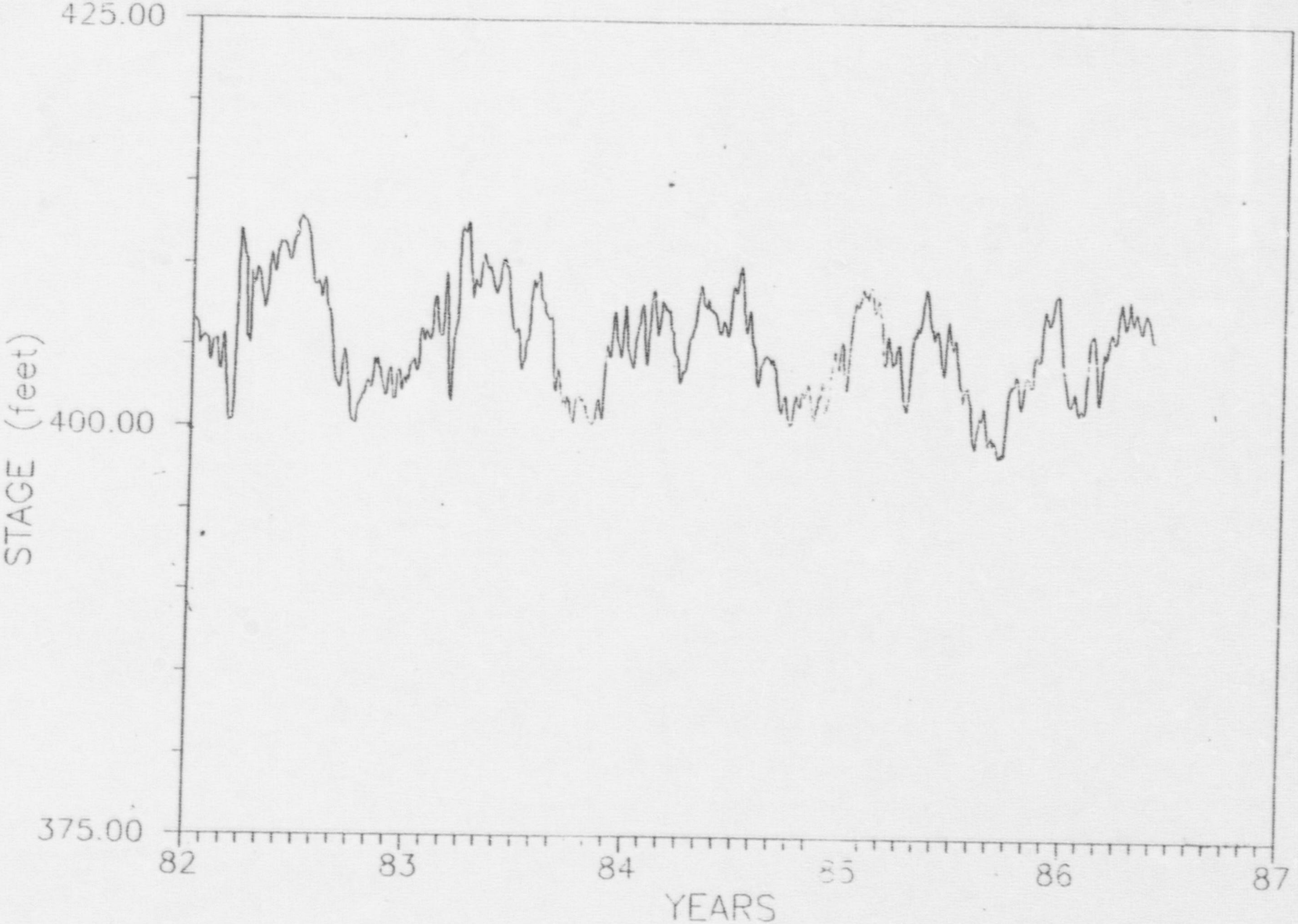

Figure 4. River stage vs. time

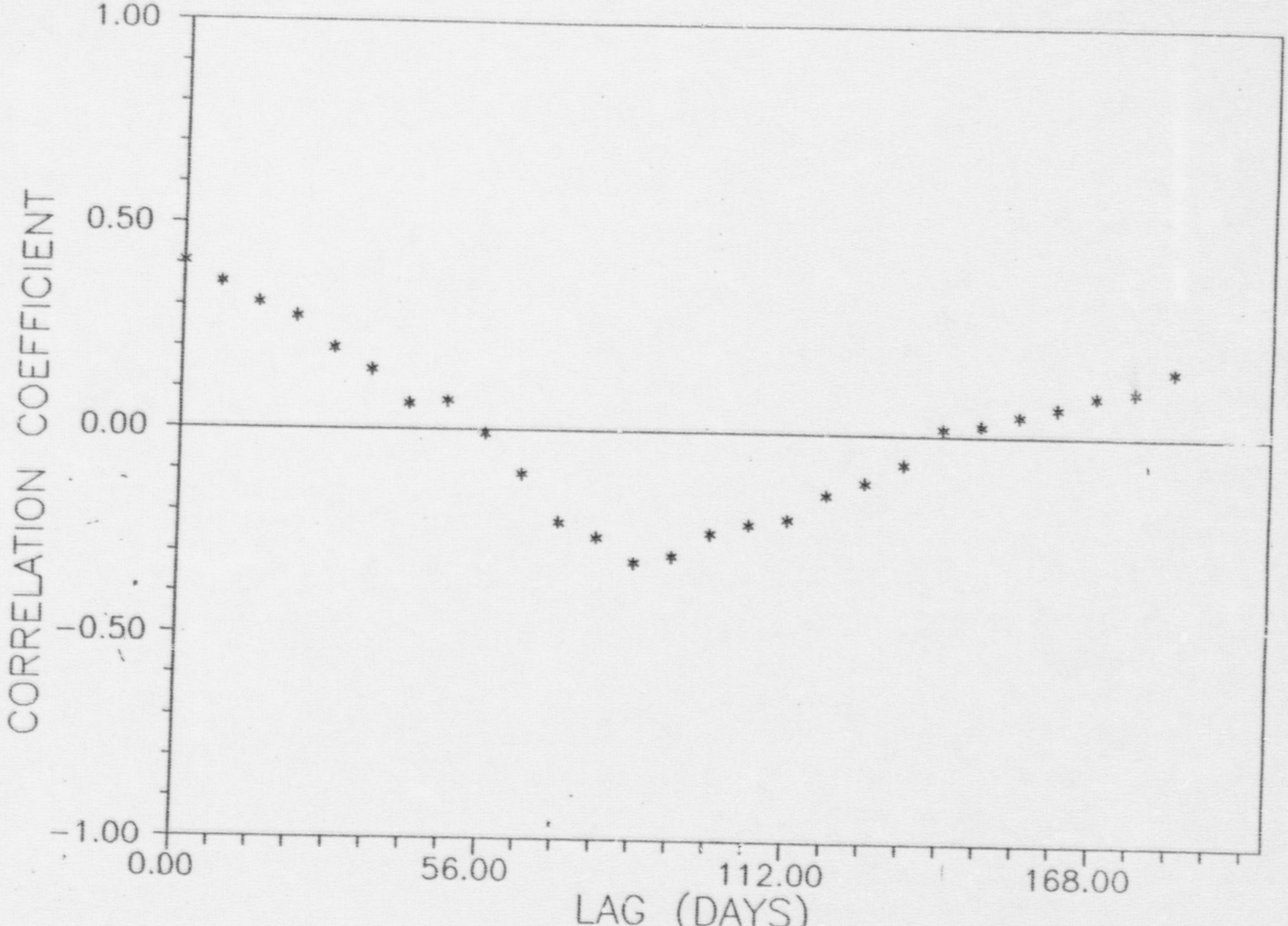

Figure 5. Correlogram of water levels in DC-15 and river stage.

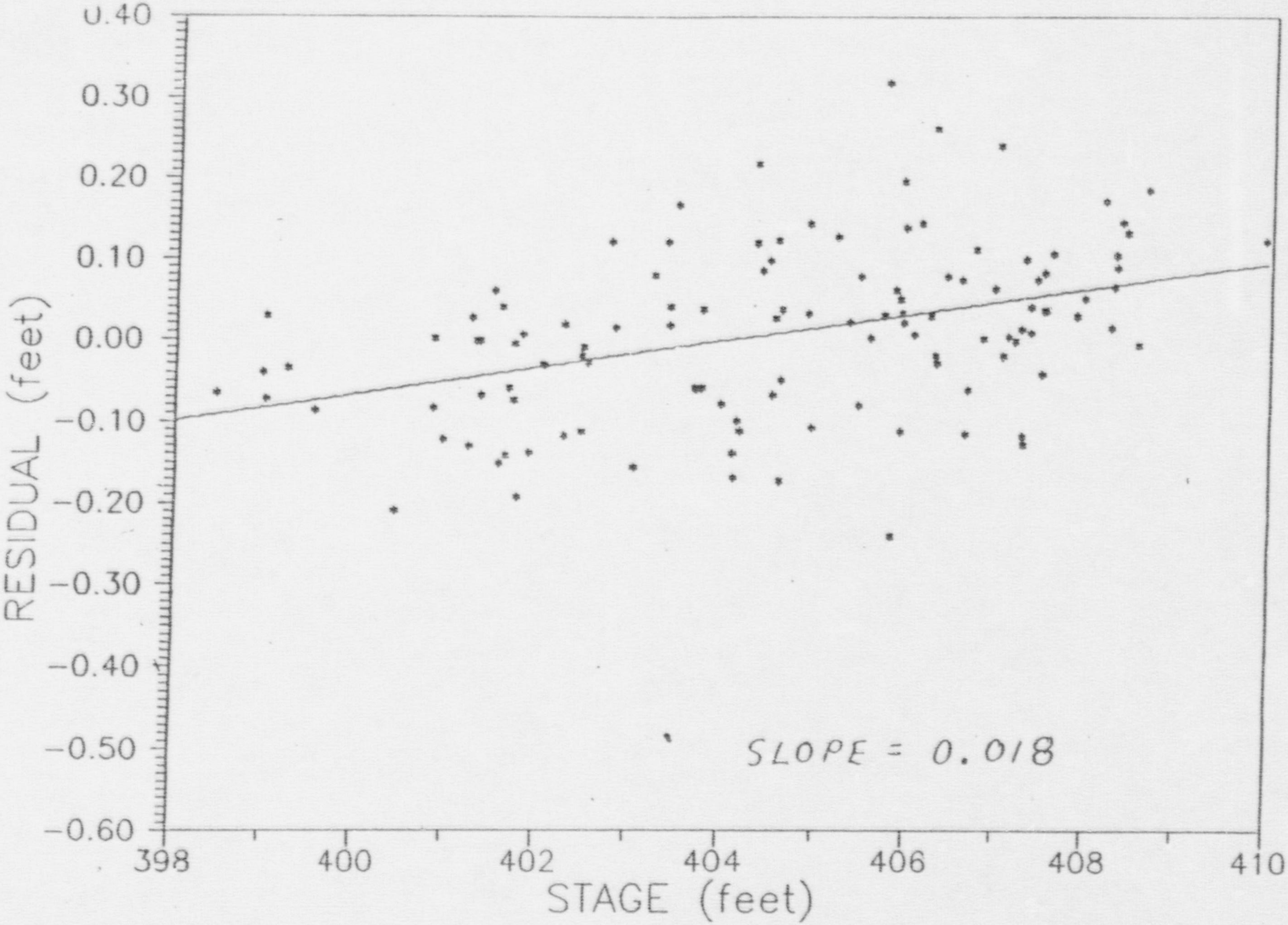

Scattergram of DC-15 residual vs. river stage.

Task 02

Drilling effects ~~at~~ of DC-23

Analysis of effects of conventional mud rotary drilling on groundwater levels in the suprabasalt and basalt sequence for DC-19, DC-20,22,23 and RRL-2 at the particular well site and other well sites.

Fluid loss for DC-19A, 19C, 19D; DC-20A, 20B, 20C, 20D; DC-22A, 22B, 22C, 22D; RRL-2B, 2C, and DC-23W was tabulated using information retrieved from the daily drilling reports for each well. The drilling footage where fluid loss occurred as well as the amount of the loss in barrels, total of loss for each lost circulation zone in barrels and gallons, and any comments dealing with the loss is given on each sheet.

When drilling basalt with the aerated mud method, lost circulation was reported as percentage estimates of total fluid returns instead of total barrels lost.

Drilling effects of DC-23 on the piezometer monitoring network was evaluated by F.A. Spane in the document SD-BWI-TI-313, "Preliminary Evaluation of the Effects of Construction Activities at DC-23W on Base-Line Monitoring at Selected Reference Repository Location Piezometer Installations". Drilling effects of DC-19,DC-20, DC-22 and the RRL-2 series on the piezometer monitoring network can be recovered from hydrograph charts which are stored in Basalt Records Management Center. Retrieval and analysis of this data is not possible because of my previous work commitments.

DRILL HOLE	LOST CIRCULATION FOOTAGE	BARRELS LOST	TOTAL LOST BARRELS/GALS	COMMENTS
DC-15A			-	NO LOST CIRCULATION REPORTED IN THE SUPRABASALT SEDIMENT
				START DRILLING BASALTS
	549-559	95%		95% CIRCULATION WHILE CORING.
	559-574			
	574-584			
	584-604			NO ESTIMATES OF FLUID LOSS GIVEN IN DAILY REPORTS
	604-614			
	624-633			
	633-638			
	638-641			
	641-659			
	683-704	90%		85% TO 95% CIRCULATION WHILE CORING
	718-735	95%		
	735-757	95%		NO ESTIMATES OF FLUID LOSS GIVEN IN DAILY REPORTS
	763-764	85%		
	764-784	95%		
	784-804	95%		

DRILL HOLE	LOST CIRCULATION FOOTAGE	BARRELS LOST	TOTAL LOST BARRELS/GALS	COMMENTS
DC-19C	229-240	160		NO LOST CIRCULATION REPORTED IN THE SUPRABASAL SEDIMENTS
	240-302	355		
	302-302	103	-	PUMPED SIX PILLS OF LOST CIRCULATION MATERIAL
		150		
		154		
		152		
		165		
		420		
	302-318	180		
	318-472	190	2029/85218	
	887-910	80	80/3360	START DRILLING BASALT WITH AERATED METHOD
	2022-2032			
	2168			DEPTH GIVEN WHERE LOST CIRCULATION OCCURRED. NO ESTIMATES OF FLUID LOSS GIVEN IN DAILY REPORT
	2363-2366			
	2559			
	3225			
	3434			
	3701			
	3834-3841			
	3841-3849			
	3882			
	3968			
	3983			

DRILL HOLE	LOST CIRCULATION FOOTAGE	BARRELS LOST	TOTAL LOST BARRELS/GALS	COMMENTS
DC-19D			-	NO LOST CIRCULATION REPORTED IN THE SUPRABASAL SEDIMENTS NO LOST CIRCULATION REPORTED IN THE BASALT DURI AERATED DRILLING

DRILL HOLE	LOST CIRCULATION FOOTAGE	BARRELS LOST	TOTAL LOST BARRELS/GALS	COMMENTS
DC-20A				
				NO LOST CIRCULATION REPORTED WHILE DRILLING THE SUPRABASALT SEDIMENTS
	564-584	75%		START CORING BASALTS
	584-604	80%		NO ESTIMATES OF FLUID LOSS GIVEN IN DAILY REPORTS
	604-634	80%		
	634-659	80%		
	659-684	85%		
	694-699	85%		
	699-724	90%		
	724-744	95%		
	744-751			TWISTED OFF AT 751 FT. PULL OUT OF HOLE. HOLE BRIDGED AT 640FT, LOST ALL CIRCULATION ATTEMPTING
	640-755			TO DRILL BRIDGE. REGAINED 50% CIRCULATION DRILLING OUT BRIDGE

DRILL HOLE	LOST CIRCULATION FOOTAGE	BARRELS LOST	TOTAL LOST BARRELS/GALS	COMMENTS
DC-20B				NO LOST CIRCULATION REPORTED WHILE DRILLING THE SUPRABASALT SEDIMENTS
	1573-1625			LOST CIRCULATION WITH NO TOTAL OF FLUID LOSS REPORTED IN THE DAILY REPORT

DRILL HOLE	LOST CIRCULATION FOOTAGE	BARRELS LOST	TOTAL LOST BARRELS/GALS	COMMENTS
DC-2?C	253-320 320-327	300 ?	300/12600	FLUID LOSS WITHIN THE SUPRABASALT SEDIMENTS
				START DRILLING BASALT AT 530 FT
	567-608			LOST APPOXIMATELY 40 TO 50 BBLS PER/HR FROM 586 TO 608 FT.
	608-719	75 80	155/6510	LOST 75 BBLS AT 615 FT, LOST 80 BBLS AT 627 FT
				START AIR DRILLING AT 1511 FT.
	2143-2251			LOST CIRCULATION AT 2197 FT, AMOUNT OF LOSS NOT GIVEN
	3137-3189			LOST CIRCULATION AT 3158 FT, AMOUNT NOT GIVEN
	3418-3451			LOST CIRCULATION, AMOUNT NOT GIVEN
	3480-3526			LOST CIRCULATION, AMOUNT NOT GIVEN

DRILL HOLE	LOST CIRCULATION FOOTAGE	BARRELS LOST	TOTAL LOST BARRELS/GALS	COMMENTS
DC-20D	280-350			LOST CIRCULATION AT 350 FT, AMOUNT OF LOSS NOT GIVEN STARTED DRILLING BASALT AT 531 FT NO REPORTED LOST CIRCULATION WHILE DRILLING BASALT

DRILL HOLE	LOST CIRCULATION FOOTAGE	BARRELS LOST	TOTAL LOST BARRELS/GALS	COMMENTS
DC-22A			-	NO REPORTED LOST CIRCULATION IN THE SUPRABASALT SEDIMENTS
				START DRILLING BASALT AT 662 FT
	691-714	95%		
	714-744	95%		START CORING BASALT, AMOUNT OF LOST CIRCULATION GIVEN IN PERCENTAGE OF FLUID RETURNS. NO ESTIMATE OF FLUID LOSS GIVEN IN DAILY REPORT
	744-754	95%		
	754-782	80%		
	782-823	85%		
	823-848	80%		
	848-860	80%		

DRILL HOLE	LOST CIRCULATION FOOTAGE	BARRELS LOST	TOTAL LOST BARRELS/GALS	COMMENTS
DC-22B				NO LOST CIRCULATION REPORTED IN THE SUPRABASALT SEDIMENTS
				START DRILLING BASALT AT 652 FT
	934-969			LOST CIRCULATION, SPENT 12 HOURS CIRCULATING MUD
	969-978			DRILL AHEAD WITH NO RETURNS
	1056-1099	55	55/2310	LOST CIRCULATION AT 1092 FT
	1718	230 CEMENT	230/9660	RUN CASING AND LOST 230 BBLS OF CEMENT

DRILL HOLE	LOST CIRCULATION FOOTAGE	BARRELS LOST	TOTAL LOST BARRELS/GALS	COMMENTS
DC-22C				NO LOST CIRCULATION REPORTED IN THE SUPRABASALT SEDIMENTS
				START DRILLING BASALT AT 658 FT
	676-695	50	50/2100	
	961-969			LOST CIRCULATION AT 969 FT, AMOUNT OF LOSS NOT GIVEN
	969-969	280	280/11760	SET CEMENT PLUG, DRILLED CEMENT AND LOST 280 BBLS
	976-996	25%		DRILLED AHEAD WITH 25% RETURNS
				START AERATED DRILLING AT 1709
	2653-2667			LOST CIRCULATION AT 2667, AMOUNT OF LOSS NOT GIVEN
	2815-2827			LOST CIRCULATION, AMOUNT OF LOSS NOT GIVEN

DRILL HOLE	LOST CIRCULATION FOOTAGE	BARRELS LOST	TOTAL LOST BARRELS/GALS	COMMENTS
DC-22D				NO LOST CIRCULATION REPORTED IN SUPRABASALT SEDIMENTS
				START DRILLING BASALT AT 658 FT
				NO LOST CIRCULATION REPORTED WHILE DRILLING BASALT

DRILL HOLE	LOST CIRCULATION FOOTAGE	BARRELS LOST	TOTAL LOST BARRELS/GALS	COMMENTS
RRL-2B	900-1045	178	178/7476	SELAH AND ESQUATZEL INNER BED
	1674-1766	520	520/21840	ROZA FLOW TOP
	2305-2310	25	25/1050	FRENCHMAN SPRINGS 3, AND 4
	2840-2858	15	15/630	ROCKY COULEE FLOW TOP

DRILL HOLE	LOST CIRCULATION FOOTAGE	BARRELS LOST	TOTAL LOST BARRELS/GALS	COMMENTS
RRL-2C				NO LOST CIRCULATION REPORTED IN THE SUPRA-BASALT SEDIMENTS
	809-917	60		LOST CIRCULATION AT 825 FT, POMONA MEMBER
	91701070	20		SELAH MEMBER
	1728-1835	12		ROZA FLOW TOP
	1945-2067	470		LOST CIRCULATION AT 2037 FT, SENTINEL GAP FLOW TOP

DRILL HOLE	LOST CIRCULATION FOOTAGE	BARRELS LOST	TOTAL LOST BARRELS/GALS	COMMENTS
DC-23W	0-37	153		DAILY REPORT NOT AVAILABLE
	37-67	351		
	67-160	239		
	160-300	82		
	300-381	22	847/35574	
	381-381	62	62/2604	
	381-437	171		
	437-592	129		
	592-663	0		
	663-809	0		
	809-937	17		
	937-1018	55		
	1018-1113	45		
	1113-1284	83		
	1285-1412	435		
	1412-1453	453	1388/58296	
	1453-1453	596		
	1453-1453	331		
	1453-1453	251	1178/49476	
	640-795	214		
	795-1244	400		
	1244-1248	81		
	1207-1258	212		
	1258-1369	255		
	1369-1455	258		
	1455-1446	239		
	1446-1301	227	1886/79212	
	1301-1301	685		
	1301-1301	151		
	1301-1301	0	836/35112	
	1239-1539	333		
	1539-1844	130		
	1844-2022	171		
	2022-2194	185		
	2194-2392	174	993/41706	

Task 02

Drilling effects at DC-23

Analysis of effects of conventional mud rotary drilling on groundwater levels in the suprabasalt and basalt sequence for DC-19, DC-20,22,23 and RRL-2 at the particular well site and other well sites.

Fluid loss for DC-19A, 19C, 19D; DC-20A, 20B, 20C, 20D; DC-22A, 22B, 22C, 22D; RRL-2B, 2C, and DC-23W was tabulated using information retrieved from the daily drilling reports for each well. The drilling footage where fluid loss occurred as well as the amount of the loss in barrels, total of loss for each lost circulation zone in barrels and gallons, and any comments dealing with the loss is given on each sheet.

When drilling basalt with the aerated mud method, lost circulation was reported as percentage estimates of total fluid returns instead of total barrels lost.

Drilling effects of DC-23 on the piezometer monitoring network was evaluated by F.A. Spane in the document SD-BWI-TI-313, "Preliminary Evaluation of the Effects of Construction Activities at DC-23W on Base-Line Monitoring at Selected Reference Repository Location Piezometer Installations". Drilling effects of DC-19,DC-20, DC-22 and the RRL-2 series on the piezometer monitoring network can be recovered from hydrograph charts which are stored in Basalt Records Management Center. Retrieval and analysis of this data is not possible because of my previous work commitments.

DRILL HOLE	LOST CIRCULATION FOOTAGE	BARRELS LOST	TOTAL LOST BARRELS/GALS	COMMENTS
DC-19A			-	NO LOST CIRCULATION REPORTED IN THE SUPRABASALT SEDIMENT
				START DRILLING BASALTS
	549-559	95%		95% CIRCULATION WHILE CORING.
	559-574			
	574-584			
	584-604			NO ESTIMATES OF FLUID LOSS GIVEN IN DAILY REPORTS
	604-614			
	624-633			
	633-638			
	638-641			
	641-659			
	683-704	90%		85% TO 95% CIRCULATION WHILE CORING
	718-735	95%		
	735-757	95%		NO ESTIMATES OF FLUID LOSS GIVEN IN DAILY REPORTS
	763-764	85%		
	764-784	95%		
	784-804	95%		

DRILL HOLE	LOST CIRCULATION FOOTAGE	BARRELS LOST	TOTAL LOST BARRELS/GALS	COMMENTS
DC-19C	229-240	160		NO LOST CIRCULATION REPORTED IN THE SUPRABASAL SEDIMENTS
	240-302	355		
	302-302	103	-	PUMPED SIX PILLS OF LOST CIRCULATION MATERIAL
		150		
		154		
		152		
		165		
		420		
	302-318	180		
	318-472	190	2029/85218	
	887-910	80	80/3360	START DRILLING BASALT WITH AERATED METHOD
	2022-2032			
	2168			DEPTH GIVEN WHERE LOST CIRCULATION OCCURRED. NO ESTIMATES OF FLUID LOSS GIVEN IN DAILY REPORT
	2363-2366			
	2559			
	3225			
	3434			
	3701			
	3834-3841			
	3841-3849			
	3882			
	3968			
	3983			

DRILL HOLE	LOST CIRCULATION FOOTAGE	BARRELS LOST	TOTAL LOST BARRELS/GALS	COMMENTS
DC-19D			-	NO LOST CIRCULATION REPORTED IN THE SUPRABASALT SEDIMENTS NO LOST CIRCULATION REPORTED IN THE BASALT DURING AERATED DRILLING

DRILL HOLE	LOST CIRCULATION FOOTAGE	BARRELS LOST	TOTAL LOST BARRELS/GALS	COMMENTS
DC-20A				NO LOST CIRCULATION REPORTED WHILE DRILLING THE SUPRABASALT SEDIMENTS
	564-584	75%		START CORING BASALTS
	584-604	80%		NO ESTIMATES OF FLUID LOSS GIVEN IN DAILY REPORTS
	604-634	80%		
	634-659	80%		
	659-684	85%		
	694-699	85%		
	699-724	90%		
	724-744	85%		
	744-751			TWISTED OFF AT 751 FT. PULL OUT OF HOLE. HOLE BRIDGED AT 640FT, LOST ALL CIRCULATION ATTEMPTING TO DRILL BRIDGE. REGAINED 50% CIRCULATION DRILLING OUT BRIDGE
	640-755			

DRILL HOLE	LOST CIRCULATION FOOTAGE	BARRELS LOST	TOTAL LOST BARRELS/GALS	COMMENTS
DC-20B				NO LOST CIRCULATION REPORTED WHILE DRILLING THE SUPRABASALT SEDIMENTS
	1573-1625			LOST CIRCULATION WITH NO TOTAL OF FLUID LOSS REPORTED IN THE DAILY REPORT

DRILL HOLE	LOST CIRCULATION FOOTAGE	BARRELS LOST	TOTAL LOST BARRELS/GALS	COMMENTS
DC-20C	253-320 320-327	300 ?	300/12600	FLUID LOSS WITHIN THE SUPRABASALT SEDIMENTS
				START DRILLING BASALT AT 530 FT
	567-608			LOST APPOXIMATELY 40 TO 50 BBLS PER/HR FROM 586 TO 608 FT.
	608-719	75 80	155/6510	LOST 75 BBLS AT 615 FT, LOST 80 BBLS AT 627 FT
				START AIR DRILLING AT 1511 FT.
	2143-2251			LOST CIRCULATION AT 2197 FT, AMOUNT OF LOSS NOT GIVEN
	3137-3189			LOST CIRCULATION AT 3158 FT, AMOUNT NOT GIVEN
	3418-3451			LOST CIRCULATION, AMOUNT NOT GIVEN
	3480-3526			LOST CIRCULATION, AMOUNT NOT GIVEN

DRILL HOLE	LOST CIRCULATION FOOTAGE	BARRELS LOST	TOTAL LOST BARRELS/GALS	COMMENTS
DC-20D	280-350			LOST CIRCULATION AT 350 FT, AMOUNT OF LOSS NOT GIVEN STARTED DRILLING BASALT AT 531 FT NO REPORTED LOST CIRCULATION WHILE DRILLING BASALT

DRILL HOLE	LOST CIRCULATION FOOTAGE	BARRELS LOST	TOTAL LOST BARRELS/GALS	COMMENTS
DC-22A				NO REPORTED LOST CIRCULATION IN THE SUPRABASALT SEDIMENTS
				START DRILLING BASALT AT 662 FT
	691-714	95%		
	714-744	95%		START CORING BASALT, AMOUNT OF LOST CIRCULATIO GIVEN IN PERCENTAGE OF FLUID RETURNS. NO ESTIMAT OF FLUID LOSS GIVEN IN DAILY REPORT
	744-754	95%		
	754-782	80%		
	782-823	85%		
	823-848	80%		
	848-860	80%		

DRILL HOLE	LOST CIRCULATION FOOTAGE	BARRELS LOST	TOTAL LOST BARRELS/GALS	COMMENTS
DC-22B				NO LOST CIRCULATION REPORTED IN THE SUPRABASALT SEDIMENTS
				START DRILLING BASALT AT 652 FT
	534-969			LOST CIRCULATION, SPENT 12 HOURS CIRCULATING MUD
	969-978			DRILL AHEAD WITH NO RETURNS
	1056-1099	55	55/2310	LOST CIRCULATION AT 1092 FT
	1718	230 CEMENT	230/9660	RUN CASING AND LOST 230 BBLS OF CEMENT

DRILL HOLE	LOST CIRCULATION FOOTAGE	BARRELS LOST	TOTAL LOST BARRELS/GALS	COMMENTS
DC-22C				NO LOST CIRCULATION REPORTED IN THE SUPRABASALT SEDIMENTS
				START DRILLING BASALT AT 658 FT
	676-695	50	50/2100	
	961-969			LOST CIRCULATION AT 969 FT, AMOUNT OF LOSS NOT GIVEN
	969-969	280	280/11760	SET CEMENT PLUG, DRILLED CEMENT AND LOST 280 BBLS
	976-996	25%		DRILLED AHEAD WITH 25% RETURNS
				START AE[illegible]TED DRILLING AT 1709
	2653-2667			LOST CIRCULATION AT 2667, AMOUNT OF LOSS NOT GIVEN
	2815-2827			LOST CIRCULATION, AMOUNT OF LOSS NOT GIVEN

DRILL HOLE	LOST CIRCULATION FOOTAGE	BARRELS LOST	TOTAL LOST BARRELS/GALS	COMMENTS
DC-22D				NO LOST CIRCULATION REPORTED IN SUPRABASALT SEDIMENTS
				START DRILLING BASALT AT 658 FT
				NO LOST CIRCULATION REPORTED WHILE DRILLING BASALT

DRILL HOLE	LOST CIRCULATION FOOTAGE	BARRELS LOST	TOTAL LOST BARRELS/GALS	COMMENTS
RRL-2B	900-1045	178	178/7476	SELAH AND ESQUATZEL INNER BED
	1674-1766	520	520/21840	ROZA FLOW TOP
	2305-2310	25	25/1050	FRENCHMAN SPRINGS 3, AND 4
	2840-2858	15	15/630	ROCKY COULEE FLOW TOP

DRILL HOLE	LOST CIRCULATION FOOTAGE	BARRELS LOST	TOTAL LOST BARRELS/GALS	COMMENTS
RRL-2C				NO LOST CIRCULATION REPORTED IN THE SUPRA-BASALT SEDIMENTS
	809-917	60		LOST CIRCULATION AT 825 FT, POMONA MEMBER
	91701070	20		SELAH MEMBER
	1728-1835	12		ROZA FLOW TOP
	1945-2067	470		LOST CIRCULATION AT 2037 FT, SENTINEL GAP FLOW TOP

DRILL HOLE	LOST CIRCULATION FOOTAGE	BARRELS LOST	TOTAL LOST BARRELS/GALS	COMMENTS
DC-23W	0-37	153		DAILY REPORT NOT AVAILABLE
	37-67	351		
	67-160	239		
	160-300	82		
	300-381	22	847/35574	
	381-381	62	62/2604	
	381-437	171		
	437-592	129		
	592-663	0		
	663-809	0		
	809-937	17		
	937-1018	55		
	1018-1113	45		
	1113-1284	83		
	1283-1412	435		
	1412-1453	453	1388/58296	
	1453-1453	596		
	1453-1453	331		
	1453-1453	251	1178/49476	
	640-795	214		
	795-1244	400		
	1244-1248	81		
	1207-1258	212		
	1258-1369	255		
	1369-1455	258		
	1455-1446	239		
	1446-1301	227	1886/79212	
	1301-1301	685		
	1301-1301	151		
	1301-1301	0	836/35112	
	1239-1539	333		
	1539-1844	130		
	1844-2022	171		
	2022-2194	185		
	2194-2392	174	993/41706	

<u>REFERENCE CASE</u>

<u>MODEL LAYER PROPERTIES</u>

LAYER	THICK (m)	T (m^2/sec)	K_h (m/sec)	K_v (m/sec)	S	S_s (1/m)
1	5.3 m	1.0E-04	2.0E-05	2.0E-05	1.0E-04	2.0E-05
2	17.9 m	?	1.0E-09	1.0E-08	1.0E-04	6.0E-06
3	53.6 m	1.0E-04	2.0E-06	2.0E-06	1.0E-04	2.0E-06
4	25.8 m		1.0E-09	1.0E-08	1.0E-04	4.0E-06
5	23.3 m	7.0E-05	3.0E-06	3.0E-06	1.0E-04	4.0E-06
6	25.9 m		1.0E-10	1.0E-09	1.0E-04	4.0E-06
7	25.9 m	2.0E-04	8.0E-06	8.0E-06	1.0E-04	4.0E-06
8	64.3 m		1.0E-10	1.0E-09	1.0E-04	2.0E-06
9	38.1 m	2.0E-04	5.0E-06	5.0E-06	1.0E-04	3.0E-06
10	50.0 m		1.0E-10	1.0E-09	1.0E-04	2.0E-06
11	7.9 m	1.0E-03	1.0E-04	1.0E-04	1.0E-04	1.0E-05
12	10.8 m		1.0E-11	1.0E-10	1.0E-04	9.0E-06

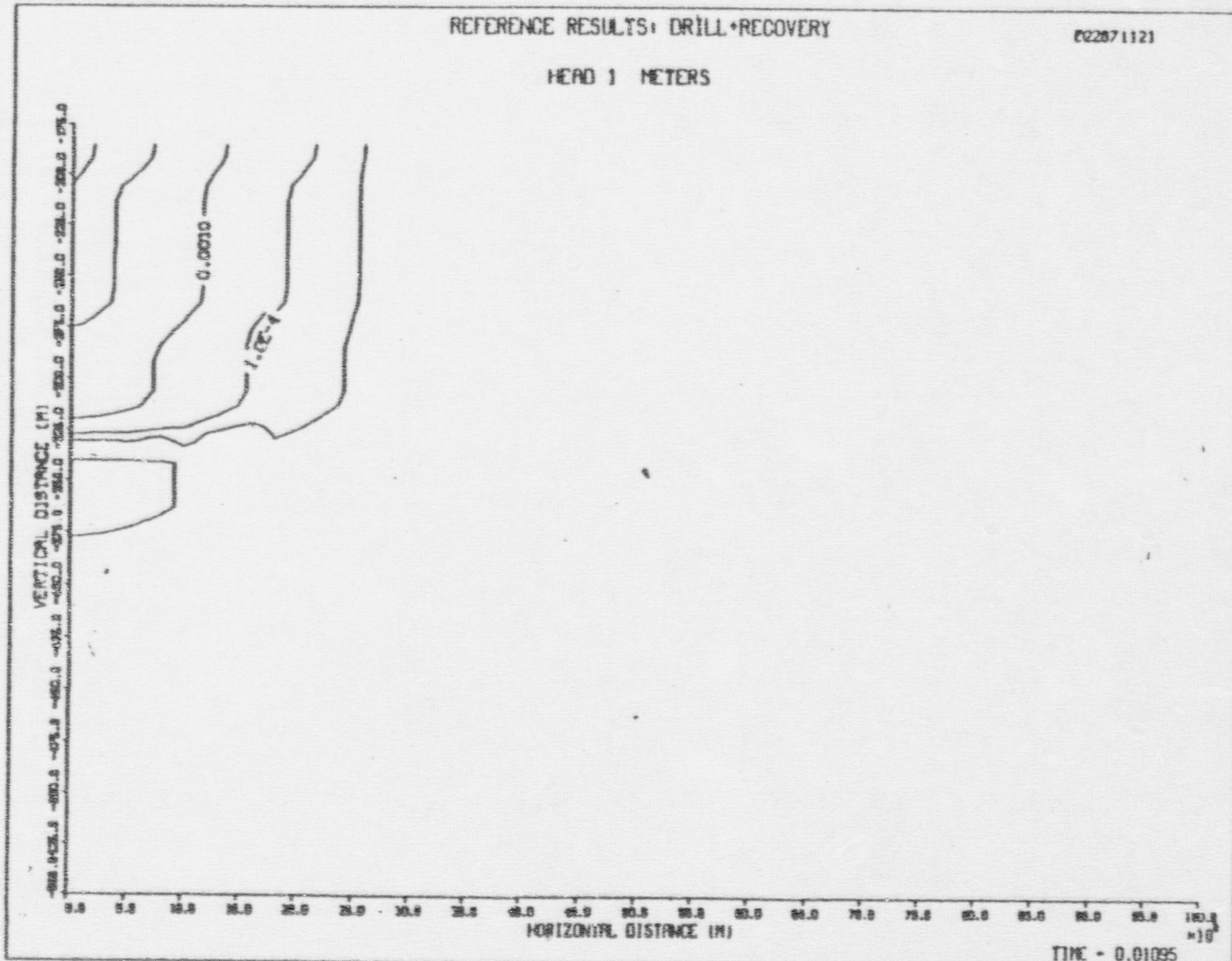
REFERENCE RESULTS: DRILL+RECOVERY
E22871121
HEAD 1 METERS
0.0010
1.0E-4
VERTICAL DISTANCE (M)
HORIZONTAL DISTANCE (M)
TIME - 0.01095

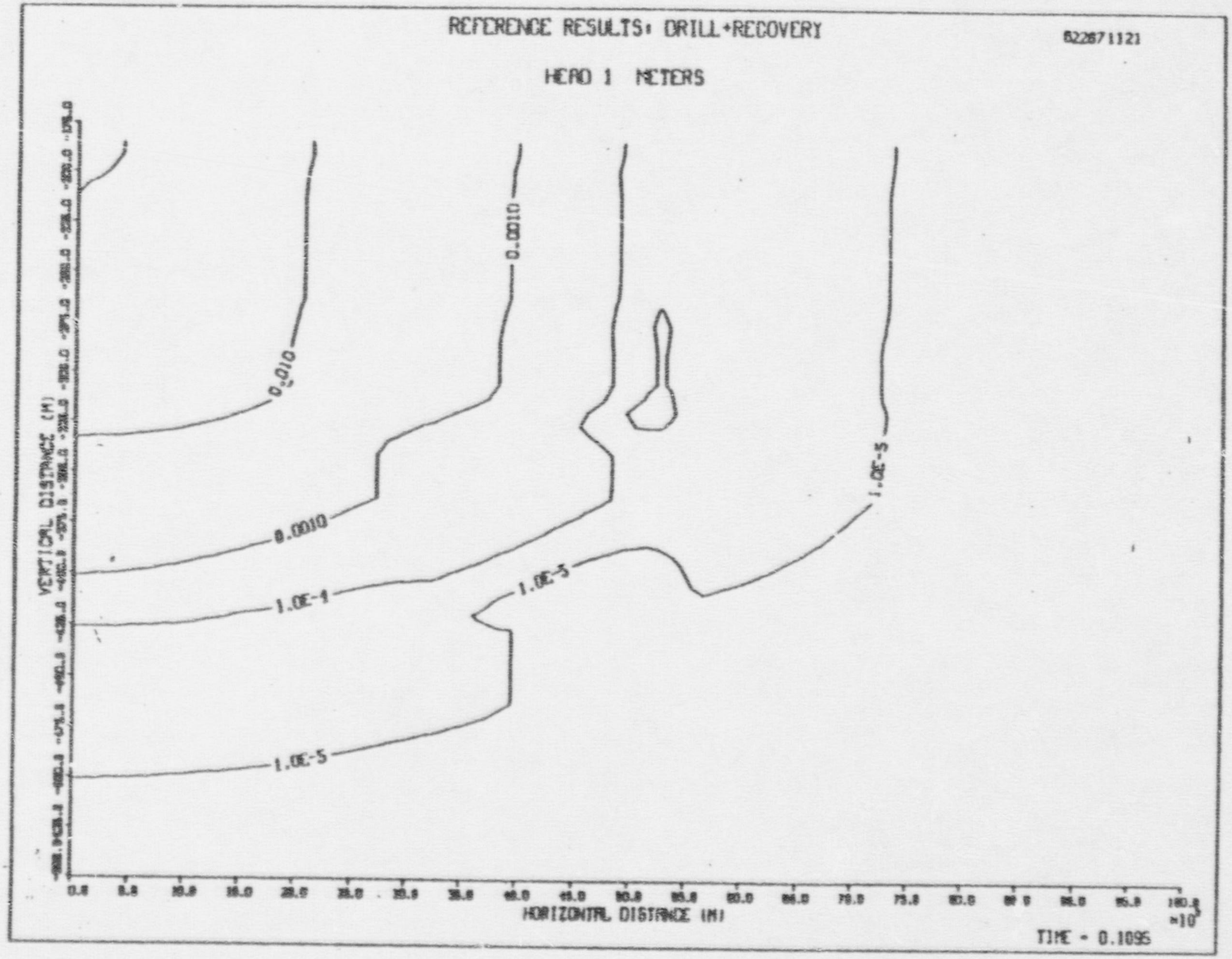
REFERENCE RESULTS: DRILL+RECOVERY
622871121
HEAD 1 METERS
0.010
0.0010
0.0010
1.0E-4
1.0E-5
1.0E-5
1.0E-5
VERTICAL DISTANCE (M)
HORIZONTAL DISTANCE (M)
TIME - 0.1095

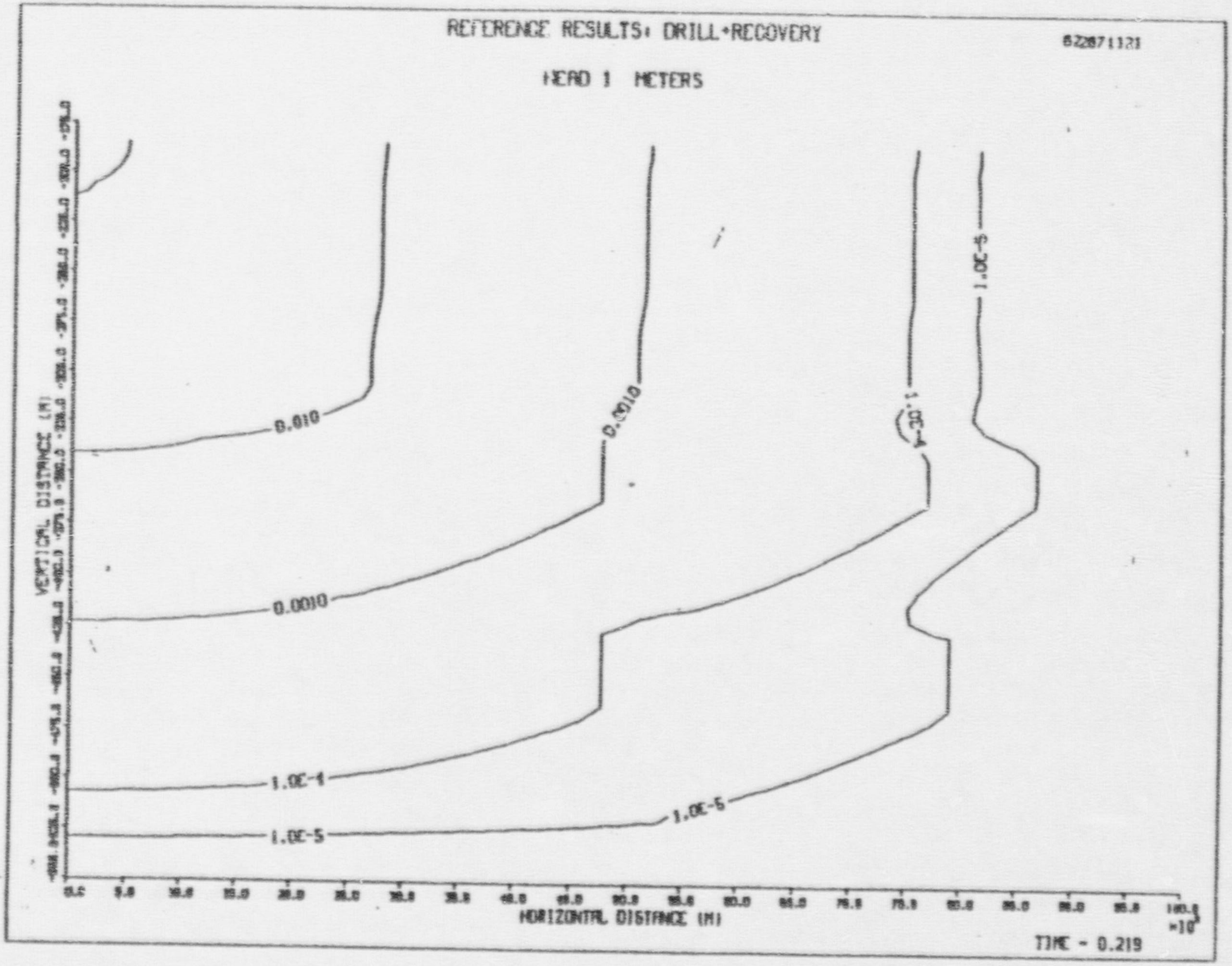
REFERENCE RESULTS: DRILL+RECOVERY
82871121
HEAD 1 METERS
VERTICAL DISTANCE (M)
HORIZONTAL DISTANCE (M)
0.010
0.0010
1.0E-4
1.0E-5
TIME - 0.219

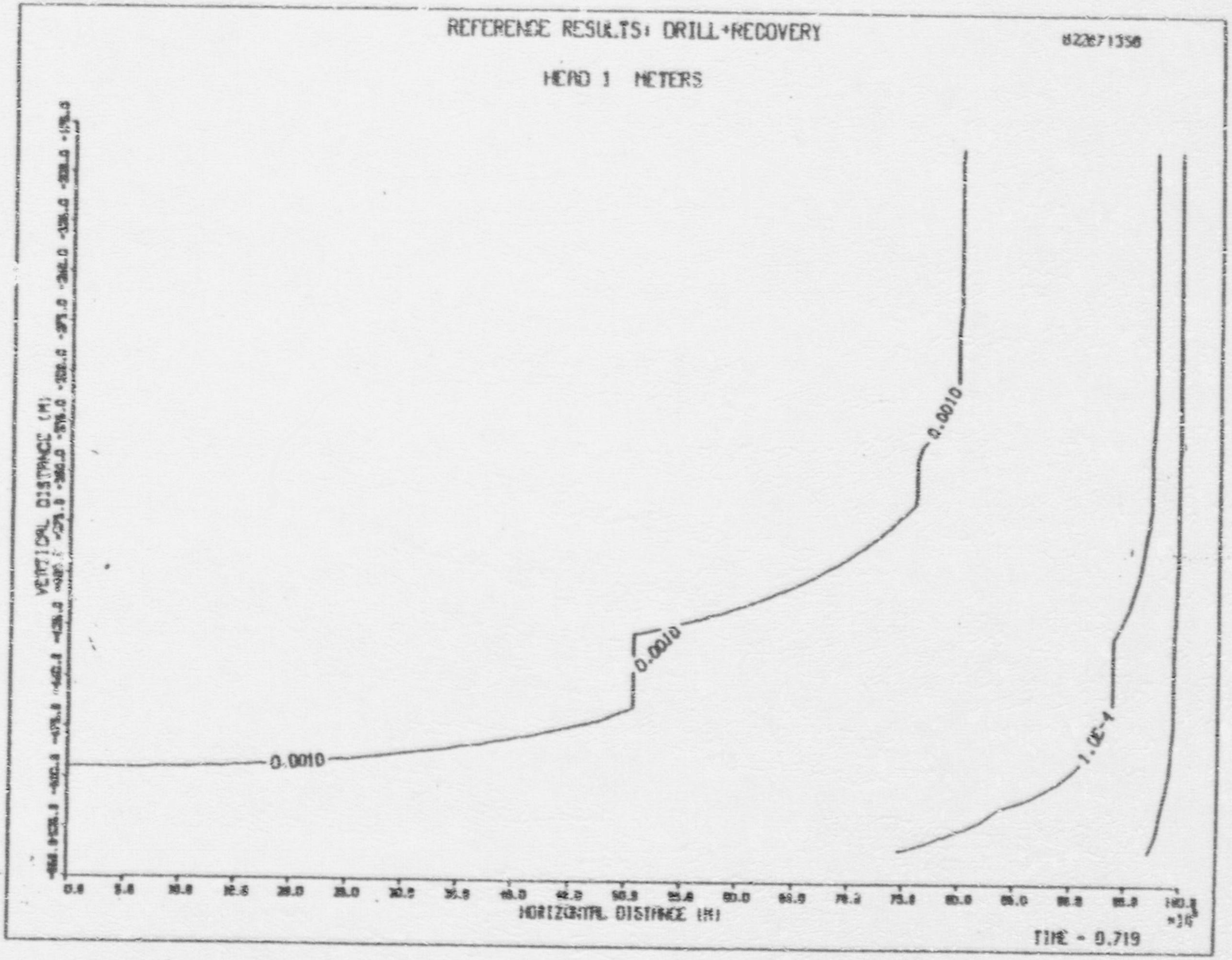
REFERENCE RESULTS: DRILL+RECOVERY
822871358
HEAD 1 METERS
VERTICAL DISTANCE (M)
HORIZONTAL DISTANCE (M)
0.0010
0.0010
0.0010
1.0E-4
TIME - 0.719

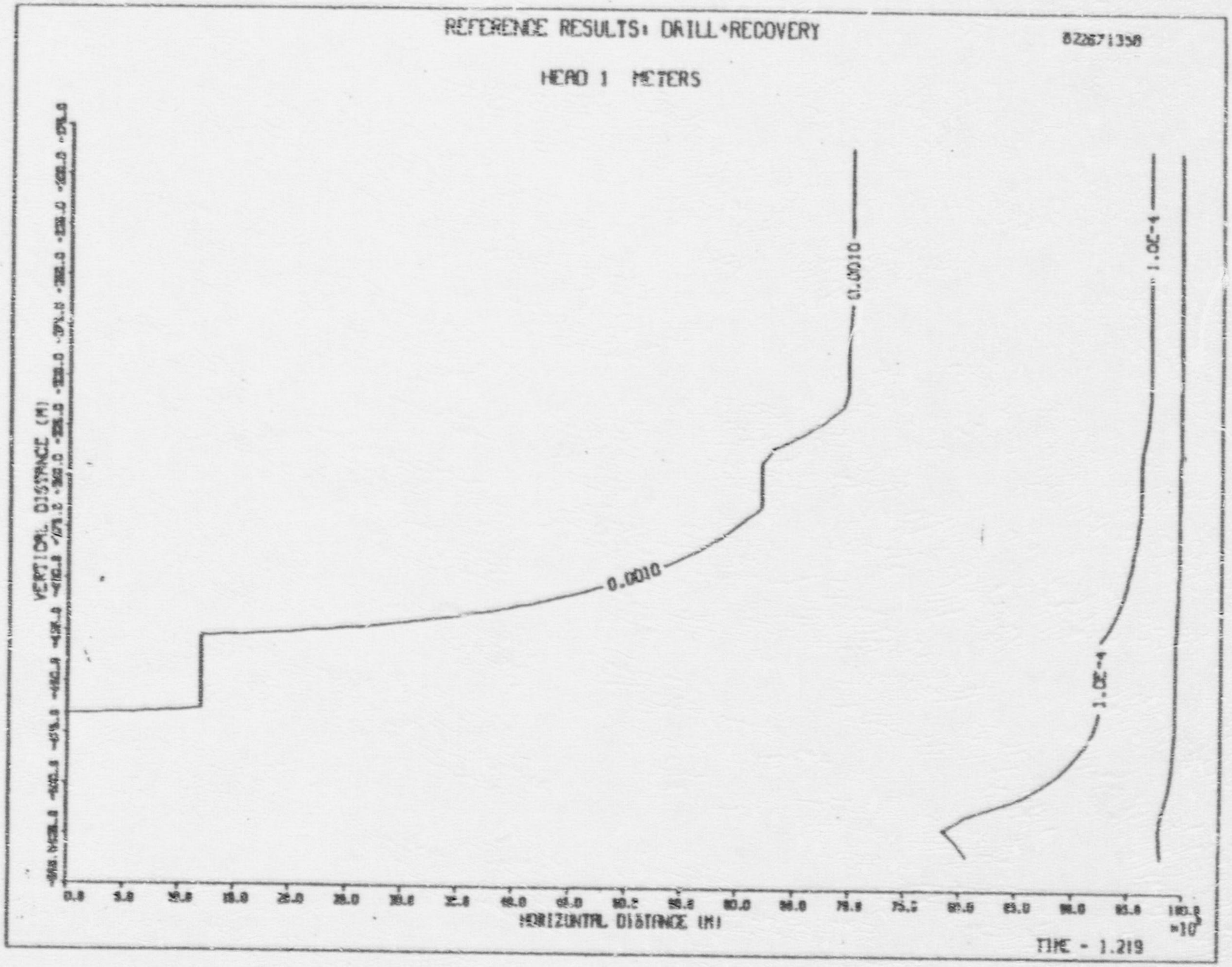
REFERENCE RESULTS: DRILL+RECOVERY
822671350
HEAD 1 METERS
VERTICAL DISTANCE (M)
0.0010
1.0E-4
HORIZONTAL DISTANCE (M)
TIME - 1.219

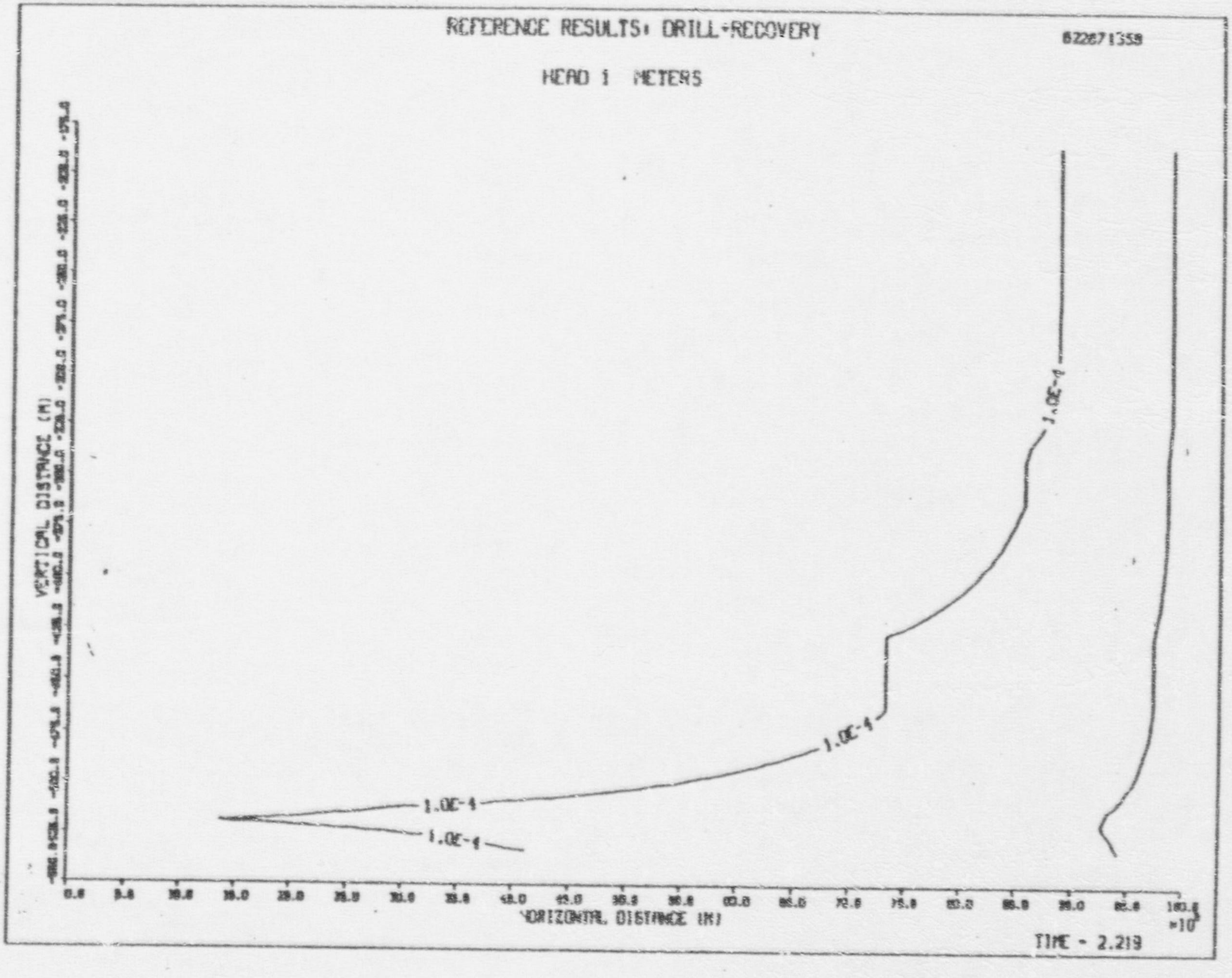
REFERENCE RESULTS: DRILL+RECOVERY
822871359
HEAD 1 METERS
VERTICAL DISTANCE (M)
1.0E-4
1.0E-4
1.0E-4
1.0E-4
HORIZONTAL DISTANCE (M)
TIME - 2.219

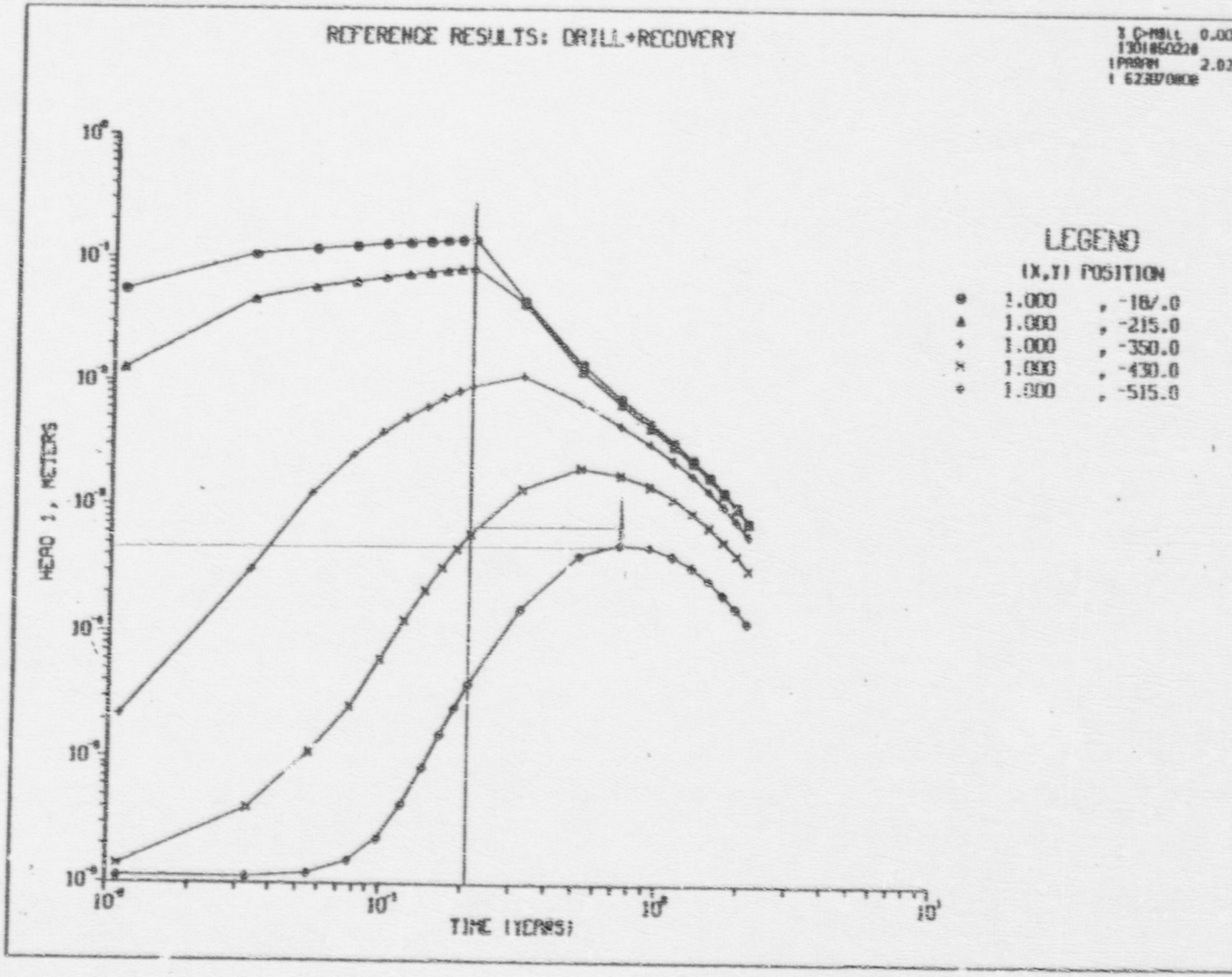

REFERENCE RESULTS: DRILL+RECOVERY
LEGEND
(X,Y) POSITION
1.000 , -187.0
1.000 , -215.0
1.000 , -350.0
1.000 , -430.0
1.000 , -515.0
HEAD 1, METERS
TIME (YEARS)

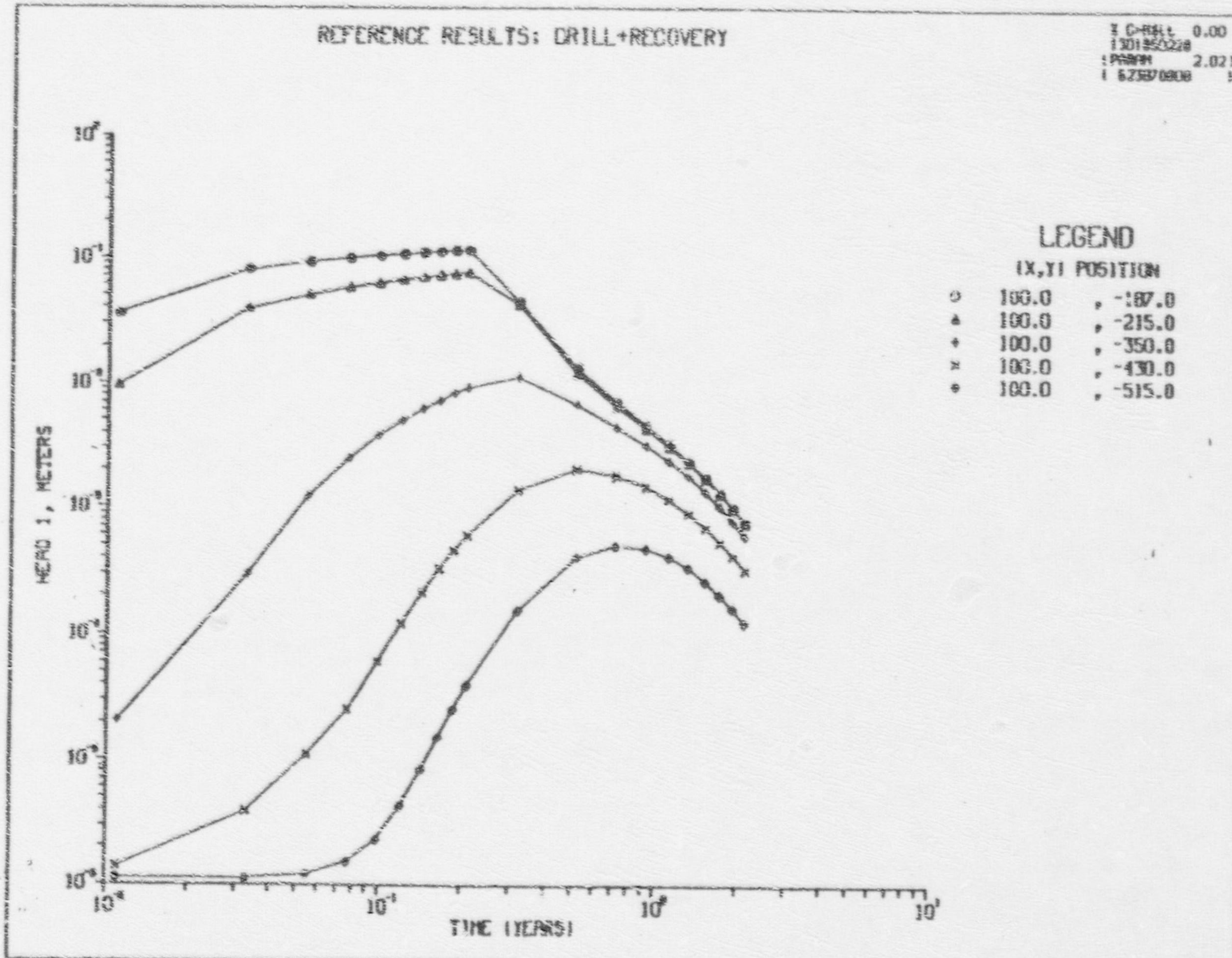

REFERENCE RESULTS: DRILL+RECOVERY
HEAD 1, METERS
TIME (YEARS)
LEGEND
(X,Y) POSITION
100.0 , -187.0
100.0 , -215.0
100.0 , -350.0
100.0 , -430.0
100.0 , -515.0

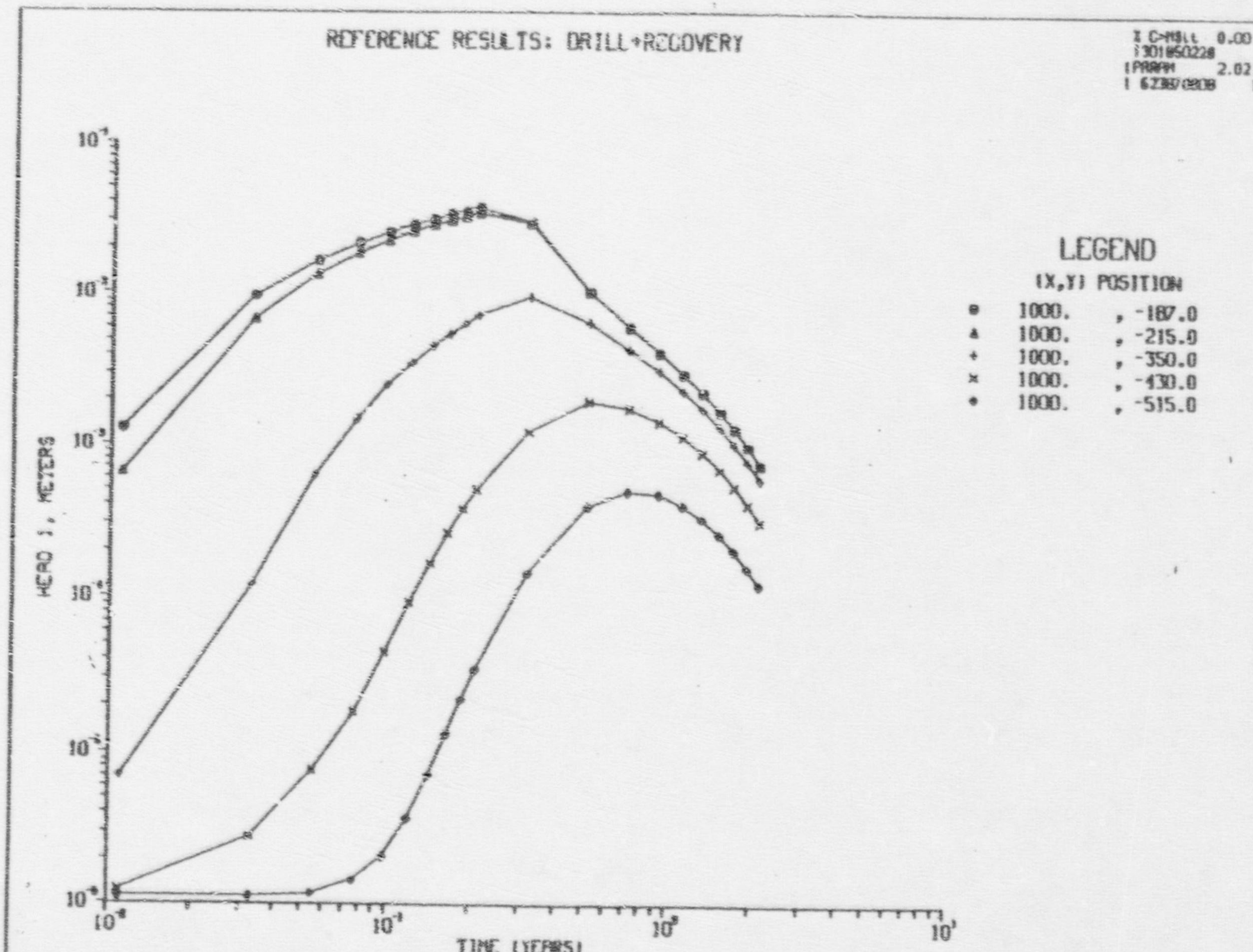
REFERENCE RESULTS: DRILL+RECOVERY
X C>MILL 0.00
301050228
PARAM 2.02
623870808
LEGEND
(X,Y) POSITION
1000. , -187.0
1000. , -215.0
1000. , -350.0
1000. , -430.0
1000. , -515.0
HEAD 1, METERS
TIME (YEARS)

CASE 2. DECREASED SPECIFIC STORAGE IN FLOW INTERIORS

MODEL LAYER PROPERTIES

CHANGES FROM REFERENCE CASE

LAYER	THICK (m)	T (m^2/sec)	K_h (m/sec)	K_v (m/sec)	S	S_s (1/m)
1	5.3 m					
2	17.9 m				1.0E-05	6.0E-07
3	53.6 m					
4	25.8 m				1.0E-05	4.0E-07
5	23.3 m					
6	25.9 m				1.0E-05	4.0E-07
7	25.9 m					
8	64.3 m				1.0E-05	2.0E-07
9	38.1 m					
10	50.0 m				1.0E-05	2.0E-07
11	7.9 m					
12	10.8 m				1.0E-05	9.0E-07

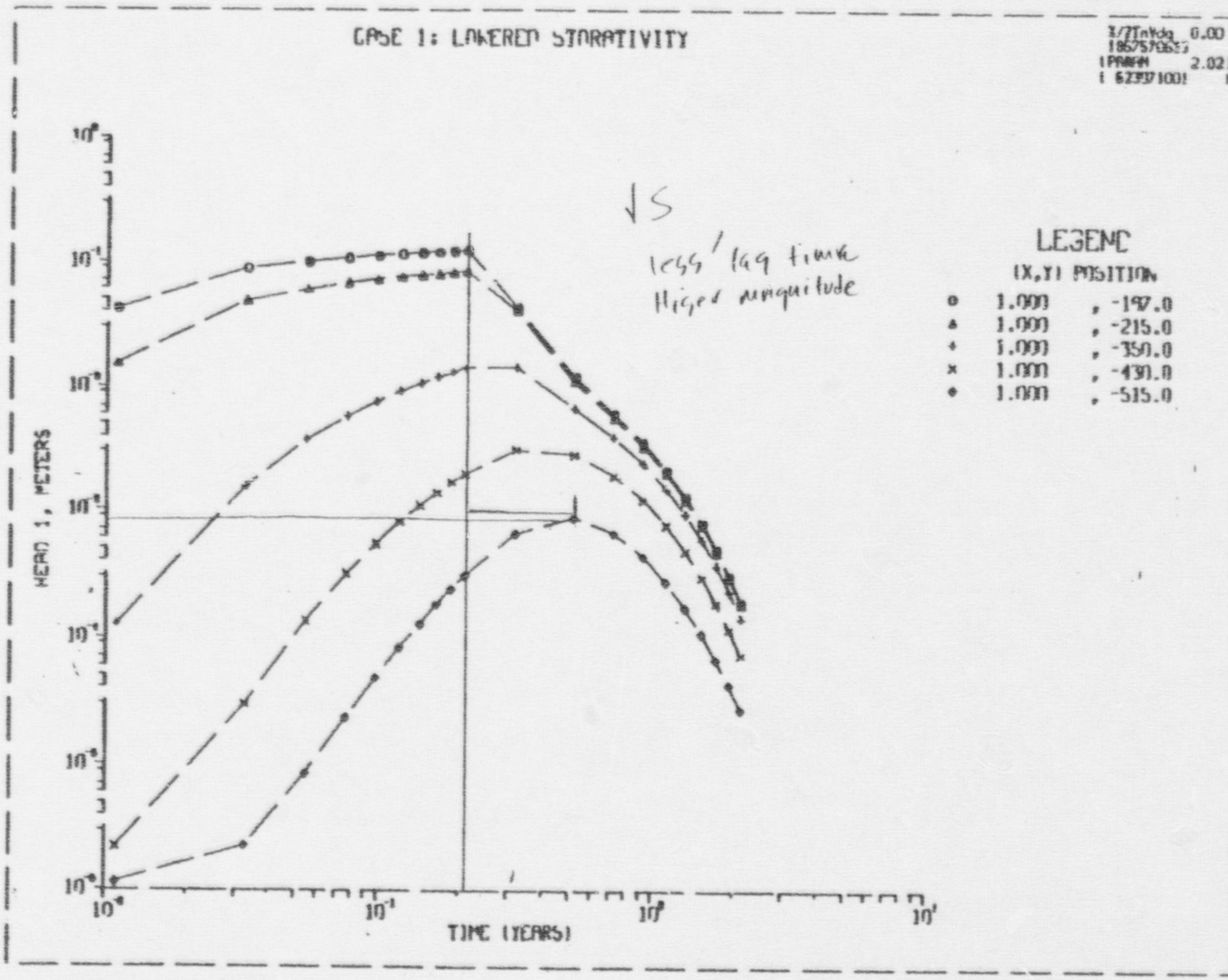
CASE 1: LAYERED STORATIVITY
3/7InVdq 0.00
1867579635
(PARAM 2.02)
(62337100) 1
↓S
less lag time
Higer magnitude
LEGEND
(X,Y) POSITION
o 1.000 , -197.0
▲ 1.000 , -215.0
+ 1.000 , -350.0
× 1.000 , -430.0
◆ 1.000 , -515.0
HEAD 1, METERS
TIME (YEARS)

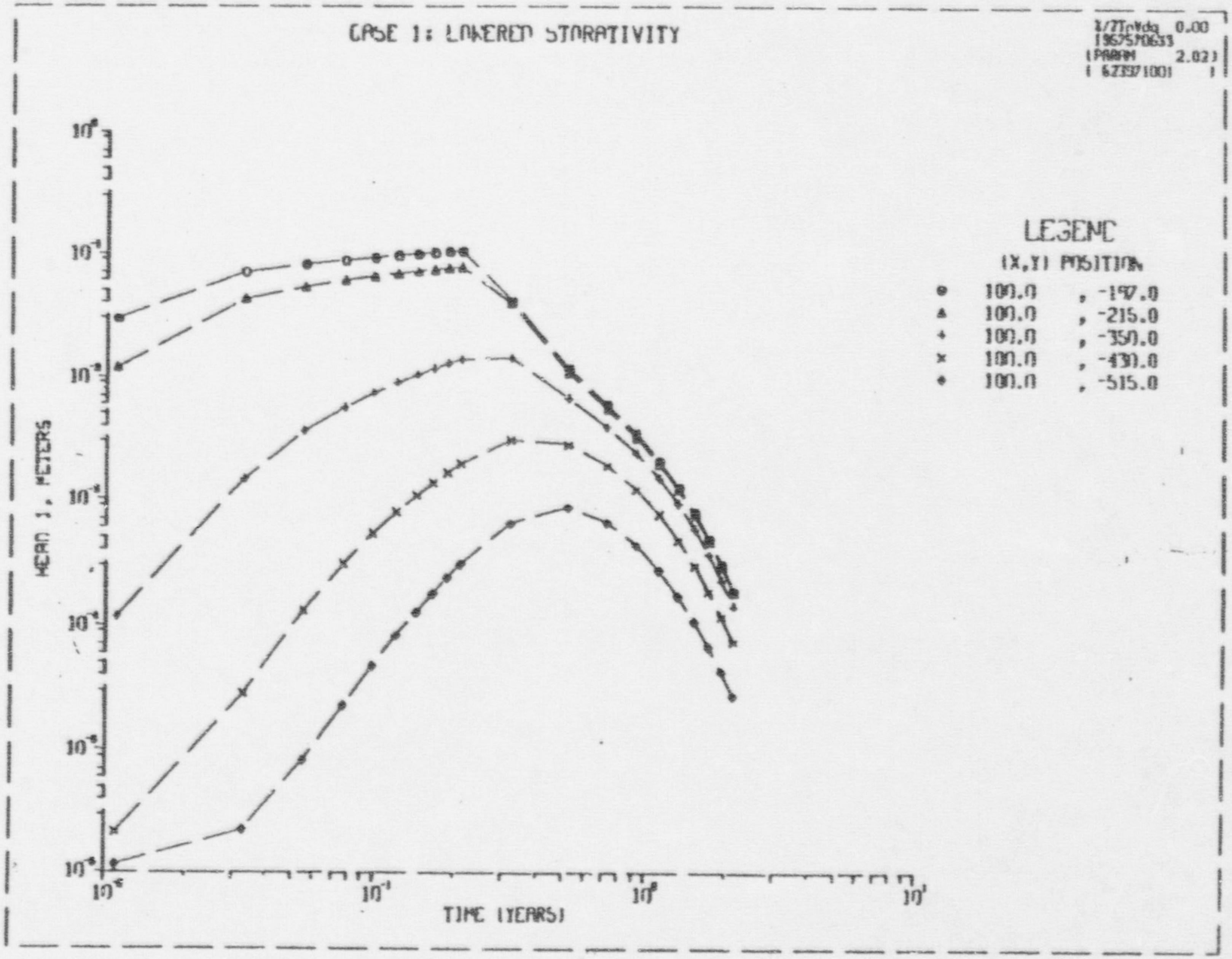

CASE 1: LOWERED STORATIVITY
MEAN J, METERS
TIME (YEARS)
LEGEND
(X,Y) POSITION
100.0 , -197.0
100.0 , -215.0
100.0 , -350.0
100.0 , -430.0
100.0 , -515.0

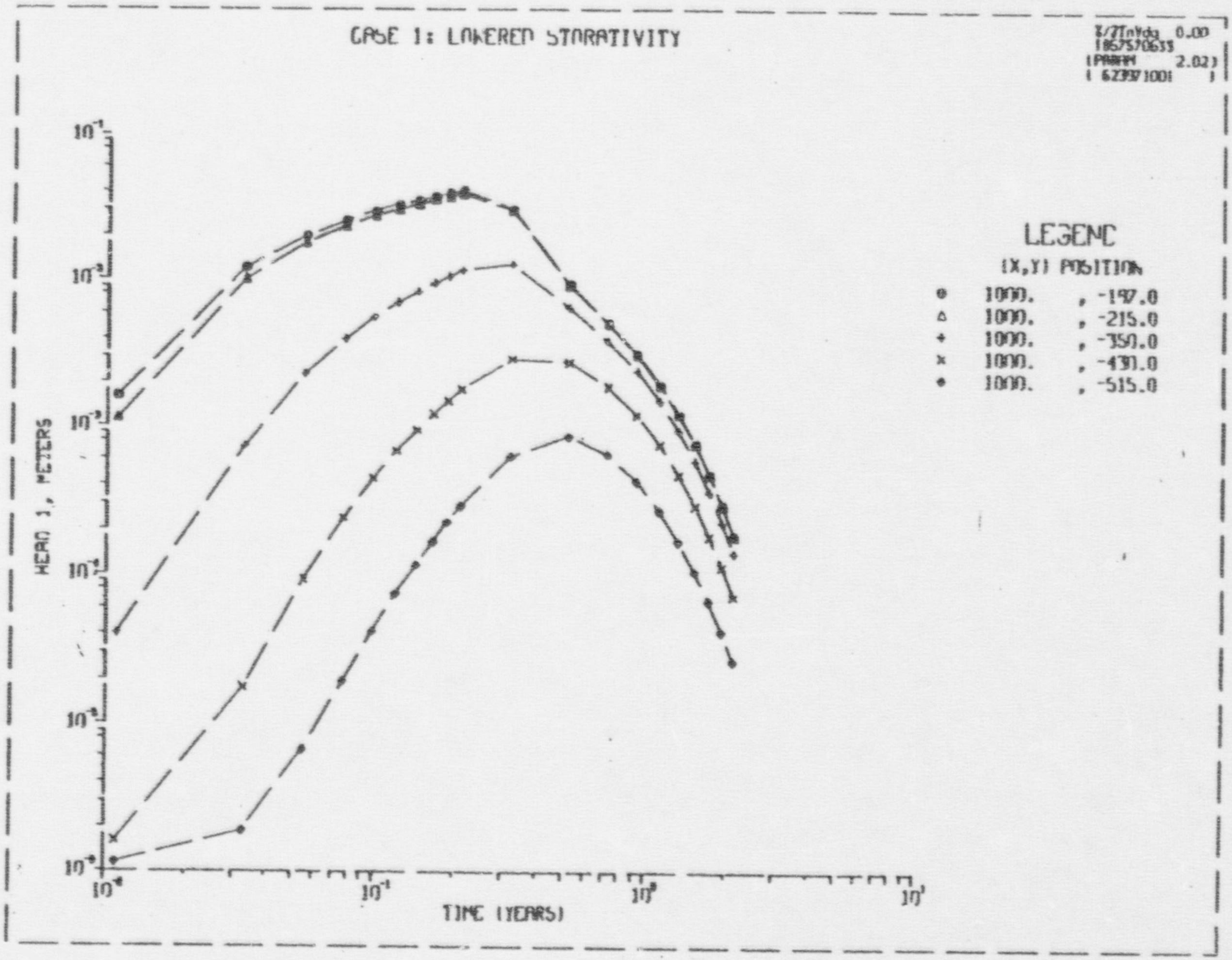
CASE 1: LOWERED STORATIVITY
HEAD 1, METERS
TIME (YEARS)
LEGEND
(X,Y) POSITION
1000. , -197.0
1000. , -215.0
1000. , -350.0
1000. , -430.0
1000. , -515.0

CASE 3. INCREASED K_v AND DECREASED S_s IN FLOW INTERIORS

MODEL LAYER PROPERTIES

CHANGES FROM REFERENCE CASE

LAYER	THICK (m)	T (m^2/sec)	K_h (m/sec)	K_v (m/sec)	S	S_s (1/m)
1	5.3 m					
2	17.9 m			1.0E-07	1.0E-05	6.0E-07
3	53.6 m					
4	25.8 m			1.0E-07	1.0E-05	4.0E-07
5	23.3 m					
6	25.9 m			1.0E-08	1.0E-05	4.0E-07
7	25.9 m					
8	64.3 m			1.0E-08	1.0E-05	2.0E-07
9	38.1 m					
10	50.0 m			1.0E-08	1.0E-05	2.0E-07
11	7.9 m					
12	10.8 m			1.0E-09	1.0E-05	9.0E-07

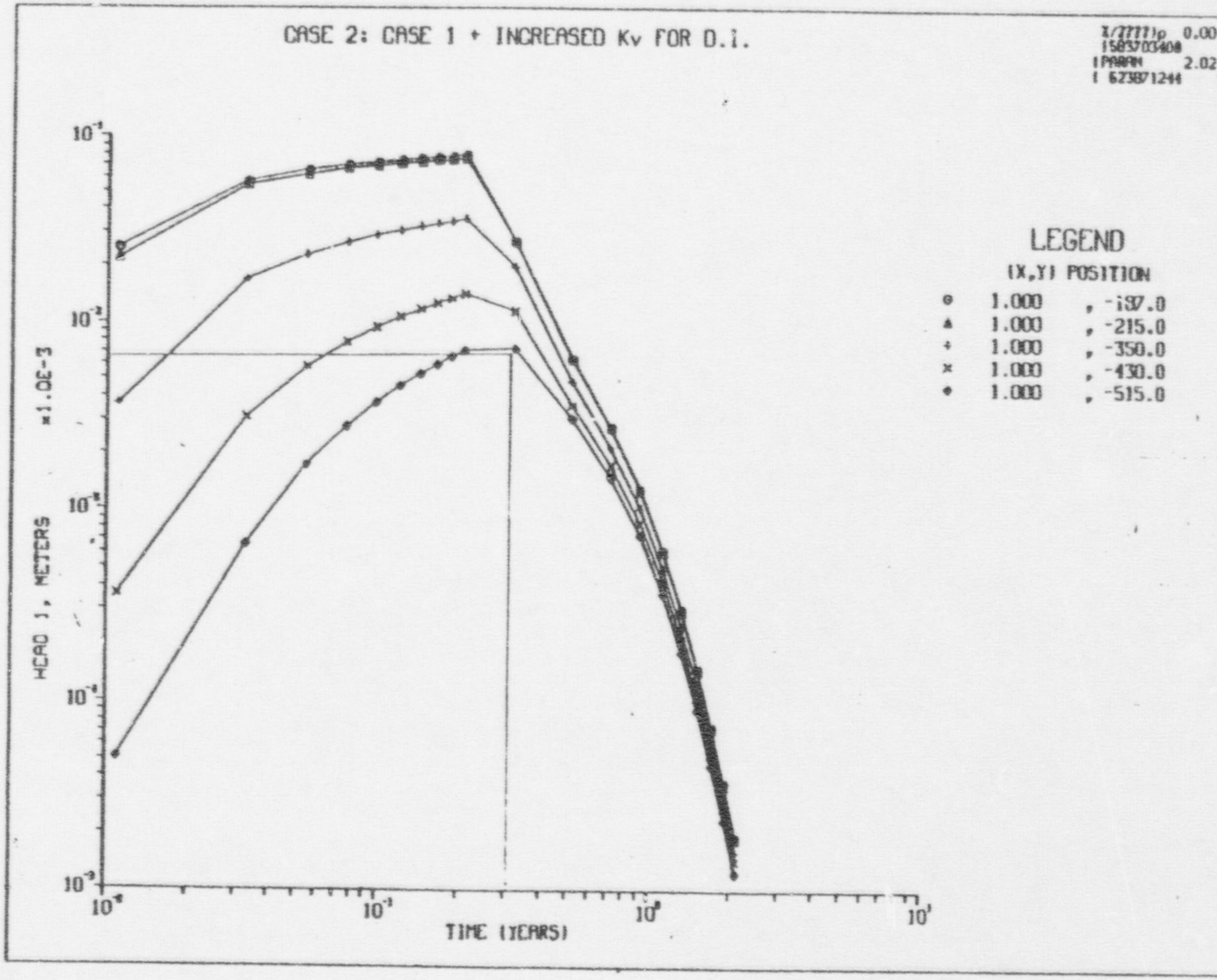

CASE 2: CASE 1 + INCREASED Kv FOR D.I.
HEAD 1, METERS ×1.0E-3
TIME (YEARS)
LEGEND
(X,Y) POSITION
1.000 , -137.0
1.000 , -215.0
1.000 , -350.0
1.000 , -430.0
1.000 , -515.0

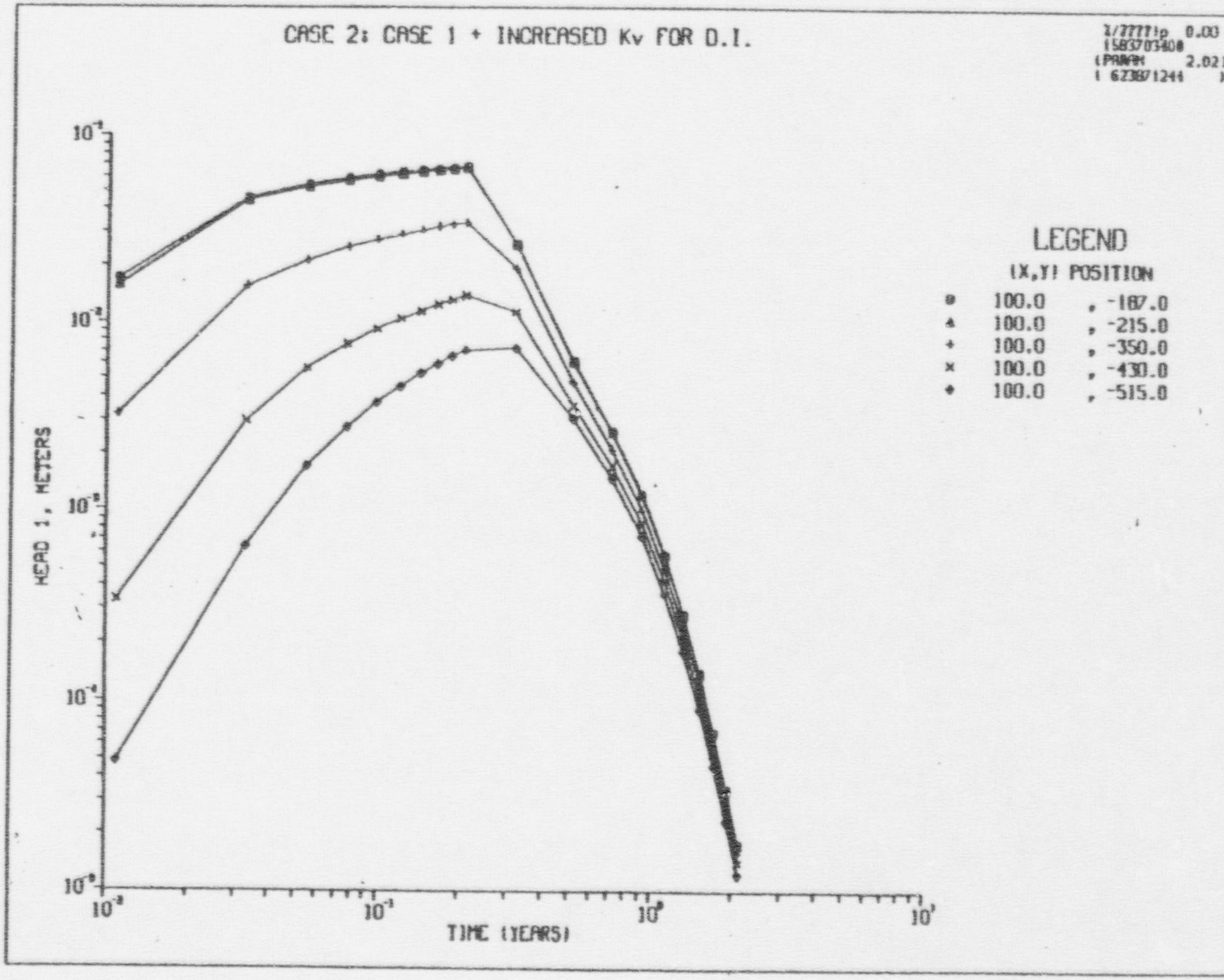
CASE 2: CASE 1 + INCREASED Kv FOR D.I.
1/7777!p 0.00
1583703408
(PARAM 2.02)
(623871244)
LEGEND
(X,Y) POSITION
100.0 , -187.0
100.0 , -215.0
100.0 , -350.0
100.0 , -430.0
100.0 , -515.0
HEAD 1, METERS
TIME (YEARS)

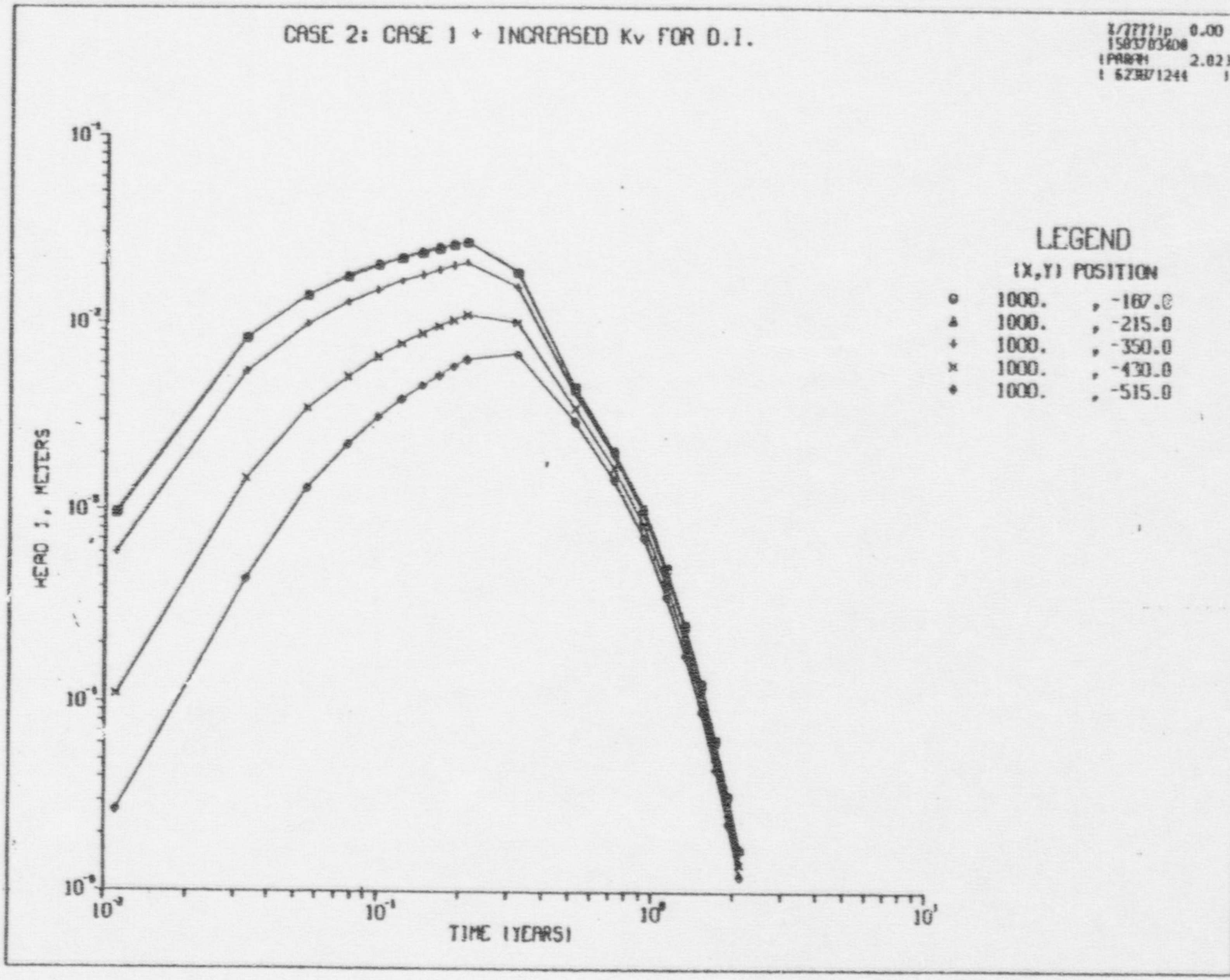
CASE 2: CASE 1 + INCREASED Kv FOR D.I.
1000. , -167.0
1000. , -215.0
1000. , -350.0
1000. , -430.0
1000. , -515.0
LEGEND
(X,Y) POSITION
HEAD 1, METERS
TIME (YEARS)

CASE A. DECREASED K_h IN FLOW TOPS, INCREASED K_v AND DECREASED S_s IN FLOW INTERIORS

MODEL-LAYER PROPERTIES

CHANGES FROM REFERENCE CASE

LAYER	THICK (m)	T (m^2/sec)	K_h (m/sec)	K_v (m/sec)	S	S_s (1/m)
1	5.3 m	1.0E-05	2.0E-06			
2	17.9 m			1.0E-07	1.0E-05	6.0E-07
3	53.6 m	1.0E-05	2.0E-07			
4	25.8 m			1.0E-07	1.0E-05	4.0E-07
5	23.3 m	7.0E-06	3.0E-07			
6	25.9 m			1.0E-08	1.0E-05	4.0E-07
7	25.9 m	2.0E-05	8.0E-07			
8	64.3 m			1.0E-08	1.0E-05	2.0E-07
9	38.1 m	2.0E-05	5.0E-07			
10	50.0 m			1.0E-08	1.0E-05	2.0E-07
11	7.9 m	1.0E-04	1.0E-05			
12	10.8 m			1.0E-09	1.0E-05	9.0E-07

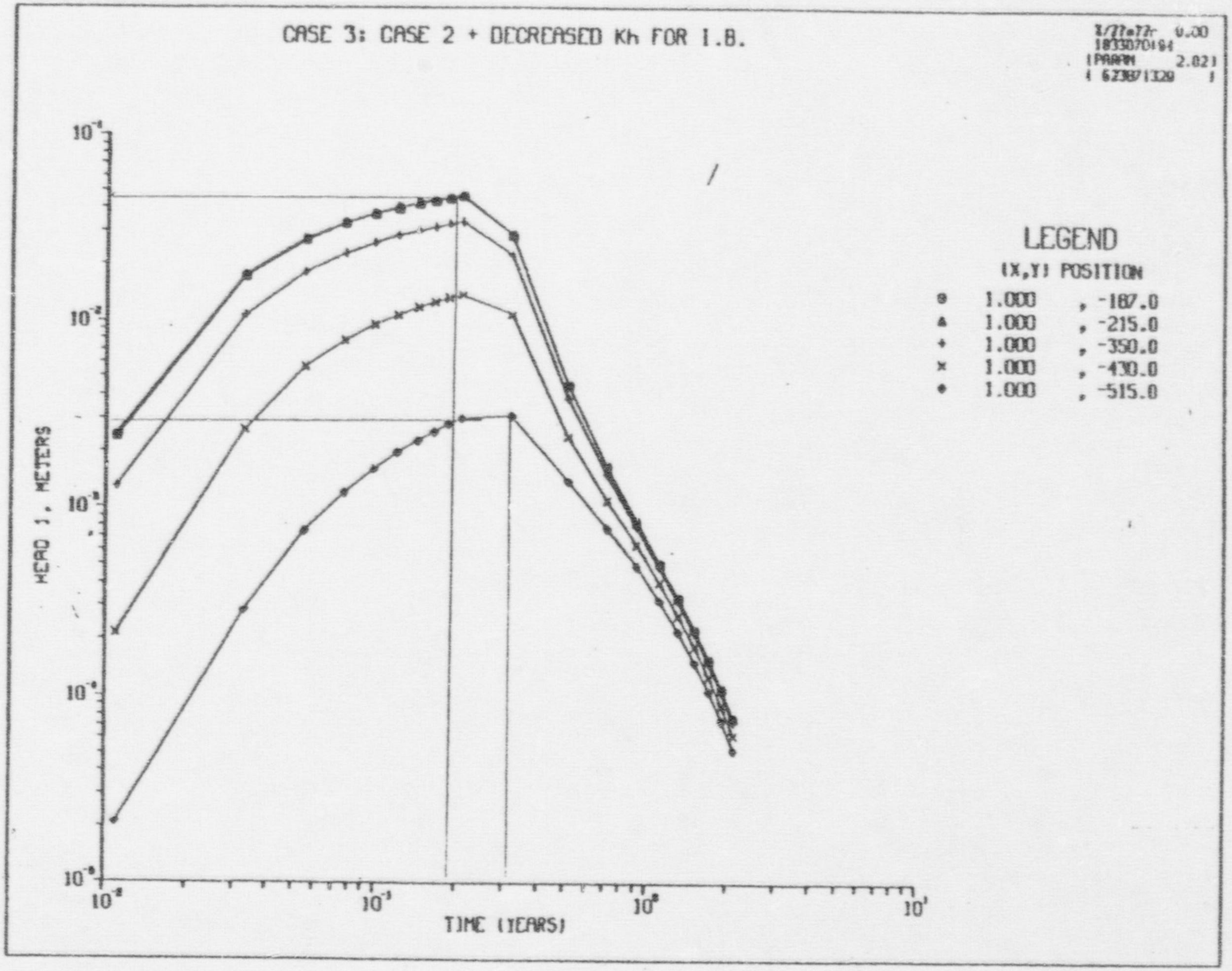

CASE 3: CASE 2 + DECREASED Kh FOR I.B.
LEGEND
(X,Y) POSITION
1.000 , -187.0
1.000 , -215.0
1.000 , -350.0
1.000 , -430.0
1.000 , -515.0
HEAD 1, METERS
TIME (YEARS)
10^{-1}
10^{-2}
10^{-3}
10^{-4}
10^{-5}
10^{-2}
10^{-1}
10^{0}
10^{1}

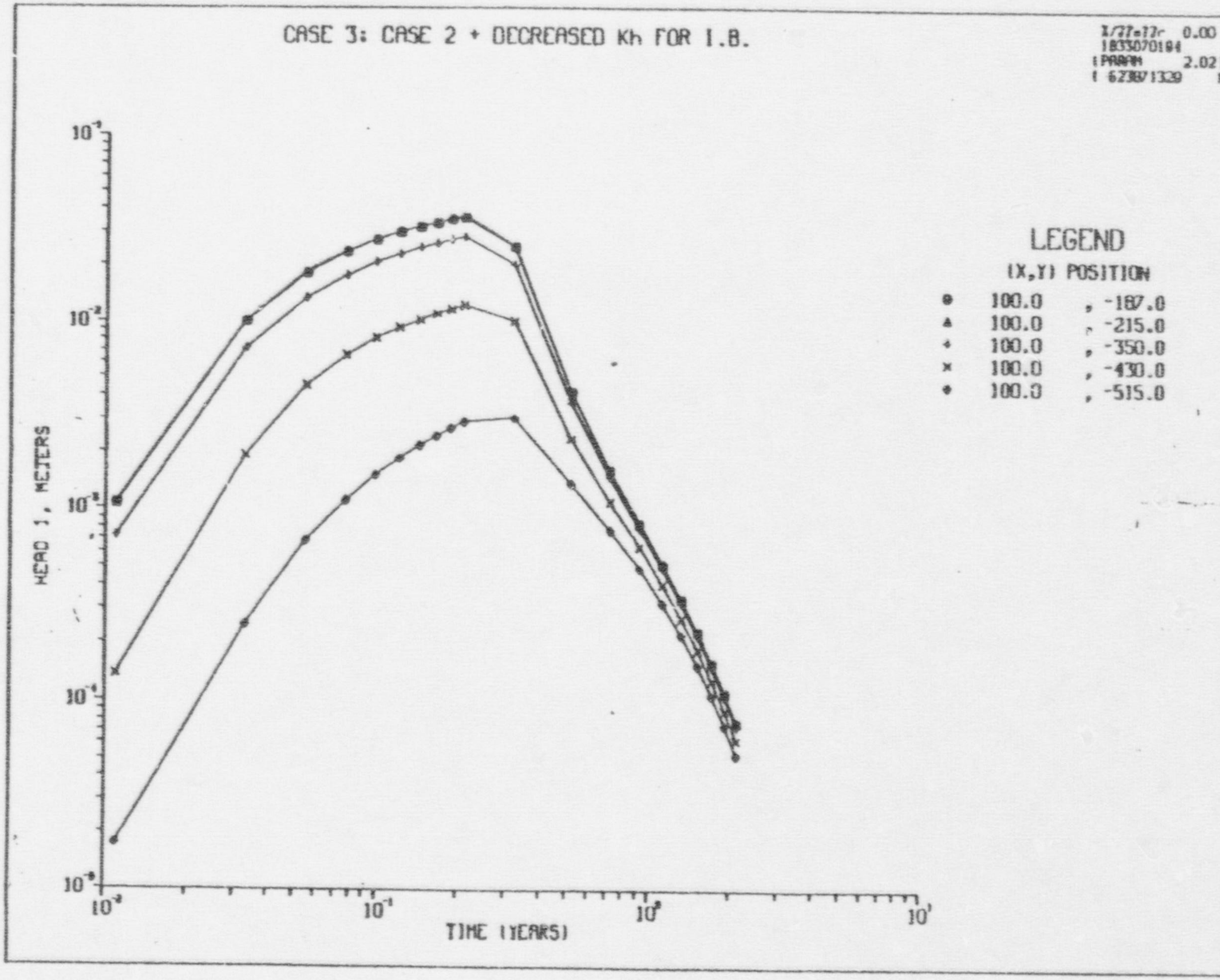
CASE 3: CASE 2 + DECREASED Kh FOR I.B.
HEAD 1, METERS
TIME (YEARS)
LEGEND
(X,Y) POSITION
100.0 , -187.0
100.0 , -215.0
100.0 , -350.0
100.0 , -430.0
100.0 , -515.0

CASE ~~5~~ 4. INCREASED K_v IN FLOW TOPS, INCREASED K_v AND DECREASED S_s IN FLOW INTERIORS

MODEL LAYER PROPERTIES

CHANGES FROM REFERENCE CASE

LAYER	THICK (m)	T (m^2/sec)	K_h (m/sec)	K_v (m/sec)	S	S_s (1/m)
1	5.3 m			2.0E-04		
2	17.9 m			1.0E-07	1.0E-05	6.0E-07
3	53.6 m			2.0E-05		
4	25.8 m			1.0E-07	1.0E-05	4.0E-07
5	23.3 m			3.0E-05		
6	25.9 m			1.0E-08	1.0E-05	4.0E-07
7	25.9 m			8.0E-05		
8	64.3 m			1.0E-08	1.0E-05	2.0E-07
9	38.1 m			5.0E-05		
10	50.0 m			1.0E-08	1.0E-05	2.0E-07
11	7.9 m			1.0E-03		
12	10.8 m			1.0E-09	1.0E-05	9.0E-07

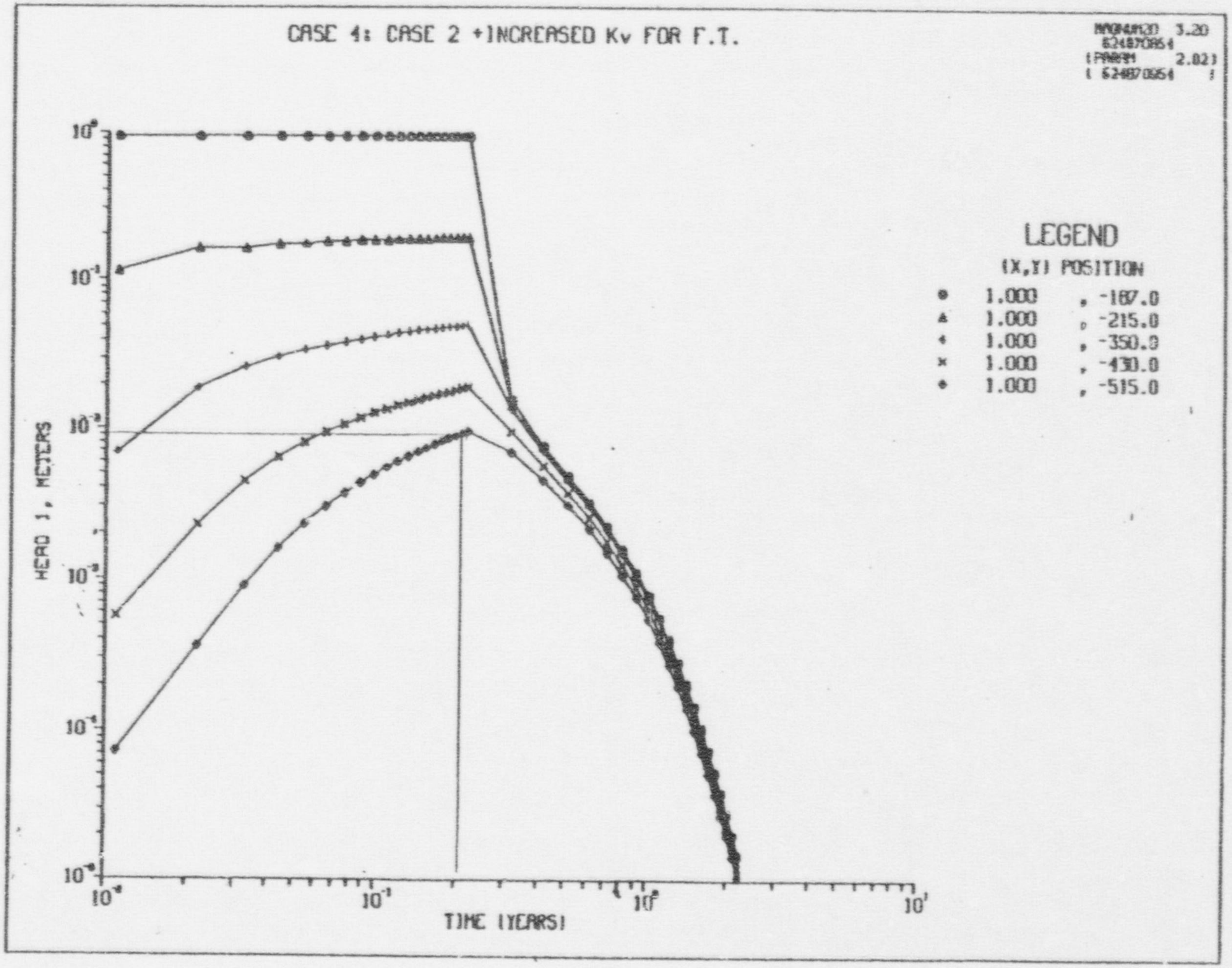
CASE 4: CASE 2 +INCREASED Kv FOR F.T.
MAGNUM2D 3.20
62487085
(PARAM 2.02)
(62487085)
LEGEND
(X,Y) POSITION
1.000 , -187.0
1.000 , -215.0
1.000 , -350.0
1.000 , -430.0
1.000 , -515.0
HEAD 1, METERS
TIME (YEARS)

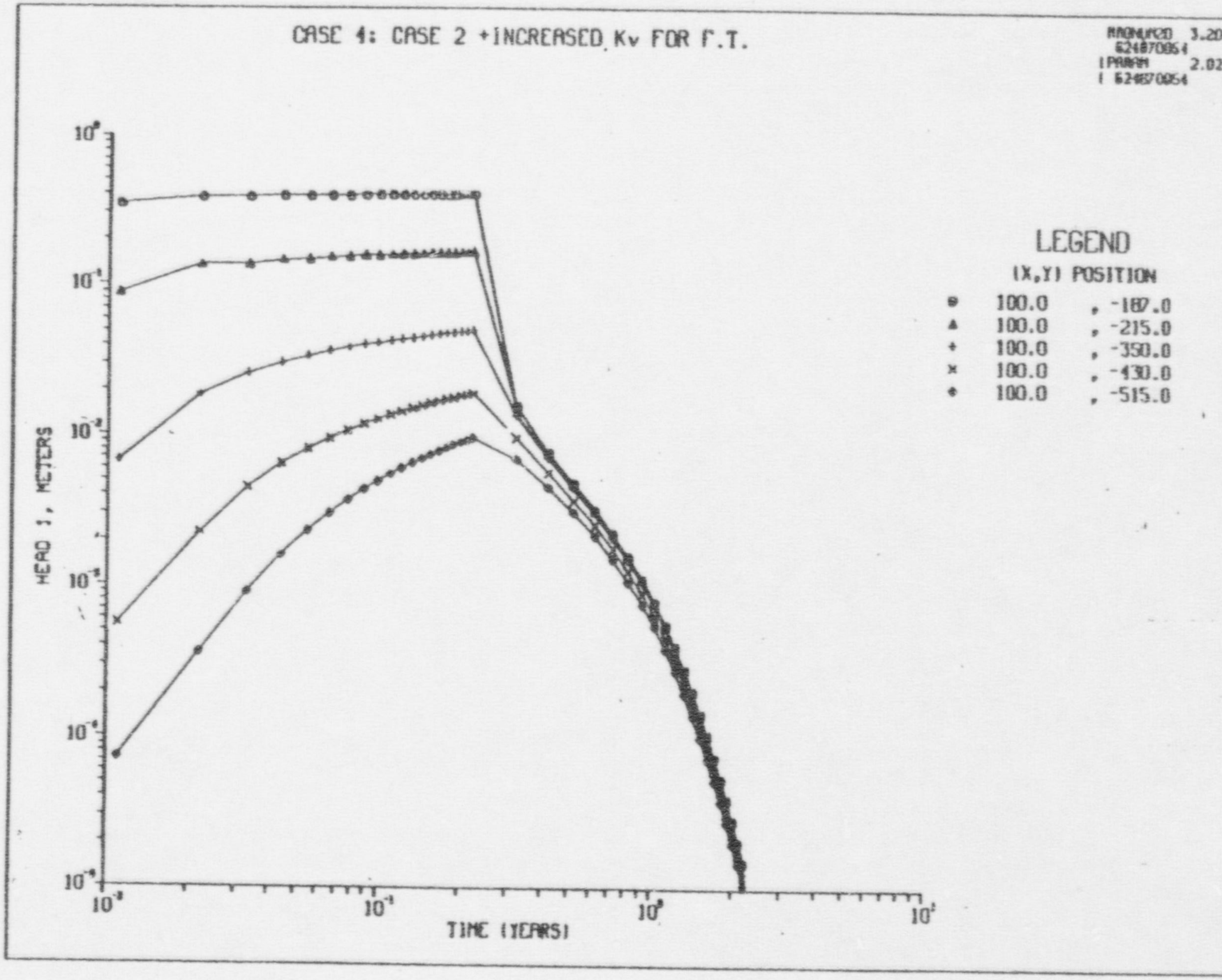
CASE 4: CASE 2 +INCREASED Kv FOR F.T.
MAGNUM2D 3.20
624870864
(PARAM 2.02)
(624870864)
LEGEND
(X,Y) POSITION
100.0 , -187.0
100.0 , -215.0
100.0 , -350.0
100.0 , -430.0
100.0 , -515.0
HEAD 1, METERS
TIME (YEARS)

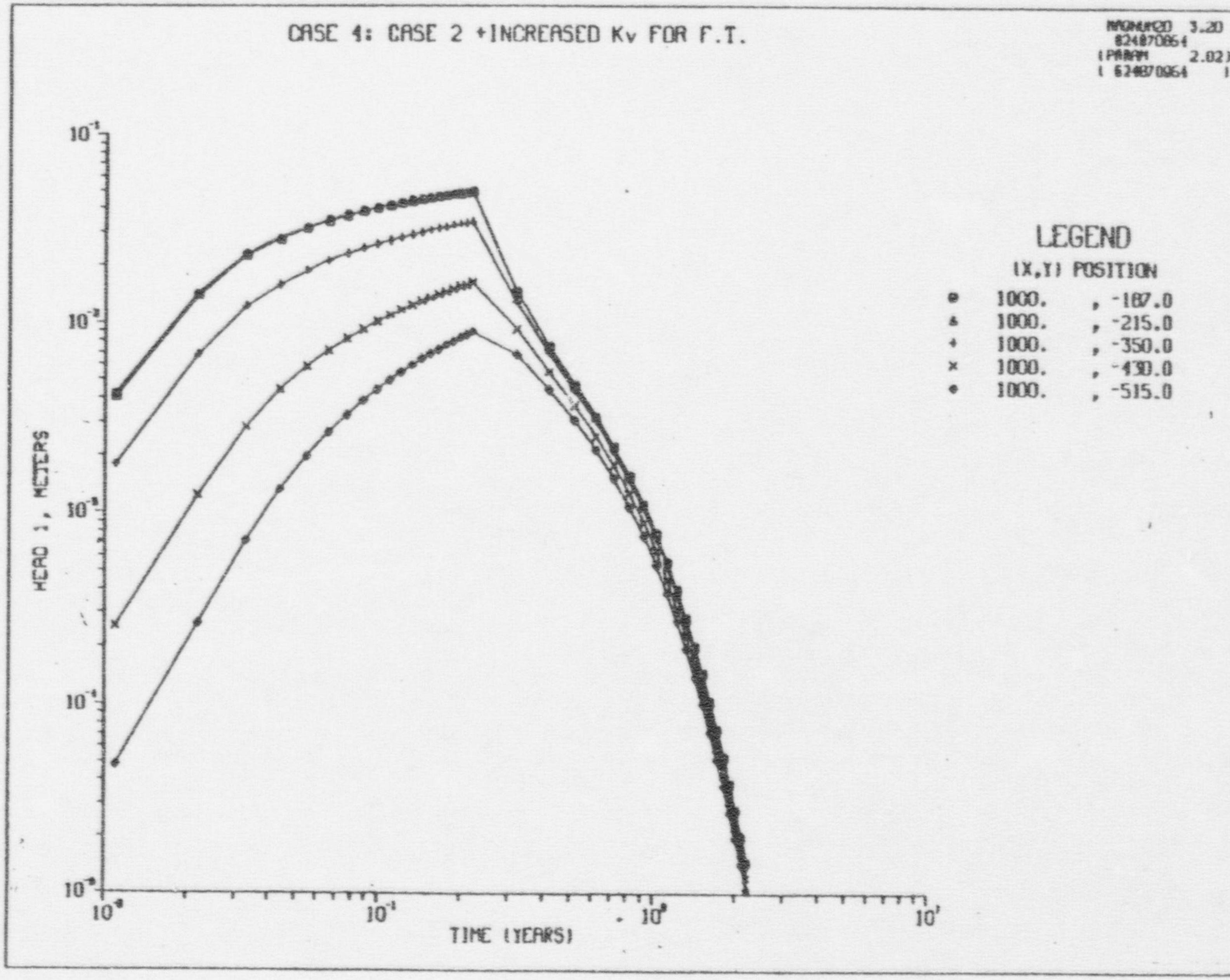

CASE 4: CASE 2 +INCREASED Kv FOR F.T.
MAGNUM2D 3.20
824870864
(PARAM 2.02)
(624870864)
LEGEND
(X,Y) POSITION
1000. , -187.0
1000. , -215.0
1000. , -350.0
1000. , -430.0
1000. , -515.0
HEAD 1, METERS
TIME (YEARS)

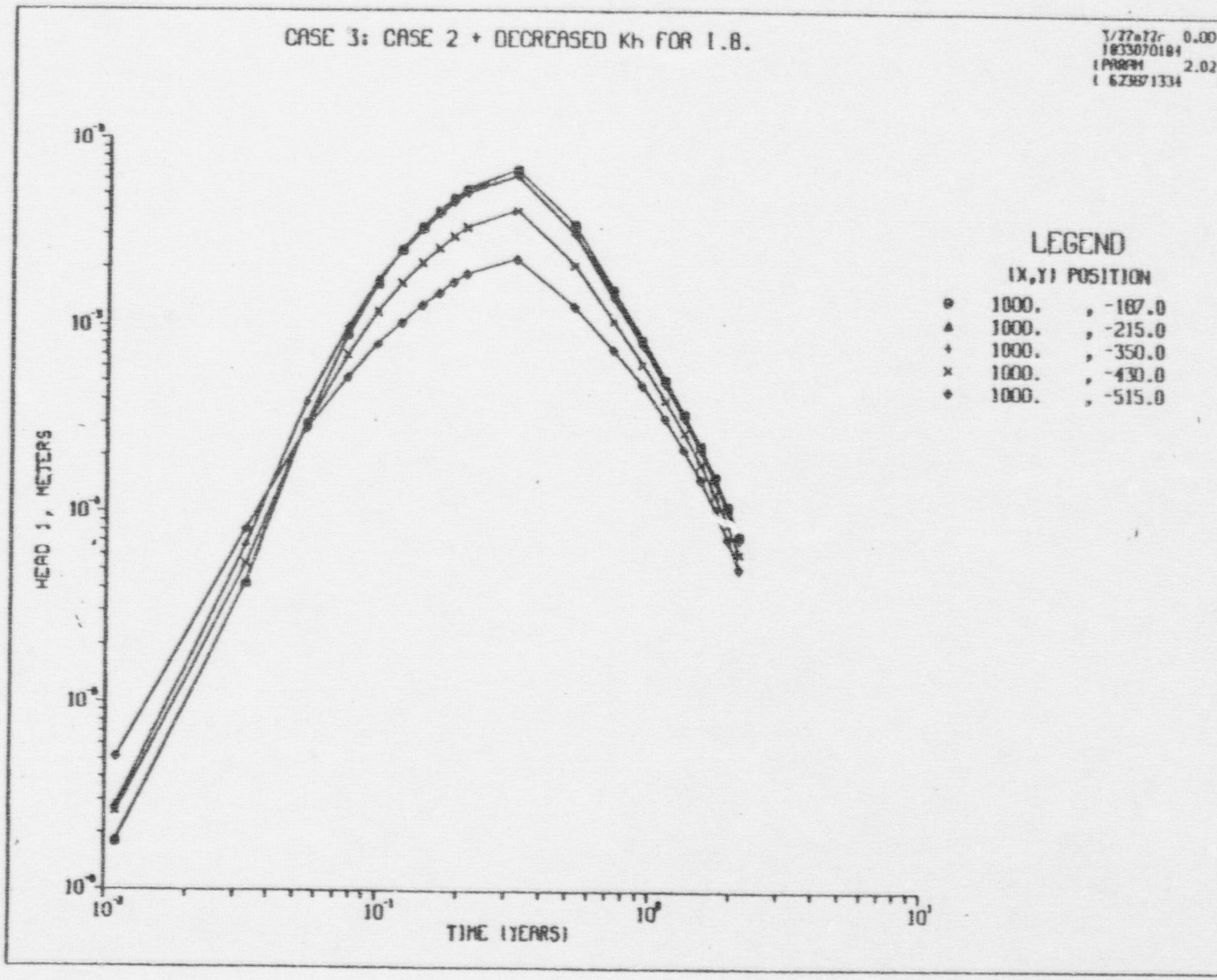

CASE 3: CASE 2 + DECREASED Kh FOR I.B.
LEGEND
(X,Y) POSITION
1000. , -187.0
1000. , -215.0
1000. , -350.0
1000. , -430.0
1000. , -515.0
HEAD 1, METERS
TIME (YEARS)

8 hr test
T= 30,000 gpd/ft
well ...

BOREHOLE: DC-20A   HYDROGEOLOGIC UNIT: BASAL RINGOLD

CONTROL DATUM ELEVATION (ft):   710.70   PROBE SEAT DEPTH (ft):   501

ADJUSTED TO A CONSTANT ATMOSPHERIC PRESSURE OF 14.437 PSI

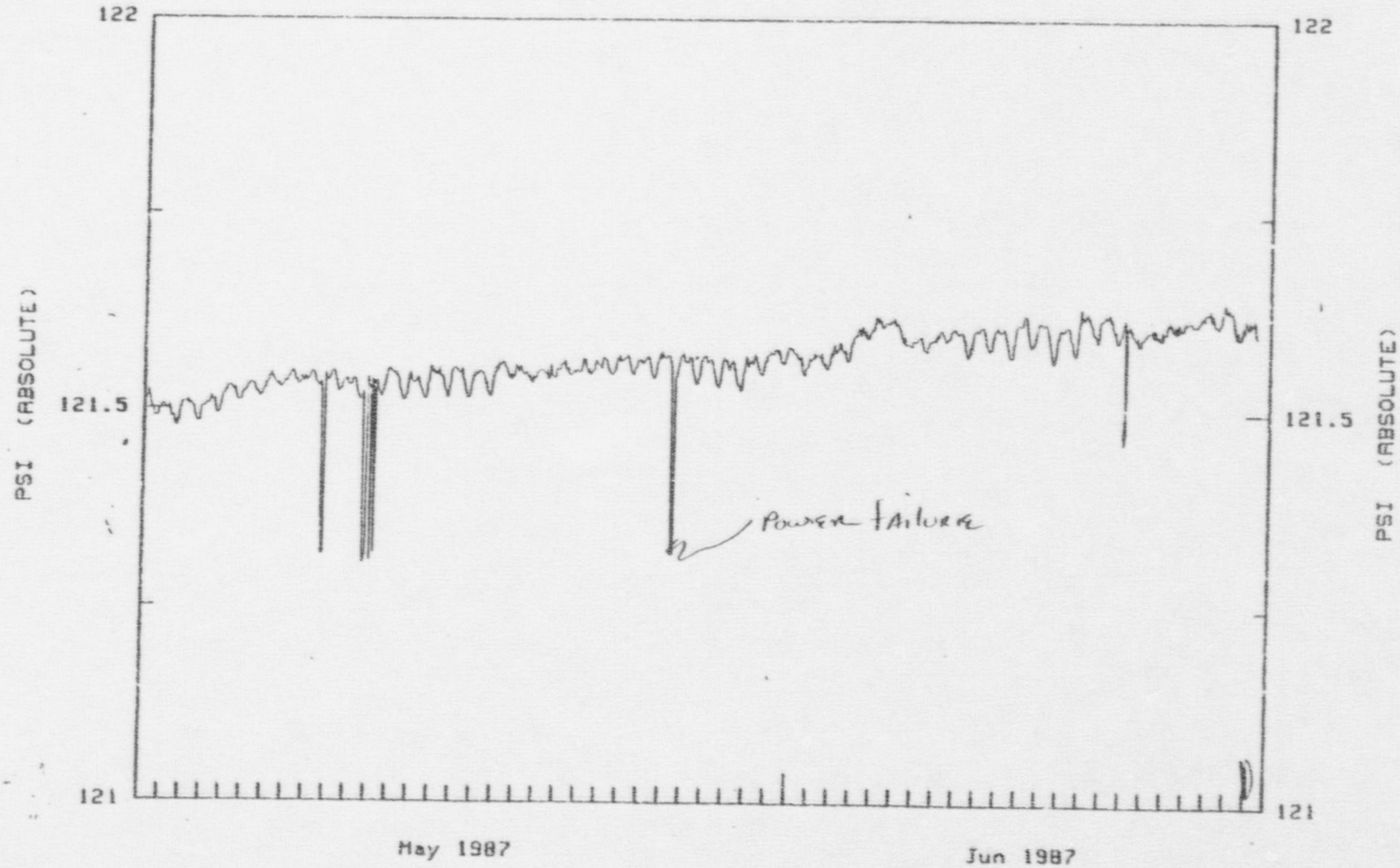

Program WHYDAT Rev 6.3   FILE: 06
Produced on: 23 Jun 1987 10: 7

BOREHOLE: DC-20A   HYDROGEOLOGIC UNIT: BASAL RINGOLD

CONTROL DATUM ELEVATION (ft): 710.70   PROBE SEAT DEPTH (ft): 501

ADJUSTED TO A CONSTANT ATMOSPHERIC PRESSURE OF 14.437 PSI

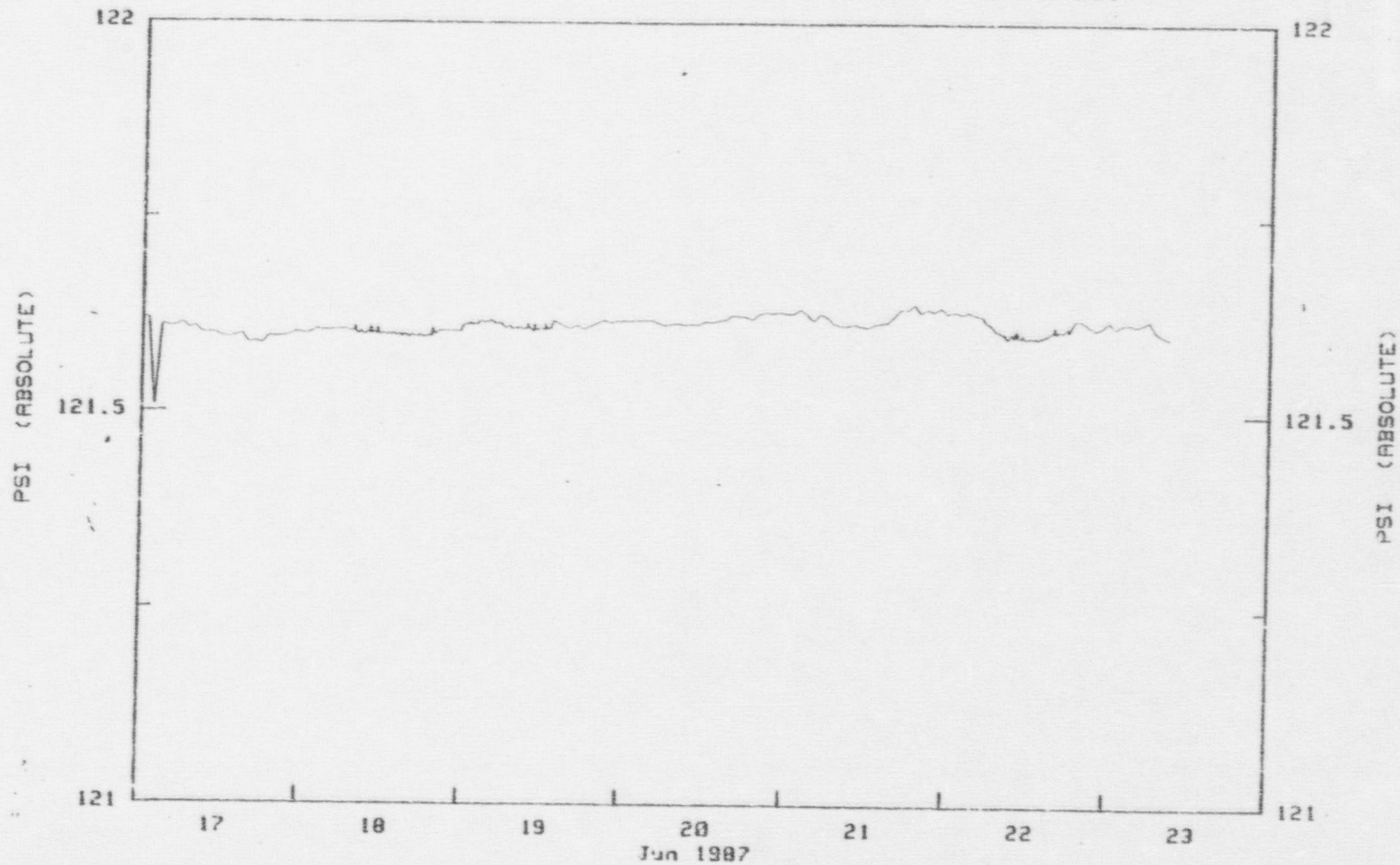

Program HHYDAT Rev 6.3   FILE: 06
Produced on: 23 Jun 1987 10:10

BOREHOLE: DC-20A HYDROGEOLOGIC UNIT: RATTLESNAKE RIDGE INTERBED

CONTROL DATUM ELEVATION (ft): 710.70 PROBE SEAT DEPTH (ft): 648

ADJUSTED TO A CONSTANT ATMOSPHERIC PRESSURE OF 14.437 PSI

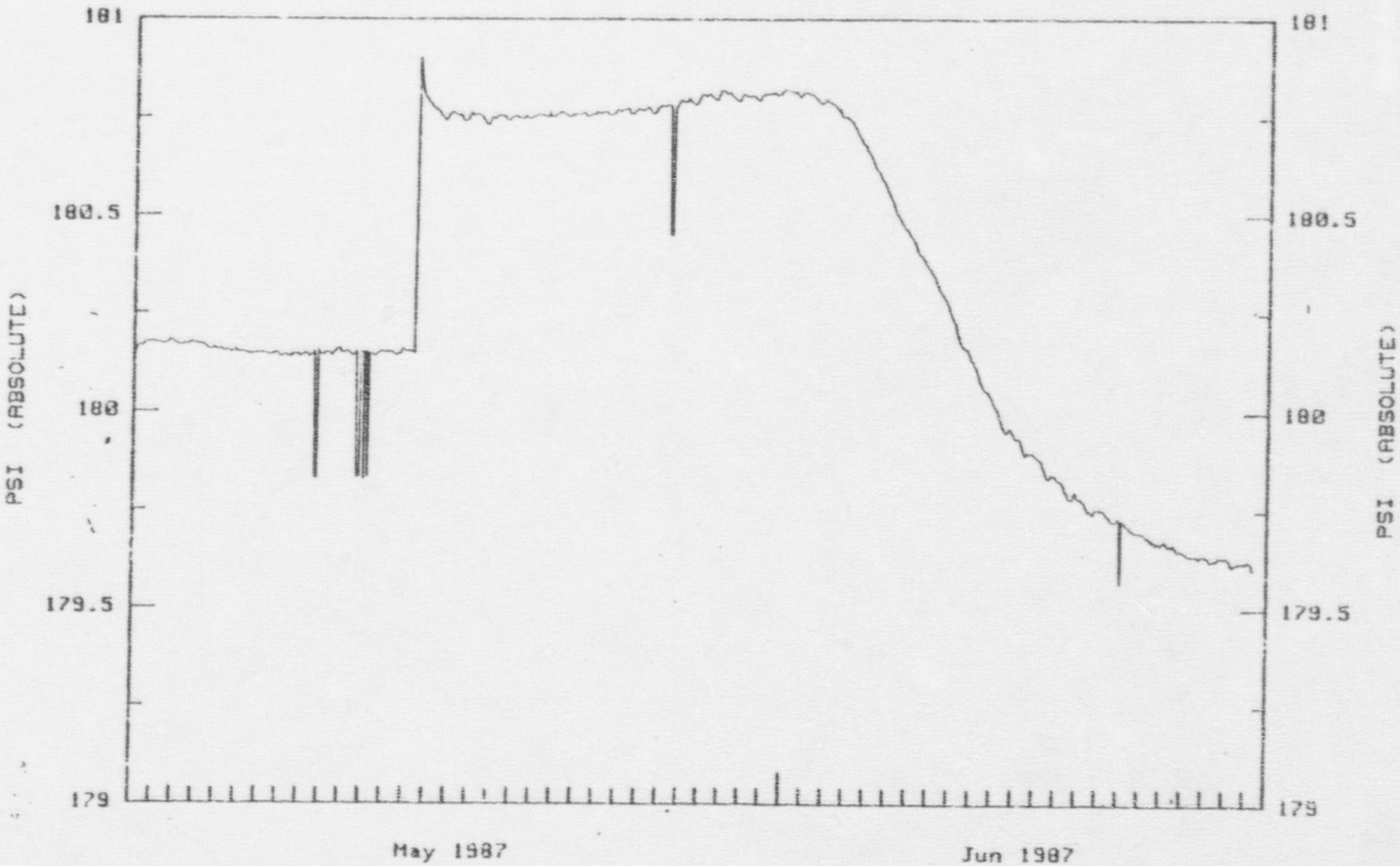

Program WHYDAT Rev 6.3 FILE: 06
Produced on: 23 Jun 1987 10:13

BOREHOLE: DC-20A   HYDROGEOLOGIC UNIT: RATTLESNAKE RIDGE INTERBED

CONTROL DATUM ELEVATION (ft): 710.70   PROBE SEAT DEPTH (ft): 648

ADJUSTED TO A CONSTANT ATMOSPHERIC PRESSURE OF 14.437 PSI

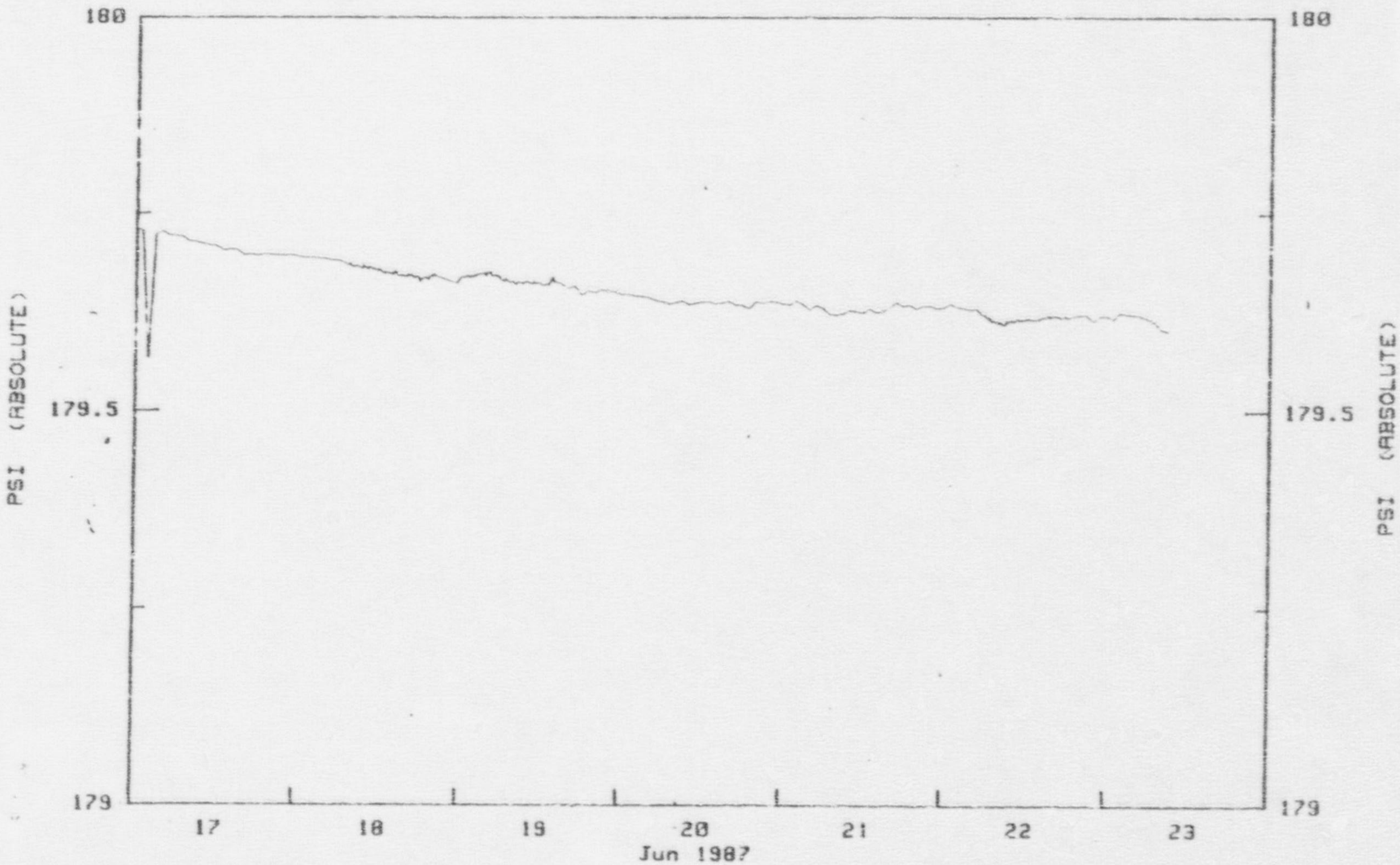

Program WHYBAT Rev 6.3   FILE: 06
Produced on: 23 Jun 1987 10:14

BOREHOLE: DC-20D   HYDROGEOLOGIC UNIT: MABTON INTERBED

CONTROL DATUM ELEVATION (ft): 710.24   PROBE SEAT DEPTH (ft): 1383

ADJUSTED TO A CONSTANT ATMOSPHERIC PRESSURE OF 14.437 PSI

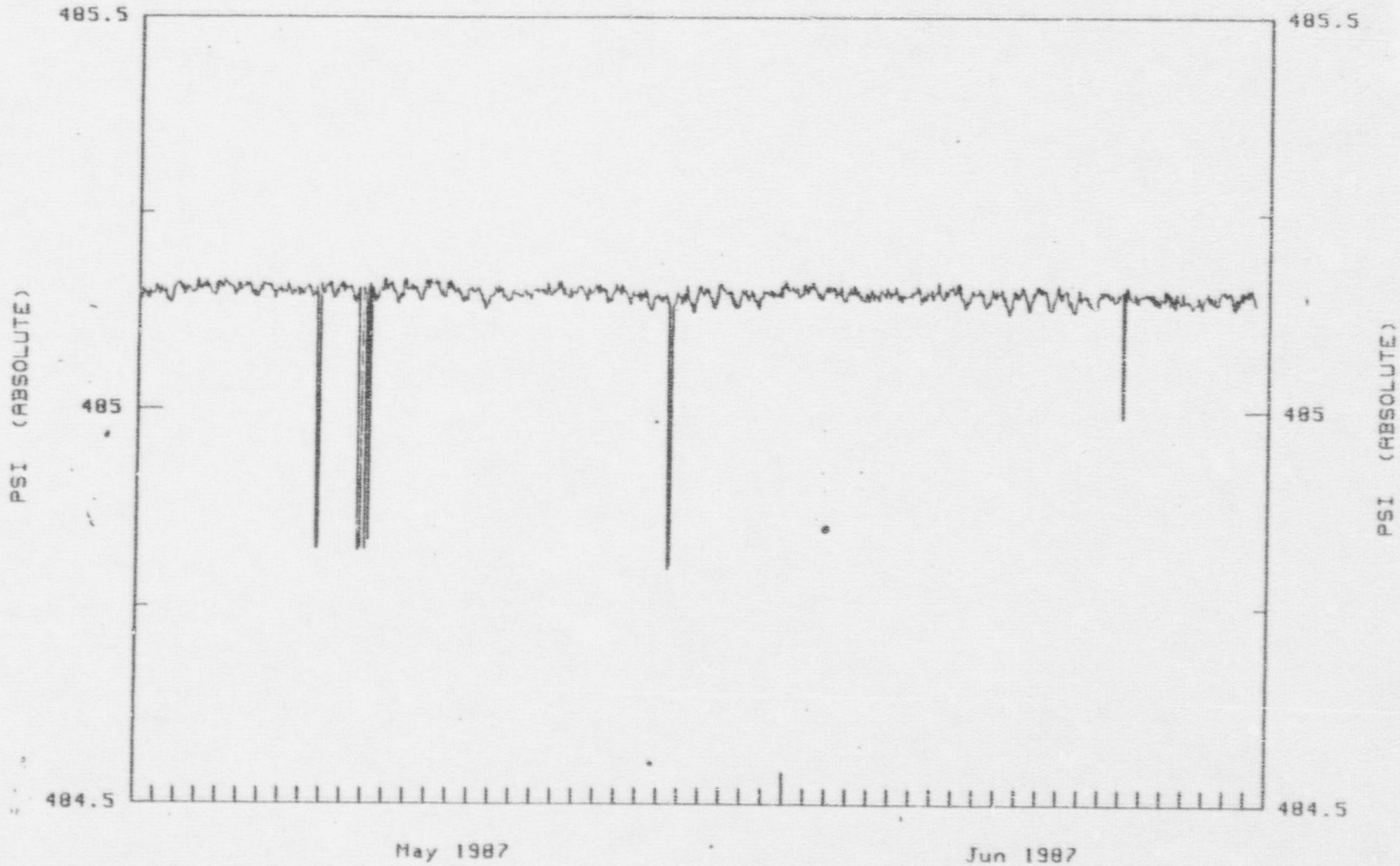

Program WHYDAT Rev 6.3   FILE: 06
Produced on: 23 Jun 1987 10:20

BOREHOLE: DC-20D HYDROGEOLOGIC UNIT: MABTON INTERBED

CONTROL DATUM ELEVATION (ft): 710.24 PROBE SEAT DEPTH (ft): 1383

ADJUSTED TO A CONSTANT ATMOSPHERIC PRESSURE OF 14.437 PSI

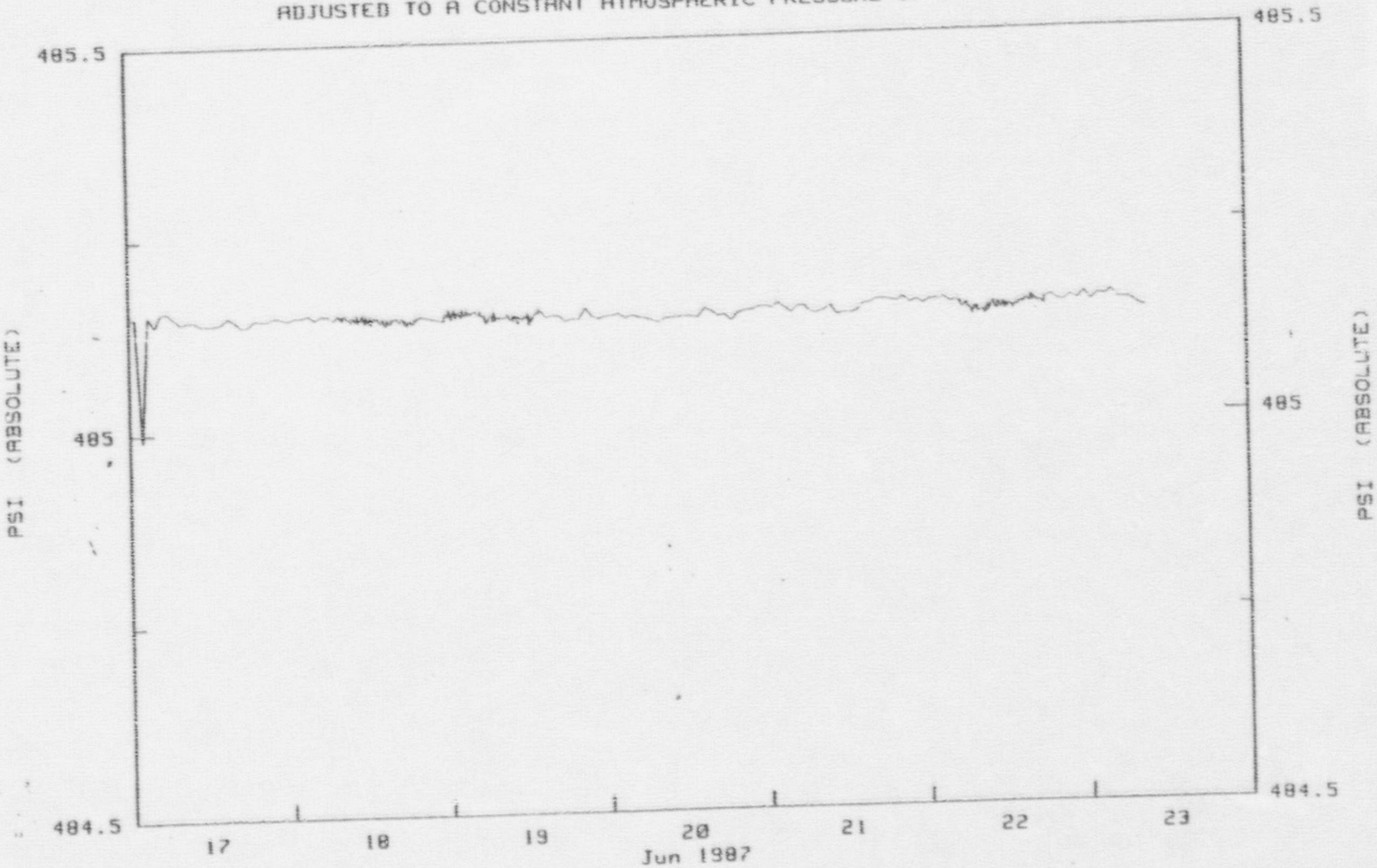

Program WHYDAT Rev 6.3 FILE: 06
Produced on: 23 Jun 1987 10:22

BOREHOLE: DC-20C   HYDROGEOLOGIC UNIT: SENTINEL GAP FLOW TOP

CONTROL DATUM ELEVATION (ft):   711.31   PROBE SEAT DEPTH (ft):   1073

ADJUSTED TO A CONSTANT ATMOSPHERIC PRESSURE OF 14.437 PSI

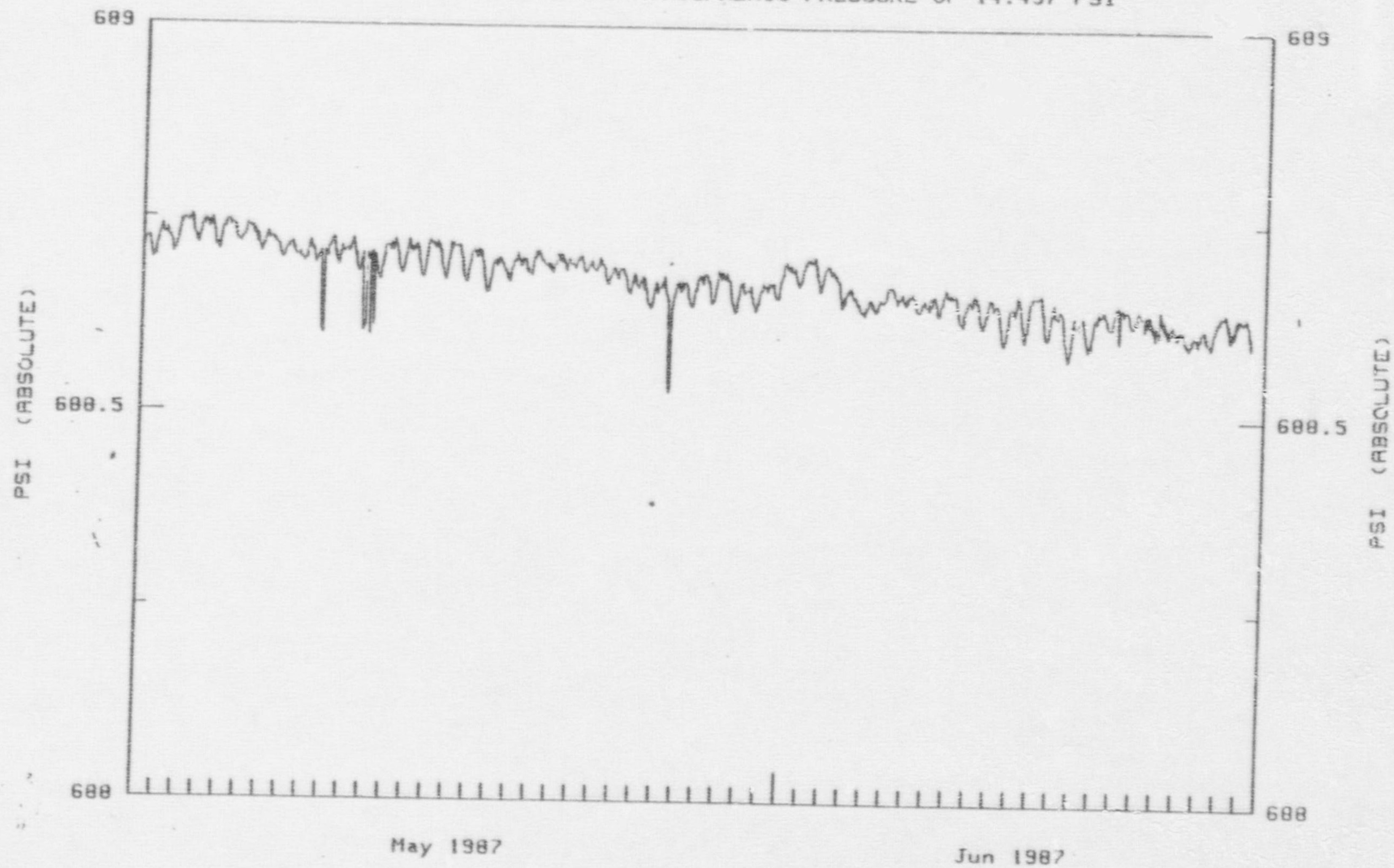

Program WHYDAT Rev 6.3   FILE: 06
Produced on: 23 Jun 1987 10:24

BOREHOLE: DC-20C HYDROGEOLOGIC UNIT: SENTINEL GAP FLOW TOP

CONTROL DATUM ELEVATION (ft): 711.31 PROBE SEAT DEPTH (ft): 1873

ADJUSTED TO A CONSTANT ATMOSPHERIC PRESSURE OF 14.437 PSI

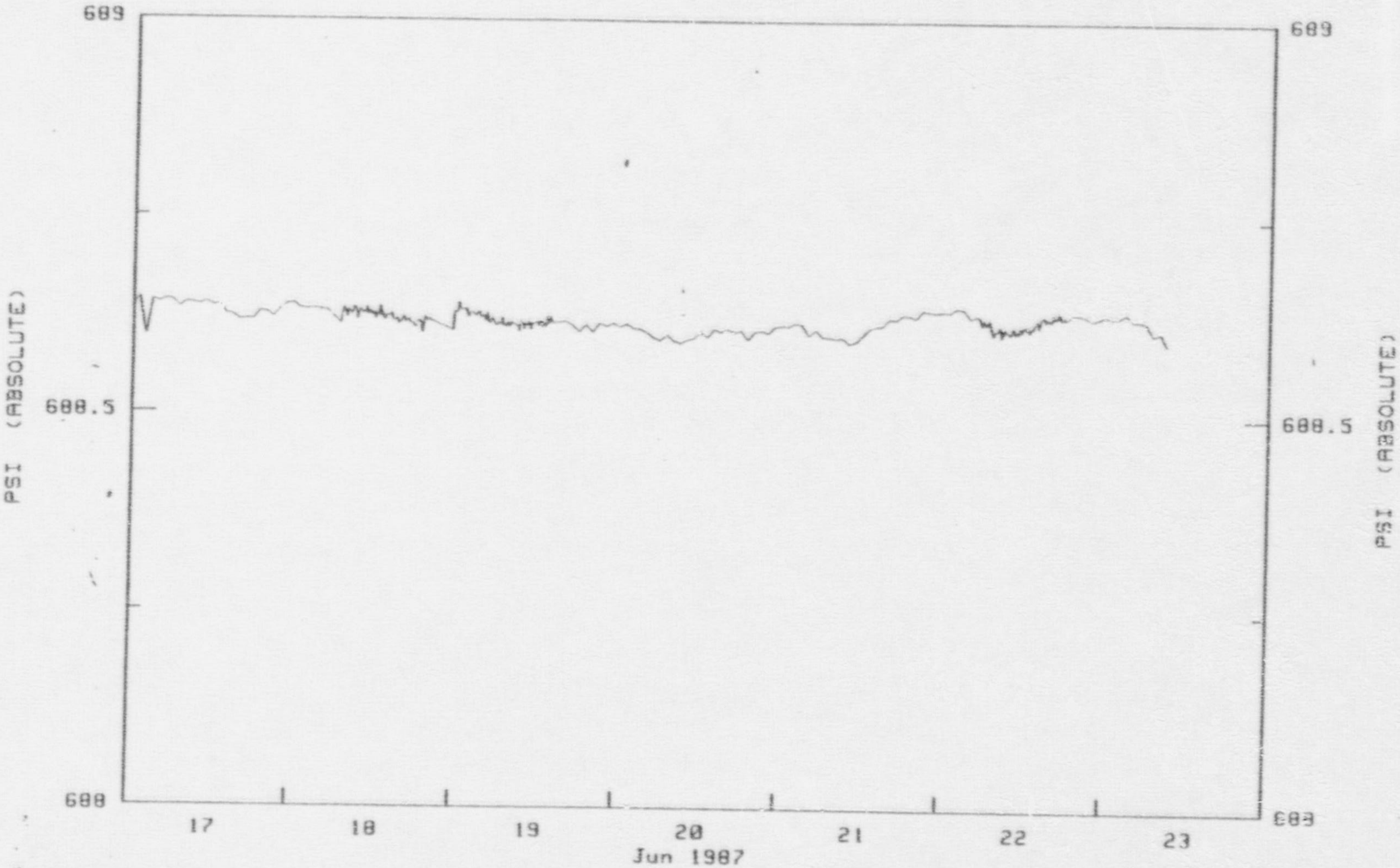

Program WHYDAT Rev 6.3 FILE: 06
Produced on: 23 Jun 1987 10:25

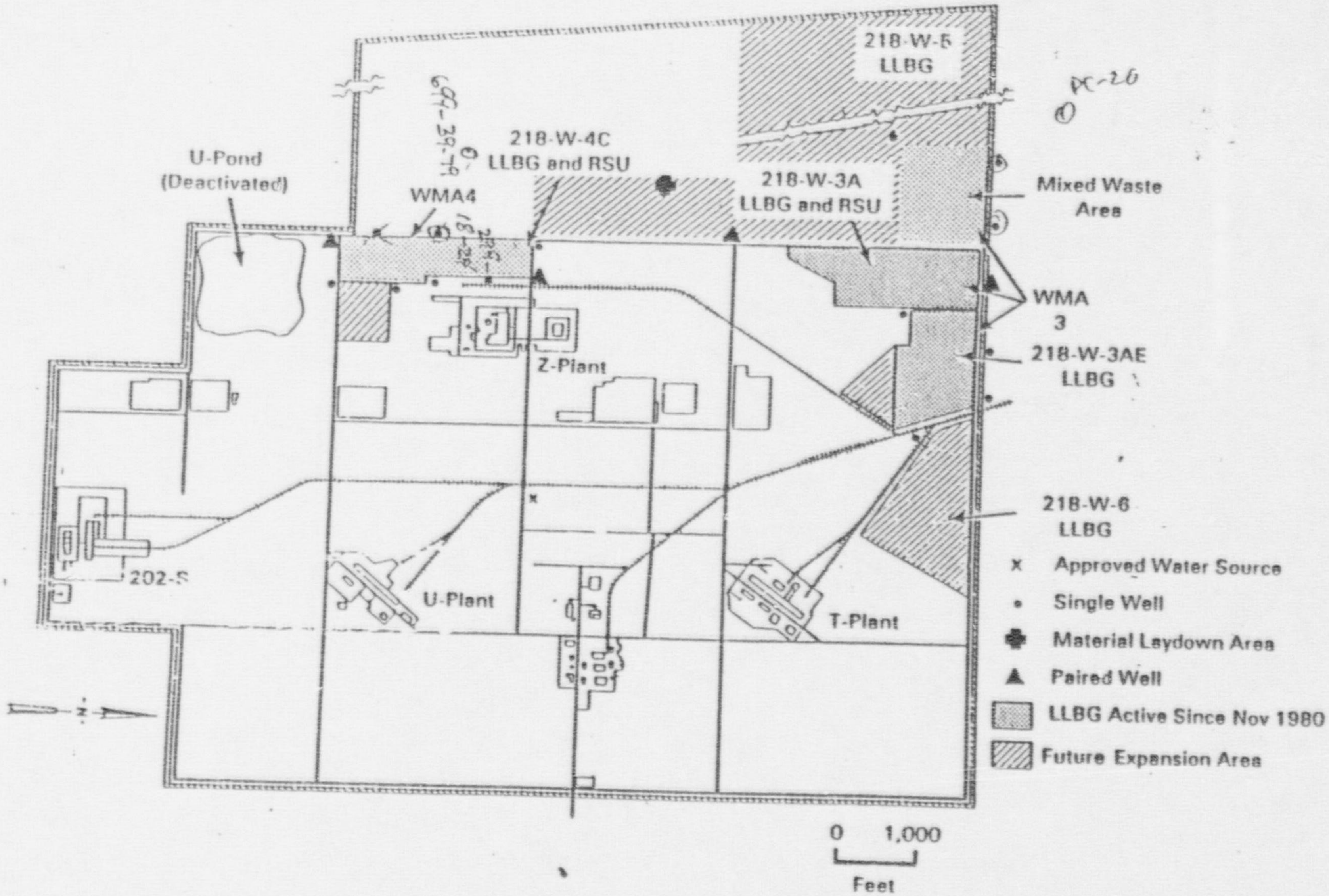

FIGURE 17. Location Map of Planned Clusters and Single Monitoring Wells in the 200-West Area